CHARACTERIZING THE *IN VIVO* ROLE OF SCABIN, A MONO ADP-RIBOSYLTRANSFERASE FROM THE COMMON SCAB PATHOGEN *STREPTOMYCES SCABIEI*

By

Hannah Claire Perry, B.Sc.

A Thesis submitted to the school of graduate studies in partial fulfilment of the requirements for the degree of

Master of Science

Department of Biology

Memorial University of Newfoundland

September 2021

St. John's Newfoundland and Labrador

ABSTRACT

Common scab is a widespread bacterial disease of potato and other root and tuber crops. The disease is characterized by the presence of superficial, raised or deep-pitted lesions on the surface of the potato tuber, and these lesions reduce the market value of the crop to cause major economic losses for farmers. To date, no fully resistant potato cultivar exists, and current management strategies are largely inadequate or inconsistent. Therefore, studying the virulence factors of the most prominent causative agent, *Streptomyces scabiei*, is of high importance. Recently, a new putative virulence factor called Scabin was identified in the genome of *S. scabiei.* Scabin is a mono ADP-ribosyltransferase that possesses *in vitro* activity towards DNA, RNA and small guanosine-containing molecules, a rare activity for this group of enzymes that typically target proteins. However, the *in vivo* target and role of Scabin remains unknown. The purpose of this study has been to investigate the function of Scabin and determine if it plays a role in *S. scabiei* pathogenesis. To achieve this, a *scabin* knockout mutant was created, and the mutant together with wild-type *S. scabiei* and a *scabin* overexpression strain were tested in several plant bioassays. The morphology of the mutant and overexpression strain was examined when the strains were cultured on several distinct agar media. The conditions under which *scabin* is expressed were investigated using RT-PCR, and subsequently, it was discovered that *scabin* is co-transcribed with a neighbouring gene, *SCAB_27781*, suggesting they are functionally linked. The distribution of Scabin and SCAB_27781 homologues in other *Streptomyces* species and the relative positions of the corresponding genes in each species were mapped out, and regions of interest in both proteins were predicted using various bioinformatic tools. This study is the first to investigate possible *in vivo* roles for Scabin.

ACKNOWLEDGEMENTS

I would like to thank everyone who has supported me through this degree. I am forever grateful to my supervisor Dr. Dawn Bignell for her understanding and guidance. Thank you to my committee members Dr. Kapil Tahlan and Dr. Linda Jewell for their time and suggestions for improving my thesis. Special thank you to Gustavo Diaz Cruz, Dr. Jingyu Liu, Dr. Yuting (Phoebe) Li, Jody-Ann Clarke, Arshad Shaikh, Brandon Piercey and Alex Byrne as well as all the other members of the Bignell lab and Tahlan lab for helping me, putting up with me, and making the lab a wonderful and fun place to work. Finally, thank you to Spencer Axford for his love and support in my everyday life outside the lab. I could not have done this without any of you.

Table of Contents

List of Figures

List of Tables

List of Abbreviations, Symbols and Nomenclature

α: alpha

µF: microfarad

µg: microgram

µL: microlitre

µm: micrometer

µM: micromolar

Ω: ohm

Φ: phi

°C: degrees Celsius

***aac(3)IV**:* apramycin resistance gene

ADP-ribose: adenosine diphosphate ribose

ApraR: apramycin resistance

ART: ADP-ribosyltransferase

***attB**:* attachment site B

BLASTP: Basic Local Alignment Search Tool for proteins

bp: basepair

C: control

cAMP: cyclic adenosine 3',5'-monophosphate

cDNA: complimentary DNA

CFA-Ile: *N*-coronafacoyl-L-isoleucine

CFU: colony forming unit

cGMP: cyclic guanosine 3',5'-monophosphate

cm: centimeter

COR: coronatine

CS: common scab

CT: cholera toxin

CT-A: cholera toxin A-subunit

C-terminal: carboxy terminal

DCW: dry cell weight

DMSO: dimethyl sulfoxide

DNA: deoxyribonucleic acid

dNTP: deoxyribonucleotide triphosphate

dsDNA: double stranded DNA

DT: diphtheria toxin

DT-A: diphtheria toxin-A subunit

DT-B: diphtheria toxin-B subunit

eEF2: eukaryotic elongation factor 2

EFR: EF-Tu receptor

EF-Tu: bacterial elongation factor-Tu

egfp: enhanced green fluorescence protein

ER: endoplasmic reticulum

ETI: effector triggered immunity

f. sp.: forma specialis

F-actin: actin filaments

FLS2: flagellin-sensing2

g: g-force

G+I: gamma distribution and invariant sites

G-actin: globular actin

GC: guanine-cytosine

GDP: guanosine diphosphate

GRP7: glycine rich RNA binding protein 7

GTP: guanosine triphosphate

GTR: general time reversal

gyrA: DNA gyrase subunit A gene

HB-EGF: heparin-binding epidermal growth factor
HPLC: high performance liquid chromatography
hr: hour
HSP90: heat shock protein 90

IAA: indole-3-acetic acid
ISP-4: International *Streptomyces* Project Medium 4
ISR: induced systemic resistance

kb: kilobase
kDa: kilodalton
kg: kilogram
KO: knockout

LB: Luria-Bertani
LRP1: low density lipoprotein receptor-related protein 1

M: molar
mART: mono-ADP-ribosyltransferase
Mb: mega base
MEGA7: Molecular Evolutionary Genetics Analysis 7
mg: miligram
min: minute
MKK5: mitogen activated protein kinase kinase 5
mL: millilitre
mm: milimeter
mM: millimolar
MMG: minimal medium with glucose
mRNA: messenger RNA

MS: Murashige and Skoog

NA: nutrient agar
NAD^+: nicotinamide adenine dinucleotide
NCBI: the National Center for Biotechnology Information
ng: nanogram
NLS: nuclear localization signal
nm: nanometer
NOI: nitrate induced
nt: nucleotide
N-terminal: amino terminal

OBA: oat bran agar
OBB: oat bran broth
OD_{600}: optical density at 600nm
OE: overexpression
oriT: origin of transfer

PAMP: pathogen associated molecular pattern
PCD: programmed cell death
PCR: polymerase chain reaction
PE: *Pseudomonas aeruginosa* exotoxin
PE-A: *Pseudomonas aeruginosa* exotoxin-A subunit
PE-B: *Pseudomonas aeruginosa* exotoxin-B subunit
PMA: potato mash agar
pmol: picomole
PT: pertussis toxin
PTI: pathogen triggered immunity
ptoDC3000: *Pseudomonas syringae* pv. *tomato* DC3000
pv.: pathovar

RhoGDI: RHO guanine nucleotide dissociation inhibitor

RNA: ribonucleic acid

rpm: rotations per minute

rpoB: β subunit of bacterial RNA polymerase

RT-PCR: reverse transcription PCR

SAR: systemic acquired resistance

***SCAB_27771/scabin*:** Scabin gene

SCAB_27781: putative toxin-B domain gene

SCAB_27791: putative regulator gene

Sec: general secretion

SFM: soy flour mannitol

SOB: super optimal broth

SOC: super optimal broth with catabolite repression

Spp.: species

ssDNA: single stranded DNA

subsp.: subspecies

Taq*: Thermus aquaticus*

TB: transformation buffer

TCAG: The Centre for Applied Genomics

TSA: trypticase soy agar

TSB: trypticase soy broth

U: units

v/v: volume per volume

V: volts

VC: vector control

w/v: weight per volume

WT: wild type

CHAPTER 1: INTRODUCTION AND LITERATURE REVIEW

1.1 General Characteristics of the Genus *Streptomyces*

Streptomyces is a genus of Gram-positive, filamentous spore-forming bacteria found ubiquitously in the environment. The genus is very large and contains over 600 described species (Wanner & Kirk, 2015). *Streptomyces* species have a single chromosome that is linear, high in GC content (~70%) and extremely large, with an average size of 8 Mb (Redenbach et al., 2000). Many species carry large linear and/or circular plasmids (Li et al., 2016; Redenbach et al., 2000). The core genome of *Streptomyces* consists of around 1,018 genes, which are usually located towards the centre of the linear chromosome (Kim et al., 2015; Lorenzi et al., 2021). Various accessory genes are situated towards the ends of the chromosome, where they are subjected to higher rates of recombination and replacement (Lorenzi et al., 2021). The pan-genome was recently calculated to contain around 106,000 genes and is predicted to be open, meaning that as new species are described, the size of the pan-genome is expected to increase significantly (Lorenzi et al., 2021).

The life cycle of *Streptomyces* is unique among bacteria. Unlike most spore-forming bacteria, which produce spores as a defense mechanism against harsh environmental conditions, the spores of *Streptomyces* are used for reproduction and dispersal, similar to the spores of fungi (Chater & Chandra, 2006). When *Streptomyces* spores land on a suitable substrate, the spores will germinate and grow, forming a dense network of branched filamentous hyphae called the vegetative mycelium (Chater, 2016). As nutrients become depleted, the organism begins producing aerial hyphae, and these eventually develop into chains of spores that disperse to restart the cycle (Chater, 2016).

Much of the research on *Streptomyces* has focused on their ability to produce numerous medically-relevant bioactive specialized metabolites, ranging from anti-cancer compounds to antibiotics. After the initial discovery of the antibiotics streptothricin in 1942 and streptomycin in 1944, *Streptomyces* and other actinobacteria became the targets of extensive specialized metabolite screening (Bérdy, 1974). During the "golden era" of antibiotic discovery from 1955 to 1962, approximately 80% of the compounds discovered were of actinomycete origin, of which members of the genus *Streptomyces* were the greatest suppliers (Bérdy, 1974; Davies, 2006). Even though novel antimicrobial compound discovery has slowed in recent years, the *Streptomyces* still remain a popular target for *in silico* genome mining and screens (Ward & Allenby, 2018). Based on the rate of antibiotic discovery, it has been estimated that there could be over 100,000 antimicrobial compounds in the totality of the genus (Watve et al., 2001). The reported compounds discovered so far only amount to roughly 3% of this value, meaning that we have likely just scratched the surface of what this genus is theoretically capable of providing (Watve et al., 2001).

Streptomyces are also interesting from an ecological viewpoint. As prominent members of the soil microbiota, they have formed complex interactions with plants, fungi and even animals (Seipke et al., 2012). For example, the beewolf solitary digger wasp (*Philanthus* spp.) coats their burrows in a species of *Streptomyces* that protects the larvae from fungal attack through production of antifungal compounds (Kaltenpoth et al., 2005). Similarly, leaf cutter ants (tribe Attine) have established a symbiotic relationship with streptomycetes producing an antifungal compound that specifically inhibits a specialized fungal pathogen from the genus *Escovopsis* (Currie et al., 1999). The ants coat their fungus garden food source with the bacteria to help protect it from the pathogenic fungus (Currie et al., 1999). Conversely, despite being

generally considered as antagonistic towards fungi as demonstrated above, there are instances of *Streptomyces* having a positive effect on fungi (Riedlinger et al., 2006). For example, *Streptomyces* strain AcH 505 produces auxofuran, which stimulates the growth of the ectomycorrhizal fungus *Amanita muscaria,* helping the fungus to establish more connections with spruce trees (Riedlinger et al., 2006). In some instances, the antimicrobial compounds produced by *Streptomyces* are thought to act as signaling molecules for interacting with the larger microbial community, rather than as tools of intermicrobial warfare (Yim et al., 2007). In this light, the extensive specialized metabolite repertoire of *Streptomyces* can be seen as necessary to integrate as members of the diverse soil ecosystem.

1.2 *Streptomyces* Associations with Plants

The genus *Streptomyces* has been estimated to have arose around 450 million years ago, closely following the arrival of green plants on land (Chater, 2006; Embley, 1994). *Streptomyces* were likely some of the first decomposers, breaking down complex polymers in the environment, including plant and fungal matter (Chater, 2006). This hypothesis is supported by the widespread distribution of several cellulose-utilization enzymes and chitinases throughout the genus (Chater et al., 2010).

Streptomyces are one of the most commonly identified groups of bacteria found living in the rhizosphere of plants and as endophytes (Taechowisan et al., 2003; Viaene et al., 2016). *Streptomyces* are able to interact with an extremely large range of plants, including both monocots and dicots. However, the recruitment of *Streptomyces* species as root endophytes seems to be somewhat specific. Plants such as *Arabidopsis thaliana* and rice *(Oryza sativa*) have been shown to have root endospheres enriched for *Streptomyces,* while other plants such

as barley (*Hordeum vulgare)* lack these bacteria (Bulgarelli et al., 2015, 2012; Edwards et al., 2015).

The vast majority of plant-associated *Streptomyces* are harmless, and many are actually beneficial to the plant. For example, some have been shown to trigger induced systemic resistance (ISR) and systemic acquired resistance (SAR) thereby priming a plant's immune response and making the plant less susceptible to infection by pathogens (Conn et al., 2008; Kurth et al., 2014). Soil inoculation of some *Streptomyces* species has been linked to an increase in the growth rate of some plants (Goudjal et al., 2013; Rungin et al., 2012; Sadeghi et al., 2012). This ability is thought to be caused by the bacterial production of plant growth phytohormones such as auxin, and by facilitating an increase in mineral availability for the plant (Goudjal et al., 2013; Rungin et al., 2012; Sadeghi et al., 2012). Finally, because *Streptomyces* are known for producing many antibiotic and antifungal compounds, they have long been regarded as antagonistic to plant pathogens in the soil (Barnett et al., 2019; Sabaratnam & Traquair, 2002). As a result, some species are being developed for use as biocontrol agents (Barnett et al., 2019; Sabaratnam & Traquair, 2002). However, in contrast to the many beneficial functions mentioned above, a small number of *Streptomyces* species have evolved to become plant pathogens and are able to exploit plants solely for their own benefit.

1.3 Plant Pathogenic *Streptomyces* and Common Scab Disease

Of the known plant pathogenic *Streptomyces*, the most well studied is *Streptomyces scabiei*, which is a causative agent of common scab (CS) disease. CS has a world-wide distribution and can affect all varieties of potato (*Solanum tuberosum*) as well as root crops such as carrot (*Daucus carota*), radish (*Raphanus sativus*), beets (*Beta vulgaris*), and parsnip

(*Pastinaca sativa*) (Goyer & Beaulieu, 1997). CS disease is characterized by the development of superficial, pitted, and/or raised scab-like lesions on the surface of the potato tuber (Figure 1.1). These lesions lower the market value of the potatoes and can lead to rejection of tubers meant for fresh market/tablestock, seed and processing uses (Wanner & Kirk, 2015). For example, tubers with 5% or more scab coverage do not meet the requirements put forth by the Canadian Food Inspection Agency for acceptable sale as Canada no.1 tablestock (Government of Canada C. F. I. A., 2021) and potatoes with 10% or more scab coverage are considered severely affected and do not meet the standards for use as seed (Government of Canada C. F. I. A., 2015). Furthermore, tubers with pitted scab lesions are undesired for processing into potato chips and fries, as a significant proportion of the tuber is lost during lesion removal (Braun et al., 2017). In addition, there is evidence that in the early stages of potato plant growth, *S. scabiei* can hinder the development of a healthy root system, and this can cause the plants to become stunted or wilted and can reduce tuber yields if the infection is severe enough (Han et al., 2008; Hiltunen et al., 2005; Loria et al., 1997). Canada is ranked 6th worldwide in the export of tablestock potatoes and 8th in the export of seed stock (Agriculture and Agri-Food Canada, 2020). Potato is the largest contributor (at 27.2%) to vegetable production in Canada (Agriculture and Agri-Food Canada, 2020). Although economic losses due to CS are not well documented, a recent survey estimated losses of at least 15.3 to 17.3 million dollars (CAN) to potato growers across Canada due to CS disease during the 2002 growing season (Hill & Lazarovits, 2005).

Figure 1.1: Common scab symptoms on the surface of a potato tuber. Image provided by Dr. Dawn Bignell.

Other pathogenic *Streptomyces* species known to cause CS include *Streptomyces europaeiscabiei, Streptomyces stelliscabiei* and *Streptomyces turgidiscabies* (Dees & Wanner, 2012). A disease related to CS is acid scab, which is caused by *Streptomyces acidiscabies* (Dees & Wanner, 2012). Acid scab produces the same symptomology on potato tubers as CS, except that it can occur in acidic soils that would otherwise inhibit CS-causing pathogens (Li et al., 2019). Netted scab is caused by *Streptomyces reticuliscabiei* and is distinguished from CS by the lesion pattern, which is always superficial and never deep-pitted, and takes on a netted shape (Scholte & Labruyere, 1985). Netted scab is associated with a higher severity of root necrosis, and increasing soil moisture increases the incidence and severity of the disease, which is opposite to the effects of soil moisture on CS (Scholte & Labruyere, 1985). *Streptomyces ipomoea* causes soil rot of sweet potato, which only affects sweet potato (*Ipomoea batatas*) and other plants in the Convolvulaceae family (Zhang et al., 2003). The symptomology is different

from CS, consisting of necrotic lesions on the storage tubers and extensive root rot (Zhang et al., 2003).

To date, efforts to manage CS disease, such as altering the soil pH, soil moisture management and crop rotation, have proven unreliable or inefficient (Braun et al., 2017). For example, reducing the soil pH has been shown to help manage CS caused by *S. scabiei*; however, other pathogenic species such as *S. acidiscabies* or *S. turgidiscabies* are able to survive in low pH soil and cause disease under such conditions (Dees & Wanner, 2012). Increasing the pH above 8.5 can suppress CS, but this negatively impacts tuber yields since potato plants grow best at a pH of 5.5 to 7.5 (Dees & Wanner, 2012; Waterer, 2002). Irrigation during tuber formation and expansion can help reduce the severity of CS, but it also promotes the development of other diseases that thrive under such conditions (Dees & Wanner, 2012). Irrigation as a disease management strategy is additionally viewed as an environmental concern in some regions since it can lead to excessive water use, and thus it has become preferable to use other strategies in order to conserve water (Collier & Else, 2014; Stead & Wale, 2004). Crop rotation can help to some degree; however, *Streptomyces* are excellent soil saprophytes and can remain in infested soils for many years (Dees & Wanner, 2012). The use of resistant potato cultivars is the most desired strategy for disease management, and while some cultivars with good resistance have been created, the mechanism behind the resistance is still largely unknown. Furthermore, no cultivar exhibits complete resistance to the disease, as disease can still develop depending on environmental conditions and the virulence of the pathogenic *Streptomyces* that are present in the soil (Braun et al., 2017; Clarke et al., 2019). Research into the virulence factors of plant pathogenic *Streptomyces* is therefore a valuable tool for both

improving the current management practices and for developing new and better strategies for disease management.

1.4 Known and Putative Virulence Factors in Pathogenic *Streptomyces*

The production of several virulence factors is what separates the plant pathogenic *Streptomyces* from related saprophytic species. Some known or putative virulence factors that have been identified thus far include thaxtomin A, Nec1, TomA, concanamycins, secreted phytohormones and *N*-coronafacoyl-L-isoleucine (CFA-Ile), expansin-like proteins, plant polymer degrading enzymes, PR-1 (pathogenesis-related) family proteins, borrelidin, demethylmensacarcin, fridamycin E and FD-891 (kamenko-byo toxin) (Bignell et al., 2010; Li et al., 2019). The following is a discussion of the known/putative virulence factors that have been characterized to date.

Thaxtomin A (Figure 1.2) is one of eleven thaxtomin analogs and is the most common analog produced by *S. scabiei* and other scab-causing *Streptomyces* species (King & Calhoun, 2009). Thaxtomins are cyclic dipeptides (2,5-diketopiperazines) that are only produced by plant pathogenic *Streptomyces* species and are synthesized via a gene cluster containing six biosynthesis genes and a regulatory gene (Bignell et al., 2014). Thaxtomin A-deficient mutants were shown to be avirulent towards potato, and the level of thaxtomin produced by a strain is positively correlated with the severity of the disease caused (Healy et al., 2000; King et al., 1991). As a result, thaxtomin A is considered the principal pathogenicity factor required for the development of scab symptoms by many pathogenic *Streptomyces* species. Under

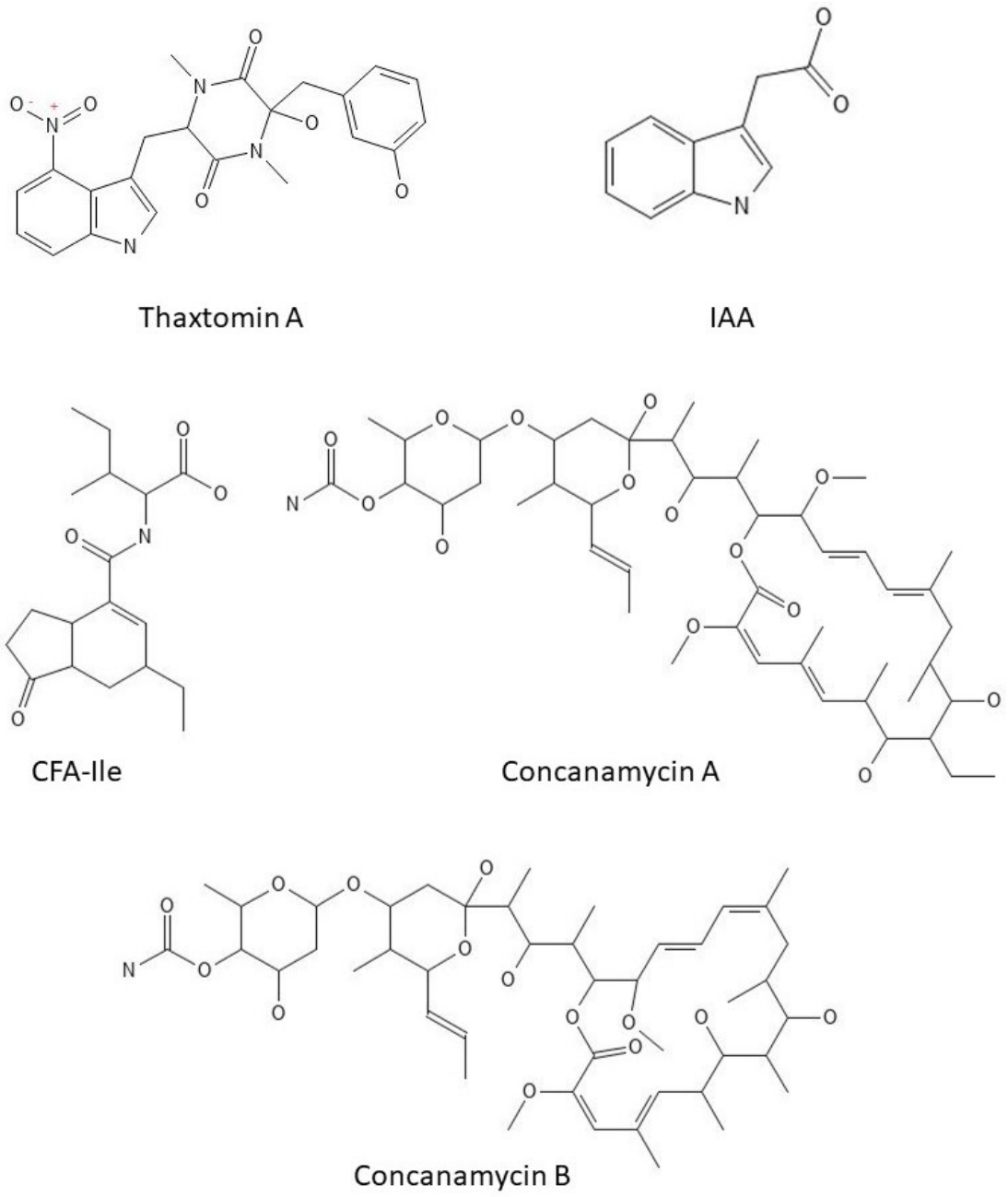

Figure 1.2: Structures of thaxtomin A, IAA, CFA-Ile, and concanamycin A/B. Structures were generated by PubChem Sketcher V2.4 from the canonical SMILES file available on PubChem.

laboratory conditions, thaxtomin A can induce necrosis of excised potato tuber tissue as well as cell hypertrophy, stunting, root swelling, and necrosis of both monocot and dicot seedlings. Further, treatment of potato mini-tubers with pure thaxtomin A leads to the development of scab-like lesions on the surface of the tubers (Li et al., 2019). Thaxtomin A is generally accepted to function as a cellulose biosynthesis inhibitor; however, the mechanism behind this activity remains a mystery (Li et al., 2019). Application of thaxtomin A to *A. thaliana* was shown to trigger a non- hypersensitive response form of programmed cell death (PCD) (Li et al., 2019). Upregulation of the plant defense-associated gene *PAL*, possibly as a response to lowered levels of cellulose in the cell, was shown to precede the PCD (Duval et al., 2005). Furthermore, a swift influx of Ca^{2+} into plant cells following treatment with thaxtomin A was linked to the induction of plant defense responses and the PCD observed (Errakhi et al., 2008).

Nec1 is a secreted protein produced by most pathogenic *Streptomyces* strains that causes necrosis of potato tuber tissue (Loria et al., 2006). It is secreted in early log phase when the *Streptomyces* are cultured on a rich medium (Joshi et al., 2007). This is in contrast to thaxtomin A, which is only produced in plant-based media such as oat bran agar, and is repressed by the addition of glucose (Babcock et al., 1993). The *nec1* gene was discovered during a screen to identify potential thaxtomin biosynthesis genes, and it was shown to confer the ability to induce tissue necrosis when transferred into the genomes of non-pathogenic *Streptomyces* species (Loria et al., 2006). The gene itself has a relatively low GC content compared to the high GC genomes of *Streptomyces* species (Joshi et al., 2007). It has therefore been hypothesized that this gene was acquired from a different unrelated taxon, though no homologues outside of the *Streptomyces* have been found to date (Joshi et al., 2007).

TomA is a secreted protein homologous to tomatinases that are found in fungal phytopathogens of tomato (Li et al., 2019). Tomatinase is part of the saponinase family of microbial effectors and is responsible for the degradation of the plant defense protein α-tomatine in tomato (*Solanum lycopersicum*) (Martin-Hernandez et al., 2000). Tomatinase was shown to be necessary for the infection of *Nicotiana benthamiana* by the fungal pathogen *Septoria lycopersici,* even though *N. benthamiana* is not known to produce α-tomatine, suggesting that it can inhibit broader disease resistance responses (Bouarab et al., 2002). Furthermore, tomatinase has been suggested as an important part of the early infection mechanism of *Fusarium oxysporum* f. sp. *lycopersici* in tomato (Pareja-Jaime et al., 2008). However, tomatinase null mutants of the bacterial pathogen *Clavibacter michiganensis* subsp. *michiganensis* and the fungal pathogen *Septoria lycopersici* did not show any attenuation in virulence (Kaup et al., 2005; Martin-Hernandez et al., 2000). Likewise in *S. scabiei,* a TomA deficient mutant did not show any reduction in virulence, and the potential role of TomA in suppression of plant defenses in potato still needs further investigation (Seipke & Loria, 2008).

Concanamycins are a family of polyketide macrolides that feature an 18-membered tetraenic macrolide ring incorporating a methyl enol ether and a b-hydroxyhemiacetal side chain (Haydock et al., 2005). Concanamycin A, B and C were found during a screen for immunologically active molecules in *Streptomyces diastastochromogenes* (Kinashi et al., 1984). They exhibit antimicrobial (excluding antibacterial) and antineoplastic activity via inhibition of V-ATPase (Haydock et al., 2005; Kinashi et al., 1984), and concanamycin A and B (Figure 1.2) have additionally been shown to act as phytotoxins (Natsume et al., 2005). Roots of rice (*Oryza sativa*), rapeseed (*Brassica napus*) and alfalfa (*Medicago sativa*) seedlings were all stunted following treatment with concanamycin A/B (Natsume et al., 2005; Natsume et al., 1996).

Production of concanamycin A/B by *S. scabiei* appears to have an effect on the type of lesion produced on the potato (Natsume et al., 2017). Sunken or deep pitted lesions were generated when potatoes were grown in pots containing *S. scabiei*, while raised scabs were produced on potatoes grown in the presence of *S. acidiscabies,* which does not produce concanamycin A/B (Natsume et al., 2017). Additionally, concanamycin A/B were more likely to be present in deep-pitted lesions from potatoes in the field (Natsume et al., 2017). Lastly, application of both concanamycin A and thaxtomin A onto potato tuber tissue produces a synergistic effect, increasing the level of necrosis (Natsume et al., 2017).

Although phytohormones are produced by beneficial plant-associated *Streptomyces* and are thought to contribute to the growth-promoting activity of these organisms, they are also implicated in the virulence of some plant pathogenic strains (Goudjal et al., 2013; Hsu, 2010). For example, many plant pathogens produce cytokinins and the auxin family molecule indole-3-acetic acid (IAA) (Figure 1.2) to modulate plant signalling systems, thereby allowing the pathogen to create a suitable environment for host colonization (Ma & Ma, 2016). Among the scab-causing pathogens, *S. turgidiscabies* is known to harbour a biosynthetic gene cluster that is predicted to produce one or more cytokinins (Kers et al., 2005). The gene cluster is expressed under the same conditions that promote thaxtomin production, a good indication that the resulting product(s) may contribute to the virulence of this pathogen (Joshi & Loria, 2007). Furthermore, culture supernatants of *S. turgidiscabies* were demonstrated to exhibit cytokinin bioactivity, indicating that the organism is capable of producing these molecules (Joshi & Loria, 2007). It is noteworthy that *S. turgidiscabies* produces particularly large and erumpent potato scab lesions when compared to other scab-causing pathogens, and no other scab pathogens are known to be able to produce cytokinins. As such, it has been hypothesized that cytokinin

production may account for the severe disease symptoms caused by *S. turgidiscabies* (Joshi & Loria, 2007). Genes related to the production of IAA have been found in *S. scabiei,* and deletion of these genes resulted in reduced necrosis on radish seedling roots (Hsu, 2010). However, unlike cytokinin production in *S. turgidiscabies,* the conditions that promote IAA production suppress the production of thaxtomin A, leading to reduced virulence (Legault et al., 2011). Therefore, the role of IAA in CS pathogenesis is still unclear.

CFA-Ile (Figure 1.2) is a member of the coronafacoyl phytotoxin group that includes the well-studied coronatine (COR) phytotoxin from the Gram-negative plant pathogen *Pseudomonas syringae* (Bignell et al., 2018). COR is associated with symptoms of leaf chlorosis, tissue hypertrophy, root stunting and changes in chloroplast structure, as well as the triggering of ethylene, anthocyanin and proteinase accumulation (Bignell et al., 2010; Li et al., 2019). Production of COR by *P. syringae* is triggered by the presence of plant cells or media derived from plant extracts (Bignell et al., 2018). Likewise, CFA-Ile production by *S. scabiei* is highest in plant-based media such as soy flour mannitol (SFM) (Fyans et al., 2015). CFA-Ile has been shown to facilitate the development of disease in the roots of tobacco seedlings and causes tissue hypertrophy when inoculated directly onto excised potato tuber tissue (Bignell et al., 2018; Cheng et al., 2019). The level of CFA-Ile produced by *S. scabiei* was positively correlated with the severity of tissue damage, suggesting that it plays a role in CS pathogenesis (Cheng et al., 2019). It has been suggested that CFA-Ile acts as a molecular mimic of the plant hormone jasmonoyl-L-Ile, which activates the plant defense response against herbivores and necrotrophic pathogens while suppressing the defense response against biotrophic pathogens (Li et al., 2019). Coronafacoyl phytotoxin biosynthetic gene clusters are not present in all pathogenic *Streptomyces* spp., and they can be found in non-pathogenic bacteria, including

Streptomyces spp., suggesting that these molecules may have functions other than as virulence factors (Bignell et al., 2018).

1.5 ADP-Ribosyltransferase Toxins: An Overview

ADP-ribosylation is a covalent modification performed by enzymes generally referred to as ADP-ribosyltransferases (ARTs) (Palazzo et al., 2017; Simon et al., 2014). ADP-ribosylation is almost ubiquitous throughout all domains of life, with examples of ADP-ribosyltransferase enzymes appearing in bacteria, eukaryotes, Archaea and even viruses (Palazzo et al., 2017; Simon et al., 2014). Even though ADP-ribosylation is quite common, the targets, the effects that the modification produces, and the structures of the enzymes are extremely diverse (Palazzo et al., 2017; Simon et al., 2014). The basic mechanism involves transferring an adenosine diphosphate ribose (ADP-ribose) moiety donated from nicotinamide adenine dinucleotide (NAD^+) onto a target molecule (Figure 1.3) (Palazzo et al., 2017). ARTs are able to add either one moiety to the target, or multiple moieties depending on the enzyme (Palazzo et al., 2017). This is referred to as mono-ADP-ribosylation and poly-ADP-ribosylation, respectively (Palazzo et al., 2017). Mono-ADP-ribosylation is most often used in bacterial pathogenesis, and thus the enzymes are often referred to as mono-ADP-ribosyltransferase (mART) toxins.

mARTs can be categorized into two major groups: Diphtheria-like toxins and Cholera-like toxins, based on the conserved catalytic motifs present in the active sites of the enzymes (Palazzo et al., 2017; Simon et al., 2014). Diphtheria toxin and Diphtheria-like toxins all share a histidine residue, two tyrosine residues, and a glutamate, otherwise known as the HYE motif,

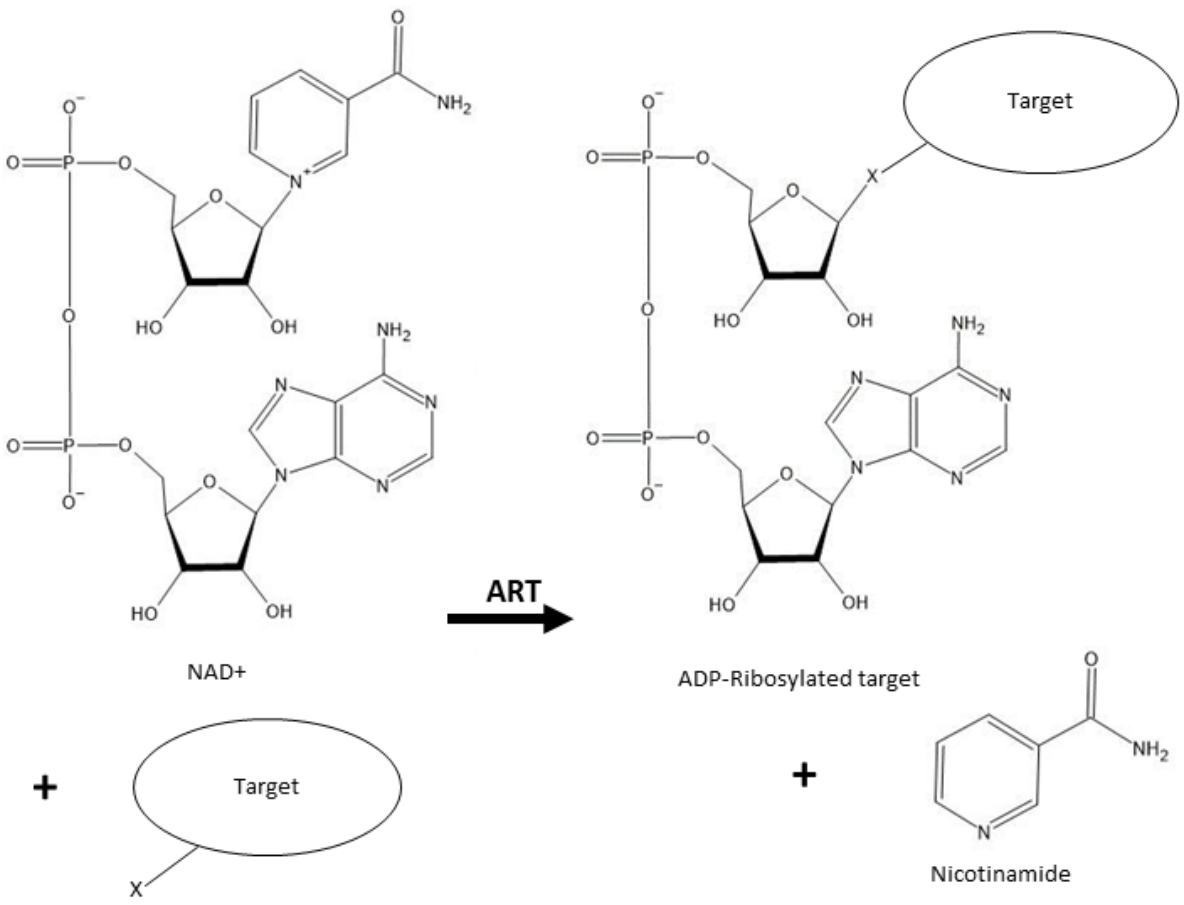

Figure 1.3: General mechanism of ADP-ribose moiety transfer performed by ARTs. Common targets for attachment include nitrogen, sulfur or oxygen (denoted by x).

in their active site (Simon et al., 2014). The active site of Cholera toxin and Cholera-like toxins consists of an arginine residue, serine- threonine- serine motif, and glutamine/glutamate-X-glutamine motif, collectively referred to as the RSE motif (Simon et al., 2014). Bacterial mART toxins containing the RSE motif can be further broken down into *Clostridium botulinum* C2-like and *Clostridium botulinum* C3-like toxins based on their target molecule and unique AB protein domain organizations (Simon et al., 2014).

The most common targets of ARTs are proteins, but some are able to attach ADP-ribose moieties to DNA and other small molecules (Lyons et al., 2016; Nakano et al., 2013; Palazzo et al., 2017). Well known eukaryotic proteins that are targets for bacterial toxins include eukaryotic elongation factor 2 (eEF2), G proteins and actin (Simon et al., 2014). Specific residues commonly used to accept the ADP-ribose moiety include arginine, asparagine, threonine, cysteine, glutamine and in some cases a modified histidine (Simon et al., 2014). In the rare instances where DNA is used as the target, the ADP-ribose moiety is usually attached to a guanosine residue (Jankevicius et al., 2016; Lyons et al., 2016; Nakano et al., 2013).

1.5.1 Diphtheria and Diphtheria-like Toxins

Diphtheria toxin (DT) is one of the most well studied bacterial toxins and is the prototypical ART toxin for the HYE group of enzymes (Holmes, 2000; Simon et al., 2014). DT is encoded by the *tox* gene located on a lysogenized corynephage within certain strains of *Corynebacterium diphtheriae* (Freeman, 1951; Holmes, 2000). The regulation of the *tox* gene has been traced to a iron-dependant repressor named DtxR (Schmitt & Holmes, 1991). The repressor senses the availability of iron in the environment and represses *tox* transcription when iron is present (Schmitt & Holmes, 1991). This allows DT to be expressed under low iron conditions, such as those found within the human body during infection (Skaar, 2010).

DT is translated as one single chain peptide proenzyme that will eventually be processed into two parts; Diptheria toxin-A (DT-A) and Diphtheria toxin B (DT-B) (Holmes, 2000; Simon et al., 2014). DT-A is located on the amino-terminal side of the peptide and possesses mART catalytic activity (Holmes, 2000). DT-B is composed of two domains: a translocation domain located in the center of the peptide, and receptor binding domain on the carboxy-terminal end (Holmes, 2000).

DT is extremely toxic, with a lethal dose of 1 ng/kg of body weight in humans (Holmes, 2000). The mechanism behind this toxicity begins with the production and release of DT during *C. diphtheriae* infection. The toxin spreads throughout the body and interacts with heparin-binding epidermal growth factor (HB-EGF), which is present on a wide variety of cells (Simon et al., 2014). The binding of HB-EGF triggers clathrin-mediated endocytosis, which brings the toxin into an early endosome (Holmes, 2000). The proenzyme is then nicked by a furin-like protease between the catalytic domain of DT-A and the translocation domain of DT-B, preparing the two for separation (Simon et al., 2014). Acidification of the endosome triggers insertion of the translocation domain into the membrane of the endosome (Holmes, 2000). The reduction of the remaining disulphate bridge between DT-A and DT-B results in the release of DT-A into the target cell cytosol (Simon et al., 2014). Once free in the cytosol, the catalytically active DT-A ADP-ribosylates eEF2 on a modified histidine residue (diphthamide), which is only found in eukaryotic and archaeal EF2 proteins (Simon et al., 2014). The addition of ADP-ribose to this modified histidine prevents eEF2 from interacting properly with the p-site of the ribosome (Simon et al., 2014). This leads to a halt in translation that eventually kills the host cell (Simon et al., 2014).

Pseudomonas aeruginosa exotoxin (PE) is another bacterial mART toxin in the HYE group (Simon et al., 2014). It is considered to be distantly related to DT, with just 18% amino acid sequence identity shared between the two, but both toxins contain a strongly conserved catalytic domain structure (Jørgensen et al., 2008; Simon et al., 2014). This trend of low sequence identity and high structural and functional similarity is common among ARTs (Feng et al., 2016; Jørgensen et al., 2008; Nakano et al., 2014; Szirák et al., 2012). As with DT, PE is

expressed as one polypeptide proenzyme with two parts, PE-A and PE-B, but in this case the catalytic domain is located on the carboxy-terminal end (Simon et al., 2014).

The first step in the mechanism of PE toxicity is binding of the toxin to low density lipoprotein receptor-related protein 1 (LRP1) (Simon et al., 2014). This triggers endocytosis via clathrin-coated pits (Simon et al., 2014). However unlike DT, PE continues past the endosome to the ER due to a KDEL sequence that marks it for retrograde trafficking (Simon et al., 2014). It is within the ER that the PE proenzyme gets cleaved by eukaryotic proteases and PE-A is able to separate from PE-B, cross the ER membrane and enter the target cell cytoplasm (Simon et al., 2014). Once released into the cytoplasm, PE targets eEF2 in the exact same way that DT does (Simon et al., 2014).

1.5.2 Cholera and Cholera-like Toxins

Cholera toxin (CT) is responsible for the rice-water stool associated with the disease cholera (Sánchez & Holmgren, 2008). The structure of CT is made up of 2 parts: the A subunit, which is subdivided into A1 (containing the catalytic domain) and A2, and the B subunit (Sánchez & Holmgren, 2008). The catalytic domain of CT is the prototypical representative for the RSE motif category of mARTs (Simon et al., 2014). The B subunit consists of a pentameric and extremely stable protein held together by hydrogen bonds and salt bridges (Sánchez & Holmgren, 2008). Unlike DT and PE, the A and B subunits of CT are encoded separately and associate in the bacterial periplasm just before leaving via a Type II secretion system (Sánchez & Holmgren, 2008).

The mechanism of CT activity begins with the B subunit attaching to its receptor, the ganglioside GM1 on the surface of intestinal epithelial cells (Simon et al., 2014). The resulting

endocytosis and subsequent pathway through the cell is not well characterized; however, it is suggested that the holoenzyme is subjected to retrograde trafficking through the ER, and the A subunit is released into the cytoplasm after interacting with the degradation system of the ER, similar to the path taken by PE (Sánchez & Holmgren, 2008; Simon et al., 2014). Once in the cytoplasm, CT-A attaches an ADP-ribose moiety to an arginine residue on the heterotrimeric G protein Gs, locking it in the GTP-bound state (Simon et al., 2014; Vogelsgesang et al., 2007). This causes the uncontrolled production of cAMP, which triggers the activation of chloride ion efflux pumps and the massive movement of chloride ions and water into the lumen of the intestines (Simon et al., 2014).

Pertussis toxin (PT) is another well studied example of bacterial ART toxins (Locht et al., 2011). It shares a similar AB5 domain organization with CT, with some slight modifications (Simon et al., 2014). The A subunit, denoted S1, has the ART catalytic domain containing the RSE motif characteristic of the cholera-like subgroup (Simon et al., 2014). The B subunit is made up of a heteropentamer consisting of two S4 chains and one S2, S3 and S5 (Locht et al., 2011). The subunits of PT are encoded by a polycistronic operon, which is activated when exposed to human body temperature (37 degrees Celsius) (Locht et al., 2011). Like with CT, the A and B subunits of PT do not associate with each other until they reach the bacterial periplasm (Locht et al., 2011). However, PT is then secreted via a dedicated Type IV secretion system called pt1 (Locht et al., 2011). Even though Type IV secretion systems usually transport bacterial effectors directly into the host cell, in the case of pt1, no cell to cell contact is needed, and PT is simply released into the extracellular space (Locht et al., 2011).

The specific receptor on the outer membrane of host cells is not known for PT, but it has been noted to interact with various glycoproteins on cell surfaces and is able to infect a wide

variety of cell types (Locht et al., 2011). The B subunit is responsible for binding of the toxin to the receptor and triggering endocytosis (Locht et al., 2011). The pathway taken by PT once inside the host cell is not fully elucidated, but it is thought to follow a retrograde path through the Golgi and ER (Locht et al., 2011). There is no obvious translocation domain in the B subunit, and so its unclear how release of the A subunit is facilitated, but the subunit does make its way into the cytoplasm (Locht et al., 2011).

The target of ADP ribosylation by PT is a cysteine residue on the heterotrimeric G protein Gi, as well as other G proteins found in a wide variety of cell types (Locht et al., 2011). This is distinct from the target of CT (Gs), and the mechanism of uncoupling is slightly different, yet as with CT, the end result is an uncontrolled accumulation of cAMP (Locht et al., 2011; Simon et al., 2014). This cAMP accumulation can trigger different responses depending on the cell type that is affected, such as histamine sensitization, islet activation and lymphocytosis (Locht et al., 2011).

1.5.3 C2 and C3 Toxins

C2 toxin from *Clostridium botulinum* is subcategorized as its own group of bacterial mART toxins within the Cholera-like toxins (Simon et al., 2014). This is due to the fact that although it shares the RSE motif that characterizes the Cholera-like toxins, the arrangement of the A and B domains is unique, and it has a unique ADP-ribosylation target within the host cell (Simon et al., 2014). C2 does not exhibit neurotoxicity as one would expect for a toxin produced by *C. botulinum* (Stiles et al., 2011). Instead, it has been shown to play a role in the development of hemorrhagic enteritis in birds (Stiles et al., 2011).

The C2 toxin is divided into 2 subunits, A and B, which are encoded by two separate genes located on a large plasmid in *C. botulinum* (Stiles et al., 2011). The two genes in the operon are transcribed in the same direction, with the A subunit gene located 247 nucleotides upstream from the B subunit gene (Stiles et al., 2011). The secretion of these products is unique in that they lack any type of secretion signal, and instead they are released after *C. botulinum* undergoes sporulation as the sporangium lyse (Stiles et al., 2011). The two components of C2 do not associate with one another to form the holotoxin until they meet at the host cell surface (Simon et al., 2014; Stiles et al., 2011). The receptor for the B domain on the host outer membrane is unknown, but once the holoenzyme is attached to the receptor, it is taken in by clathrin-coated pit-mediated endocytosis (Stiles et al., 2011). Subsequently, C2 is engulphed in an early endosome, where acidification of the vesicle triggers a conformation change in the B subunit (Stiles et al., 2011). The B subunit then inserts itself into the endosomal membrane similar to the entry mechanism of DT (Simon et al., 2014; Stiles et al., 2011). However, unlike DT, C2 is shown to exit the endosome unfolded with the help of chaperones HSP90 and cyclophilinA (Stiles et al., 2011). Once free in the cytoplasm, the molecular target of ADP-ribosylation is the monomer form of actin, globular actin (G-actin) (Simon et al., 2014; Stiles et al., 2011). The attachment of ADP-ribose to an arginine residue produces steric hinderance that prevents G-actin from interacting with and polymerizing into actin filaments (F-actin) (Stiles et al., 2011; Vogelsgesang et al., 2007). This leads to the collapse of the actin cytoskeleton (Stiles et al., 2011). Consequences of this include disruption of vesicle transport, disruption of intracellular signalling and inability to form epithelial barriers (Stiles et al., 2011). Without these processes, the cells die. This contributes to the formation of necrotic lesions and

accumulation of lethal amounts of fluid in the intestinal track, which is characteristic of avian hemorrhagic enteritis (Stiles et al., 2011).

The C3 toxin from *C. botulinum* is unusual among the bacterial mARTs. Instead of the typical A and B subunit organization, C3 consists of a single A subunit with no associated B subunit (Simon et al., 2014; Vogelsgesang et al., 2007). Due to this, the mechanism by which C3 and other A-only C3-like toxins enter the host cell to cause toxicity has not yet been fully elucidated (Fellermann et al., 2020; Vogelsgesang et al., 2007). Some suggestions for potential mechanisms of entry involve invasion of host cells by the entire bacterial cell, which then secretes the toxin into the host cytoplasm (Vogelsgesang et al., 2007). This entry method was shown to be utilized by the C3-like toxin C3stau2 from *Staphylococcus aureus* (Molinari et al., 2006). Alternatively, intermediate filament protein vimentin may play a role in uptake of C3 into some cell types or the concentration of C3 surrounding host cells may be so high that some nonspecific toxin uptake by the host cell is unavoidable (Fellermann et al., 2020; Vogelsgesang et al., 2007). Once inside, C3 ADP-ribosylates RHO proteins, which are a class of low molecular weight G proteins involved in the regulation of actin formation as well as a variety of other systems (Simon et al., 2014; Vogelsgesang et al., 2007). The ADP-ribosylation of an asparagine residue amplifies the affinity of RHO for RHO guanine nucleotide dissociation inhibitor (RhoGDI) (Simon et al., 2014). This sequesters RHO in the cytoplasm so it can no longer function in the regulation of actin polymerization, leading to destruction of the cytoskeleton and disruption of cell endothelial barriers, as well as hindering migration of immune cells and inhibition of phagocytosis in macrophages (Vogelsgesang et al., 2007).

1.5.4 Plant Pathogenic ADP-Ribosyltransferase Toxins

Despite the widespread use of mART toxins by human and animal pathogens, mART virulence effectors in plant pathogenic microbes are an emerging area of study, with only a handful of toxins characterized to date. One of the best studied plant pathogenic mART toxins is HopU1 from *Pseudomonas syringae* pv. *tomato* DC3000 (ptoDC3000) (Jeong et al., 2011). Homologues of HopU1 are present in the phytopathogens *P. syringae* pv. *maculicola, P. syringae* pv. *persicae, Pseudomonas viridiflava* and *Pseudomonas amygdali* pv. *lachrymans* (Hwang et al., 2005). It is similar to the C3 toxin in that it has a Cholera-type catalytic motif and no associated B domain (Jeong et al., 2011). However, unlike C3, the entry of HopU1 into host cells is achieved via injection directly into the host cytosol by the syringe-like Type-III secretion system (Fu et al., 2007). HopU1 was shown to suppress pathogen triggered immunity (PTI), allowing *P. syringae* to proliferate within the plant (Fu et al., 2007; Nicaise et al., 2013). The target of HopU1 is glycine rich RNA binding protein 7 (GRP7), which is modified by attachment of the ADP-ribose moiety to an arginine residue within the RNA binding domain of the protein (Nicaise et al., 2013). It is believed that attachment of the ADP-ribose interferes with the ability of GRP7 to bind and stabilize the mRNA transcripts for the pathogen associated molecular pattern (PAMP)-sensing proteins flagellin-sensing2 (FLS2), which recognizes bacterial flagellar protein, and EF-Tu receptor (EFR), which recognizes bacterial elongation factor-Tu (Nicaise et al., 2013). Reduced stabilization of these mRNAs result in decreased expression of FLS2 and ERF and a lower overall PTI response in the plant (Nicaise et al., 2013).

HopF2 is a second mART toxin produced by PtoDC3000 (Wang et al., 2010). In contrast to HopU1, HopF2 is a Diphtheria-like mART, but HopF2 is similar to HopU1 in that it

only contains an A domain and is injected into host cells via the same Type-III secretion system (Singer et al., 2004). HopF2 was shown to target *Arabidopsis* mitogen activated protein kinase kinase 5 (MKK5) as well as other MKKs (Wang et al., 2010). The ADP-ribose receiving amino acid on MKK5 is the Arg-313 on the C-terminal end of the protein (Wang et al., 2010). MKKs are upstream activators of PTI signalling cascade responses such as callose deposition, and ADP-ribosylation effectively shuts down this pathway (Wang et al., 2010). In addition to its PTI quelling abilities, HopF2 can target *At*RIN4 to prevent an effector triggered immunity (ETI) response to another ptoDC300 virulence factor, AvrRpt2 (Wilton et al., 2010). In some resistant plants, AvrRpt2 will cleave *At*RIN4, and this cleavage is detected by the plant protein RPS2, which triggers the hypersensitive response and leads to the death of the pathogen (Day et al., 2005; Kim et al., 2005). The cleavage of *At*RIN4 can be averted by HopF2-mediated ADP-ribosylation, thereby preventing the ETI pathway (Wang et al., 2010). Similar to HopF2, the putative mART toxin HopF1 from the bean pathogen *P. syringae* pv. *phaseolicola* can inhibit both PTI and ETI responses in bean (*Phaseolus vulgaris*) (Hou et al., 2011). HopF1 shares 48% amino acid sequence identity with HopF2 and has all of the required catalytic residues to be considered a mART (Hou et al., 2011). However, HopF1 has not been shown to ADP-ribosylate any substrates *in vitro,* and its exact target *in planta* is currently unknown (Hou et al., 2011; Wang et al., 2010).

AvrRPM1 is a Type-III secreted Diphtheria-like mART toxin produced by the cauliflower (*Brassica oleracea* var. *botrytis*) pathogen *P. syringae* pv. *maculicola* (Redditt et al., 2019). The target of AvrRPM1 is likely the Asp-153 residue in the nitrate induced (NOI) domain of RIN4. RIN4 is a negative regulator of plant PTI, and ADP-ribosylation of its NOI domain causes the protein to be locked in the active state (Chung et al., 2011; Redditt et al.,

2019), thereby allowing the bacteria to proliferate unchecked within the plant. Some plant varieties have developed resistance to this mechanism by employing the monitoring protein RPM1 (Grant et al., 2000). RPM1 can sense when RIN4 has been modified by AvrRPM1 and triggers a hypersensitive response (Grant et al., 2000). The specific ADP-ribosylation site on RIN4 used by AvrRPM1 is likely different than the site used by HopF2. This is because while the activity of AvrRMP1 can activate RPM1-mediated ETI in resistant plants, the activity of HopF2 does not. Furthermore, the end-goal behind ADP-ribosylation of RIN4 by these two effectors is different. AvrRPM1 targets RIN4 in order to supress PTI, while HopF2 targets RIN4 to stop RPS2-mediated ETI.

A third mART from the ptoDC3000 genome has recently been discovered and characterized. This mART, called HopO1-1, is secreted through the Type-III secretion system and is targeted to the plant plasmodesmata, which is the microscopic channels that connect the cytoplasm of adjacent plant cells (Aung et al., 2020). Here, HopO1-1 functions to increase intercellular trafficking of other pathogenicity effectors, allowing a greater area of the plant to be colonized by the pathogen (Aung et al., 2020). Although the ADP-ribosylation activity of HopO1-1 was found to be relatively weak *in vitro,* it is still considered essential as a catalytically inactive version of the enzyme could not produce the same increased trafficking effect (Aung et al., 2020). The targets of HopO1-1 are predicted to be PDLP5 and PDLP7 based on their interaction with HopO1-1 in a coimmunoprecipitation assay and bimolecular fluorescence complementation assay (Aung et al., 2020). PDLP5 is involved in mediating PTI-triggered callose deposition in the plasmodesmata and is therefore a biologically relevant target for HopO1-1 (Aung et al., 2020; Lee et al., 2011). However, their interaction *in planta* has yet to be demonstrated.

1.6 Scabin: A Novel Mono-ADP-Ribosyltransferase in *S. scabiei*

Recently, a gene encoding a mART was found in the genome of *S. scabiei* (Lyons et al., 2016). Scabin was identified as a 22 kDa single domain Cholera-like mART with an attached N-terminal secretion signal (Lyons et al., 2016). While the vast majority of mART toxins target proteins for ADP-ribosylation, Scabin attaches an ADP-ribose moiety to the exocyclic NH_2 of guanosine residues in DNA, RNA, and smaller molecules such as cyclic guanosine 3',5'-monophosphate (cGMP) and guanosine diphosphate (GDP) *in vitro* (Vatta et al., 2021). However, the *in vivo* target of Scabin has yet to be elucidated. Strikingly, Scabin shows higher activity towards potato DNA compared to bacterial DNA, and this is promising evidence that it may function as a virulence factor for *S. scabiei* (Lyons et al., 2016).

Outside of the *Streptomyces* genus, Scabin is most closely related to the Pierisin toxin from the white cabbage butterfly (*Pieris rapae),* sharing about 40% amino acid sequence identity (Lyons et al., 2016). Pierisin induces apoptosis in mammalian cell lines *in vitro,* but it is unclear what the biological role the toxin plays *in vivo* (Nakano et al., 2014). It has been suggested that Pierisin could be a protective agent against bacterial invasion and/or parasitization by wasps (Nakano et al., 2014), This prediction is supported by the finding that Pierisin is upregulated during parasite entry and shows lethality towards parasitic wasp eggs and larvae (Nakano et al., 2014). Another suggested role for Pierisin is in the apoptosis-induced removal of certain tissues during the remodeling of metamorphosis (Nakano et al., 2014). This is supported by the marked upregulation of Pierisin during stages of metamorphosis followed by its gradual downregulation once metamorphosis is complete (Nakano et al., 2014).

Unlike Scabin, Pierisin possesses a known toxin B subunit consisting of ricin-like domains attached to the C-terminal end of the toxin (Carpusca et al., 2006). It is currently

unknown how Scabin would enter a target plant cell once secreted. It has been suggested that a nearby gene, *SCAB_27781*, could potentially encode the associated B subunit (Lyons et al., 2016), or that Scabin is an A-domain only toxin like C3, HopU1, HopF1, HopO1-1 and AvrRPM1.

Another mART that has been characterised within the genus *Streptomyces* is ScARP from the non-pathogenic species *Streptomyces coelicolor*. ScARP shares 76% amino acid identity with Scabin, and was originally thought to target endogenous proteins as a way to control morphological differentiation (Szirák et al., 2012). The ADP-ribosylation profile of a ScARP disruption mutant showed slightly less ADP-ribose modified proteins compared to wild type and the complement strain (Szirák et al., 2012). Strengthening this idea, the ScARP disruption mutant had reduced sporulation on certain media compared to the wild type, and production of the antibiotic actinorhodin was affected (Szirák et al., 2012). However, it was later discovered that ScARP targets guanosine-containing molecules similar to the activity of Scabin (Nakano et al., 2013). Despite sharing guanosine as a common target, the binding pocket of ScARP, Scabin and Pierisin are slightly different, resulting in slight substrate preference changes. Pierisin has a large basic area and strongly binds double stranded DNA (dsDNA) but not single stranded DNA (ssDNA) or mononucleotides (Oda et al., 2017). Scabin has a smaller basic region compared to Pierisin and can bind dsDNA, ssDNA and guanosine containing mononucleotides (Vatta et al., 2021; Yoshida & Tsuge, 2018). However, Scabin shows a preference for DNA as a substrate compared to mononucleotides (Vatta et al., 2021). ScARP, on the other hand, has no discernable basic region and shows a strong preference for mononucleotides compared to DNA (Nakano et al., 2013).

1.7 Research Objectives

Scabin has the potential to be a novel virulence factor for *S. scabiei,* since mART toxins are important for the virulence phenotype of other bacterial pathogens, including phytopathogens. While the *in vitro* characteristics of Scabin have been extensively studied, the *in vivo* role of Scabin has yet to be described. Therefore, the objectives of this study were to investigate the contribution of Scabin to the pathogenic phenotype of *S. scabiei*, and to determine whether SCAB_27781, the suggested toxin B domain, is functionally linked to Scabin. Homology searches for Scabin and SCAB_27781-like proteins in other *Streptomyces* species were conducted in order to examine their distribution among pathogenic and non-pathogenic species. To help elucidate potential roles and to identify regions of interest in both Scabin and SCAB_27781, the amino acid sequences were examined using several protein feature prediction software programs such as SignalP 5.0, HHpred and pfam. The expression of both the *scabin* and *SCAB_27781* genes and their possible co-transcription was assessed using semi-quantitative RT-PCR. Finally, a *scabin* gene deletion mutant was created in *S. scabiei* 87-22. This mutant was evaluated for changes in virulence using a potato tuber slice bioassay, a radish seedling bioassay and a *Nicotiana benthamiana* leaf infiltration assay. The morphology of the mutant compared to the wild type was investigated by culturing the strains on different agar media.

CHAPTER 2: MATERIALS AND METHODS

2.1 Bacterial Strains and Plasmids

Bacterial strains and plasmids used in this study are listed in Table 2.1.

Table 2.1: Bacterial Strains and Plasmids Used in this Study

Bacterial strain or Plasmid	**Description**	**Antibiotic resistance**	**Reference or source**
***Escherichia coli* strains**			
DH5α	General cloning host	none	Gibco-BRL
Top10	General cloning host	none	Invitrogen
ET12567/pUZ8002	Non-methylating conjugation strain	Kanamycin, Chloramphenicol, Tetracycline	(Kieser et al., 2000; MacNeil et al., 1992)
BW25113/pIJ790	Host for REDIRECT PCR targeting system	Chloramphenicol	(Gust et al., 2003)
***Streptomyces scabiei* strains**			
87-22	Wild-type strain	none	(R. Loria et al., 1995)
scabin KO	87-22 derivative in which the s*cabin* gene (*SCAB_27771*) is replaced with a [ApraR+*oriT*] cassette	Apramycin	This study

Bacterial strain or Plasmid	**Description**	**Antibiotic resistance**	**Reference or source**
87-22/pDBHP1	*scabin* overexpression strain derived from 87-22; contains the pDBHP1 plasmid integrated into the ΦC31 *attB* site	Apramycin	(Perry, 2019)
87-22/pIJ8641	Vector control strain derived from 87-22; contains the pIJ8641 plasmid integrated into the ΦC31 *attB* site	Apramycin	(Perry, 2019)
Plasmids			
pIJ773	Template for amplification of the [ApraR+*oriT*] cassette	Apramycin	(Gust et al., 2003)
pCR4-TOPO	Cloning vector for PCR products	Kanamycin, Ampicillin	Invitrogen
pIJ8641	*Streptomyces* integrative plasmid harbouring the *egfp* gene downstream of the *ermE*p* promoter	Apramycin	J. Sun, unpublished
pDBHP1	pIJ8641 derivative in which the *egfp* gene was replaced with the *scabin*	Apramycin	(Perry, 2019)

Bacterial strain or Plasmid	Description	Antibiotic resistance	Reference or source
	(*SCAB_27771*) coding sequence		
pDBHP3	*scabin* deletion plasmid; contains the [ApraR+*oriT*] cassette flanked a 1.1 kb and 1.5 kb fragment of *S. scabiei* genomic DNA in pCR4-TOPO	Apramycin, Kanamycin, Ampicillin	This study

2.2 General DNA Methods

2.2.1 Oligonucleotide Primers

Oligonucleotide primers used in this study are listed in Table 2.2. Primers were purchased from Integrated DNA Technologies (USA) and purified by standard desalting.

Table 2.2: Primers Used in this Study

Primer	**Sequence (5′ → 3′)***	**Use**
HP5	TCAGTGCCAGGGCTCGTAGTGC GGGTTGCCCACGCACTC TGTAGGCTGGAGCTGCTTC	PCR amplification of [ApraR+*oriT*] for deletion of *SCAB_27771* (*scabin* gene) using Redirect PCR targeting – reverse primer
HP6	GTGCGGCGCCGGGCCGCCGCC GTCGTCCTGTCCCTCTCC ATTCCGGGGATCCGTCGACC	PCR amplification of [ApraR+*oriT*] for deletion of *SCAB_27771* (*scabin* gene) using Redirect PCR targeting – forward primer
HP9	TCGAACGACAGGAGCTTGTC	PCR amplification of the *SCAB_27771/SCAB_27781* locus – forward primer
HP10	CTGGTTCGAGATGAGGGTCG	PCR amplification of *SCAB_27771/SCAB_27781* locus – reverse primer
HP11	GGGCAGTACGACATCGAGAG	RT-PCR analysis of *SCAB_27771* (*scabin* gene) – forward primer
HP12	GTAGCCGGACTTGTACCAGG	RT-PCR analysis of *SCAB_27771* (*scabin* gene) – reverse primer
HP13	CGAGGATGAAGGTGATCGGG	RT-PCR analysis of *SCAB_27781* – forward primer
HP14	ATGTCGGCGATGTAGAACCG	RT-PCR analysis of *SCAB_27781* – reverse primer
HP15	TCGTCGAACCGGGGACAG	RT-PCR analysis for detecting *SCAB_27771/SCAB_27781* co-transcription – forward primer
HP16	GCAGGACGTGAAGATCTCCC	RT-PCR analysis for detecting *SCAB_27771/SCAB_27781* co-transcription – reverse primer
ApraR for	TCGATGGGCAGGTACTTCTC	PCR detection of *aac(3)IV* (apramycin resistance gene) – forward primer

Primer	Sequence (5′ → 3′)*	Use
ApraR rev	ACCGACTGGACCTTCCTTCT	PCR detection of *aac(3)IV* (apramycin resistance gene) – reverse primer
DRB23	GGACATCCAGACGTACA	RT-PCR analysis of g*yrA* – forward primer
DRB24	CTCGGTGAGCTTCTCCT	RT-PCR analysis of g*yrA* – reverse primer

* Non homologous extensions are underlined

2.2.2 Polymerase Chain Reaction (PCR) Conditions

For construction of the *scabin* deletion plasmid (Section 2.4.4), a 3.2 kb region from the *S. scabiei* chromosome was amplified using Phusion high fidelity DNA polymerase (New England Biolabs, Canada) following the manufacturer's protocol with the adjustments shown in Table 2.3 below. Amplification of the [ApraR+*oriT*] cassette from pIJ773 (Section 2.4.4), as well as PCRs used for the verification of mutants and plasmid inserts were performed using *Taq* DNA polymerase (New England Biolabs, Canada) following manufacturer's guidelines with the adjustments shown in Tables 2.4 and 2.5 below.

Table 2.3: PCR Protocol using Phusion DNA Polymerase

Reaction component	**Volume or amount**	**Final concentration**
5× Phusion GC Buffer (containing $MgCl_2$)	4 µL	1×
dNTPs (10 mM each)	0.4 µL	200 µM
Forward primer (10 pmol/µL)	1 µL	0.5 pmol/µL
Reverse primer (10 pmol/µL)	1 µL	0.5 pmol/µL
DMSO (100% v/v)	1 µL	5% v/v
DNA template	70 ng	3.5 ng/µL
Phusion DNA polymerase (2U/µL)	0.2 µL	0.02 U/µL
Water	To 20 µL final volume	

Thermal cycling conditions:

Initial denaturing 98°C for 2 minutes

Followed by 30 cycles of:

- Denaturing at 98°C for 10 seconds
- Annealing at 71.2°C for 20 seconds
- Extension at 72°C for 1.5 minutes

Final extension at 72°C for 5 minutes

Table 2.4: Amplification of the [ApraR+*oriT*] Cassette using *Taq* DNA Polymerase

Reaction component	**Volume or amount**	**Final concentration**
10× Standard *Taq* buffer	5 µL	1×
dNTPs (10 mM each)	1 µL	200 µM
Forward primer (10 pmol/µL)	1 µL	0.5 pmol/µL
Reverse primer (10 pmol/µL)	1 µL	0.5 pmol/µL
DMSO (100% v/v)	2.5 µL	5% v/v
DNA template	200 ng	4 ng/µL
Taq DNA Polymerase (5U/µL)	0.25 µL	0.0625 U/µL
Water	To 50 µL final volume	

Thermal cycling conditions:

Initial denaturing 95°C

Followed by 10 cycles of:

- Denaturing at 95°C for 45 seconds
- Annealing at 50°C for 45 seconds
- Extension at 68°C for 1.5 minutes

Then 15 cycles of:

- Denaturing at 95°C for 45 seconds
- Annealing at 55°C for 45 seconds
- Extension at 68°C for 1.5min

Final extension at 68°C for 5 minutes

Table 2.5: Typical PCR Protocol for Verification of Mutant Strains and Plasmids using *Taq* DNA Polymerase

Reaction component	**Volume or amount**	**Final concentration**
10× Standard *Taq* buffer	2 µL	1×
dNTPs (10 mM each)	0.4 µL	200 µM
Forward primer (10 pmol/µL)	1 µL	0.5 pmol/µL
Reverse primer (10 pmol/µL)	1 µL	0.5 pmol/µL
DMSO (100% v/v)	1 µL	5% v/v
DNA template	30 to 400 ng	1.5 to 20 ng/µL
Taq DNA Polymerase (5U/µL)	0.125 µL	0.03125 U/µL
Water	To 20 µL final volume	

Thermal cycling conditions:

Initial denaturing 95°C for 2 minutes

Followed by 30 cycles of:

Denaturing at 95°C for 10 seconds

Annealing at 58°C (ApraR for/ApraR rev) or 60°C (HP11/HP12) for 30 seconds

Extension at 68°C for 15 seconds

Final extension at 68°C for 5 minutes

2.2.3 Gel Electrophoresis

DNA was analyzed by electrophoresis on a 1% w/v agarose gel at 100 V in 1× TBE buffer (pH = 8.3) for 1 to 1.5 hours. Samples were first mixed with loading dye (New England Biolabs, Canada) to a final concentration of 1× before loading onto the gel. A 1 kb DNA ladder (FroggaBio, Canada) or 100 bp DNA ladder (Fermentas, Canada) was used depending on the size of the expected band. Gels were either pre-stained by adding GelRed® (Biotinum, USA) to

a final concentration of 1× to the molten gel before casting, or stained after electrophoresis by soaking in ethidium bromide (2.0 µg/mL in 1× TBE buffer) for 25 minutes followed by soaking in 1× TBE buffer to de-stain for 12 minutes. Gels were imaged by exposure to UV light followed by photographing using a Chemi-Imager Gel Documentation System with a Fluorchem HD2 upgrade (Alpha Innotech, USA) when stained with ethidium bromide, or a GelDoc38It®TS2 310 Imager (UVP Analytik Jena, USA) when stained with GelRed®.

2.2.4 Gel Extraction

DNA fragments were extracted from the agarose gel after electrophoresis (Section 2.2.3) by first exposing the gel to UV light and quickly excising the band of interest using a scalpel. The piece of gel was then placed into a 1.5 mL pre-weighed microcentrifuge tube, and either the Wizard SV Gel and PCR Clean-Up kit (Bio Basic Inc., Canada) or the T1020S Monarch® Gel Extraction Kit (New England Biolabs, Canada) was used to extract the DNA from the gel following the manufacturer's protocol.

2.2.5 Digestion of DNA

Restriction digestion was performed to confirm the successful cloning of the *scabin* gene and flanking sequences into the pCR4-TOPO vector (Section 2.4.4). The digestion was conducted in a 10 µL volume using the EcoRI-HF restriction enzyme (New England Biolabs, Canada) as per the manufacturer's protocol. The reaction was incubated at 37°C for 1 hour before being analyzed by agarose gel electrophoresis (Section 2.2.3).

2.2.6 Nucleic Acid Quantification and Sequencing

Quantification of DNA and RNA samples was performed using a P300 Nanophotometer (Implen Inc., USA) as per manufacturers instructions. Samples were sent for sequencing to The Centre for Applied Genomics (TCAG) in Toronto, Canada. Samples were first prepared for sequencing following the guidelines found on the center for applied genomics website: http://www.tcag.ca/facilities/dnaSequencingSynthesis.html#3.

2.3 General *E. coli* Culturing, Storage, and Manipulation

2.3.1 Growth and Storage Conditions

E. coli strains were routinely cultured at 37°C unless otherwise stated. Liquid cultures were typically grown with shaking (180 to 200 rpm) in Luria-Bertani (LB) broth (Fisher Scientific, Canada), super optimal broth (SOB) (Inoue et al., 1990) or super optimal broth with catabolite repression (SOC) (Sun et al., 2009), while LB containing 1.5% w/v agar was used for solid plate cultures. The antibiotics apramycin (50 µg/mL final concentration; Goldbio, USA), ampicillin (100 µg/mL final concentration; Sigma-Aldrich, Canada), kanamycin (50 µg/mL final concentration; Sigma-Aldrich, Canada) and/or chloramphenicol (25 µg/mL final concentration; Sigma-Aldrich, Canada) were included in the culture media when required.

Glycerol stocks of *E. coli* strains were prepared by mixing 500 µL of a dense *E. coli* liquid culture with 500 µL of 40% v/v sterile glycerol. The resulting 20% v/v glycerol stock was stored for long term at -80°C. For short term storage, a streak plate or spread plate showing single colonies was kept at 4°C.

2.3.2 Preparation of Chemically Competent *E. coli* Cells

Chemically competent cells of *E. coli* Top10 (Table 2.1) were purchased from Invitrogen Canada, Inc., while competent cells of *E. coli* DH5α and ET12567/pUZ8002 were prepared following a previously described protocol (Inoue et al., 1990) with some slight alterations as follows. The *E. coli* cells were cultured overnight in 3 mL of LB broth. Five hundred microlitres were then sub-cultured into 50 mL of SOB broth, and the cells were incubated with shaking until an OD_{600} of 0.5 was reached. Next, the cells were chilled on ice for approximately 10 minutes and were then pelleted at 1789 × *g* for 10 minutes at 4°C. The pellet was resuspended in 20 mL of freshly prepared ice cold TB buffer (Inoue et al., 1990), and the suspension was left to sit on ice for 10 minutes. The cells were pelleted again at 1789 × *g* for 10 minutes at 4°C, and the pellet was resuspended in 1.25 mL of TB buffer containing 7% v/v DMSO. The cell mixture was then aliquoted into 100 µL volumes in microcentrifuge tubes, and the tubes were flash frozen in a dry ice/ethanol bath and were stored at -80°C.

2.3.3 Transformation of DNA into Chemically Competent *E. coli*

Transformations were conducted following a previously described protocol (Inoue et al., 1990) with some slight changes. A tube of competent cells was thawed on ice for 10 minutes before the addition of 10 µL of plasmid DNA or ligation mixture. After mixing gently via pipetting up and down, the cells were incubated on ice for 30 minutes. Then, the cells were heat shocked at 42°C for 45 seconds, after which they were immediately placed on ice and left for 10 minutes. SOC medium (1 mL) was added, and the cells were incubated with shaking for 1 hour. Finally, the cells were spread plated onto LB agar containing the appropriate antibiotics, and the plates were incubated for 24 hours.

2.3.4 Preparation of Electrocompetent *E. coli* Cells

Electrocompetent cells of *E. coli* BW25113/pIJ790 were prepared following a previously described protocol (Gust et al., 2003) with the following minor changes. The *E. coli* cells were inoculated into 5 mL of LB broth with appropriate antibiotics and were incubated overnight at 28°C with shaking. Then, 500 µL of the overnight culture was sub-cultured into 50 mL of SOC broth containing the appropriate antibiotics and 500 µL of 1M L-arabinose (final concentration 10 mM) when required (see Section 2.4.4). The culture was incubated with shaking at 28°C until an OD_{600} of 0.6 was reached. Next, the cells were pelleted by centrifugation at 1789 × *g* for 5 minutes at 4°C, after which they were resuspended in 50 mL of ice-cold sterile 10% v/v glycerol. The cells were pelleted again as before, and were resuspended in 25 mL of ice-cold sterile 10% v/v glycerol. Finally, the cells were pelleted as above, and the pellet was resuspended in the remaining ~100 µL of glycerol. The cell suspension was then used immediately for electroporation.

2.3.5 Transformation of DNA into Electrocompetent *E. coli*

A 50 µL aliquot of freshly prepared electrocompetent *E. coli* cells was mixed with 100 ng (1 to 2 µL) of DNA in a pre-chilled electroporation cuvette (1 mm gap, VWR International, Canada) Electroporation was carried out using a Gene Pulser Xcell (Bio-Rad, Canada) with the following settings: 200 Ω, 25 µF, and 1.4 kV. Afterwards, the cells were immediately transferred into 1 mL of ice-cold SOC and were incubated with shaking at 28°C for one hour. One hundred microliters of the cells were spread onto LB agar plates containing the appropriate antibiotics, and the plates were incubated overnight at 28°C if the pIJ790 plasmid was still required for downstream manipulations, or at 37°C to induce the loss of the pIJ790 plasmid (see Section 2.4.4).

2.3.6 Purification of Plasmid DNA from *E. coli*

E. coli cultures were grown overnight with shaking in 5 mL of LB broth. Plasmid DNA was extracted from the overnight cultures using the EZ-10 Spin Column Plasmid DNA kit BS614-250Preps (Bio Basic Inc., Canada) following the manufacturer's protocol.

2.4 General *Streptomyces* Culturing, Storage, and Manipulation

2.4.1 Growth and Storage Conditions

S. scabiei strains were routinely cultured at 28°C unless otherwise stated. Liquid cultures were grown with shaking (125 to 200 rpm) in trypticase soy broth (TSB; BD Biosciences, Canada) or oat bran broth (OBB) (Johnson et al., 2007), while potato mash agar (PMA) (Fyans et al., 2015), International *Streptomyces* Project Medium 4 (ISP-4; Himedia Laboratories LLC, USA), minimal medium with glucose (MMG; (Kieser et al., 2000)) nutrient agar (NA; BD Biosciences, Canada), soy flour mannitol (SFM) agar (Kieser et al., 2000), oat bran agar (OBA) (Johnson et al., 2007) and trypticase soy agar (TSA; BD Biosciences, Canada) were used for solid plate cultures. Where necessary, the antibiotics nalidixic acid (50 µg/mL final concentration; Sigma-Aldrich, Canada), apramycin (50 µg/mL final concentration), and/or kanamycin (50 µg/mL final concentration) were added to the media.

Strains were stored as spore stocks in 20% v/v glycerol at either -20°C for short term storage or -80°C for long term storage. To prepare quantified spore stocks, 3 mL of a 0.01% v/v Tween-20 solution in water was added to a well-sporulated plate of *S. scabiei*. The spores were aseptically scraped into the Tween-20 solution, and the suspension was transferred into a sterile 15 mL conical tube. Next, the suspension was sonicated for 5 minutes in a sonication bath to help separate the spores from the mycelia, and then it was filtered through sterile non-absorbent

cotton in order to remove the mycelial fragments. The collected spores were pelleted via centrifugation at 1789 × *g* for 10 minutes at room temperature, and the supernatant was discarded. The spores were washed with sterile water to remove the Tween-20, and following centrifugation, the pellet were resuspended in 100 to 1000 µL of sterile 20% v/v glycerol to give a dense suspension. An aliquot of the spore stock was serially diluted in sterile water, and different dilutions were plated onto NA in duplicate to determine the CFU/mL of spores in the stock using the standard plate count method.

To prepare a *S. scabiei* spore stock for storage purposes only (not quantified), the spores were aseptically scraped from a well-sporulated plate into a sterile 1.5 mL microcentrifuge tube, and 500 µL of sterile 20% v/v glycerol was added. The tube was then vortexed to create a suspension.

2.4.2 Conjugation with *E. coli*

Plasmids were introduced into *S. scabiei* via conjugation with *E. coli* as described before (Kieser et al., 2000) with the following minor changes. *S. scabiei* was cultured on a PMA plate until well sporulated (4 to 7 days). *E. coli* ET12567/pUZ8002 that had been previously transformed with the plasmid of interest (see Section 2.3.3) was grown overnight in 5 mL of LB broth with chloramphenicol, kanamycin and apramycin. Five hundred microliters of the overnight *E. coli* culture were subcultured into 50 mL of LB with antibiotics, and the cells were grown to an OD_{600} of 0.5. The culture was then centrifuged at 2264 × *g* for 10 minutes to pellet the cells, and the supernatant was discarded. The *E. coli* cells were resuspended in fresh LB broth to remove any remaining antibiotics, and following a second round of centrifugation, the cells were resuspended in 250 µL of LB broth. *S. scabiei* spores were aseptically scraped from ¼ to ½ of the PMA plate, and the spores were added to the *E. coli* cell suspension. The mixture

was then vortexed briefly, and the suspension was spread onto plates of SFM agar medium containing 10 mM $MgCl_2$. The plates were incubated at 28°C for 24 hours, after which they were overlayed with 1 mL of an aqueous solution containing apramycin and nalidixic acid, with the final concentration of each being 50 μg/mL in the agar medium. The plates were then returned to 28°C and were incubated until colonies arose.

2.4.3 *Streptomyces* Genomic DNA Extraction

S. scabiei was cultured in 10 mL of TSB with shaking in 50 mL spring flasks until the culture was dense (2 to 4 days). One milliliter of culture was transferred to a 3 mL bead beater tube filled with just enough silica beads (400 μm; OPS Diagnostics, USA) to cover the bottom of the tube. The tubes were then centrifuged at 1743 × *g* for 10 minutes, and the supernatant removed with a pipette. This was repeated 3 to 5 times until a significant amount of cells were collected at the bottom of the tube. The cells and beads were then resuspended in 200 μL of buffer AL and 200 μL of buffer ATL from the QIAamp DNA Mini Kit (Qiagen Inc., Canada). The cells were lysed using a SpeedMill PLUS tissue homogenizer (Analytik Jena, USA) set to "bacteria". Following lysis, the cells were centrifuged at 8609 × *g* for 5 minutes, and the supernatant was transferred to a clean 1.5 mL microcentrifuge tube. Then, 200 μL of 95% ethanol was added to the supernatant, and the mixture was vortexed. The mixture was added to a spin column from the QIAamp DNA Mini Kit, and the column was centrifuged at 5510 × *g* for 1 minute. The flow-through was discarded, and 500 μL of buffer AW2 from the QIAamp DNA Mini Kit was added to the column. The column was centrifuged again at 16,873 × *g* for 3 minutes, followed by another spin for 1 minute to dry the column. The column was transferred to a clean 1.5 mL microcentrifuge tube, and 50 μL of water was added to the column filter.

Following a 2 to 5 minute incubation at room temperature, the column was centrifuged at 8609 × *g* for 1 minute to collect the eluted DNA.

2.4.4 Creation of the *scabin* Gene Deletion Mutant

The *scabin* deletion mutant (*scabin* KO) was created using the Redirect PCR targeting system (Gust et al., 2003). To begin, A 3,200 bp fragment of *S. scabiei* genomic DNA containing the gene of interest and flanking sequences (approximately 1,100 bp and 1,500 bp on each side) was PCR-amplified using the conditions outlined in Table 2.3 and the custom designed primers HP9 and HP10 (Table 2.2). The resulting PCR product was A-tailed as outlined in the TOPO TA cloning kit (Invitrogen) protocol before ligation into the pCR4-TOPO vector following manufacturer's instructions. The presence of the correct insert in the pCR4-TOPO vector was verified by restriction digestion (Section 2.2.5) and DNA sequencing (Section 2.2.6). Next, the TOPO vector + insert was electroporated into *E. coli* BW25113/pIJ790 following the protocol described in Section 2.3.5. PCR primers (HP5 and HP6 in Table 2.2) were designed with 39 nt extensions that are homologous to the ends of the *scabin* gene, and 19 or 20 nt of sequence matching the ends of the [ApraR+*oriT*] cassette in pIJ773. The [ApraR+*oriT*] cassette was PCR-amplified using primers HP5 and HP6 following the conditions outlined in Table 2.4, and the cassette was gel extracted and purified (see Section 2.2.4) before being electroporated into the *E. coli* BW25113/pIJ790 strain containing the created TOPO vector + insert (Section 2.3.5). During this second electroporation, arabinose was added to the *E. coli* culture to induce the expression of the lambda Red genes located on pIJ790. The resulting proteins were required to promote recombination of the [ApraR+*oriT*] cassette with the TOPO plasmid, leading to replacement of the *scabin* gene with the cassette. Following this

electroporation, the cells were incubated at 37°C to promote the loss of pIJ790, thereby preventing further recombination.

Plasmid DNA was extracted (Section 2.3.6) from the *E. coli* colonies that arose, and the DNA was tested for the presence of the [ApraR+*oriT*] cassette via PCR using the ApraR for and ApraR rev primers (PCR conditions were as shown in Table 2.5) followed by sequencing (Section 2.2.6). The confirmed mutant plasmid (pDBHP3; see Table 2.1) was then introduced into wild-type *S. scabiei* 87-22 via conjugation (Section 2.4.2). Apramycin resistance exconjugants that arose were patched onto NA plates containing kanamycin to screen for kanamycin sensitivity. Successful double cross-over mutants were expected to be apramycin resistant and kanamycin sensitive. Exconjugants with this phenotype were streaked for single colonies onto ISP-4 with the nalidixic acid and apramycin. Spores from a single isolated colony were used to inoculate an entire PMA plate, and following growth and sporulation of the organism, a glycerol stock was prepared as described in Section 2.4.1.

2.5 General RNA Methods

2.5.1 Growth and Sampling

To grow wild-type *S. scabiei* for RNA sampling, sterile cellophane disks (7.5cm diameter) were placed onto the surface of 12 SFM, 12 TSA and 12 OBA plates. Then, 10^6 spores from a quantified spore stock (Section 2.4.1) in 50 µL of sterile water was spread over the entire surface of the cellophane disk on each plate. The plates were incubated for 24, 48 and 72 hours, after which the mycelia were scraped from 1 to 5 plates of each medium using a small sterile spatula. The cell material (80 to 200 mg) was transferred into 2 mL microcentrifuge tubes

containing beads and was immediately flash frozen using a dry ice/ethanol bath. The samples were then stored at -80°C until the RNA extraction could be performed.

2.5.2 RNA Extraction

The commercially available innuSPEED Bacteria-Fungi RNA Kit (Analytik Jena, USA) was used to extract total RNA from the frozen samples of *S. scabiei* following the manufacturer's instructions. After extraction, the samples were treated with DNase I (New England Biolabs, Canada) following manufacturer's protocol, and then the RNA was precipitated by mixing with 3 M DEPC-treated NaOAc and 95% v/v ethanol and leaving overnight at -20°C (Sambrook & Russell, 2001). The RNA was pelleted by centrifugation at 16,873 × *g* for 10 minutes and the supernatant discarded. The pellet was washed twice with 70% v/v ethanol and then left to dry for approximately 15 minutes. After drying, the RNA was resuspended in 50 µL of RNase-free water and was quantified (Section 2.4.5). Two micrograms of the RNA were then electrophoresed on a 1% w/v agarose gel made with RNase-free 1× TBE and using a tank cleaned with 0.5% w/v SDS and rinsed with RNase free water and 100% ethanol. The agarose gel contained GelRed® for visualization of the RNA following electrophoresis (Section 2.2.3). The RNA extraction was only performed once.

2.5.3 Reverse Transcription-PCR (RT-PCR)

cDNA was synthesized from 2 µg of total *S. scabiei* RNA using the SuperScriptTM III kit (Invitrogen) with random hexamer primers and following the manufacturer's instructions. A control reaction was performed for each RNA sample where the reverse transcriptase was omitted from the reaction. The resulting cDNA samples were used as template in PCR reactions with gene-specific primers (Table 2.2) as outlined in Table 2.6.

Water was used in place of cDNA as the template in control reactions. PCR reactions using cDNA from OBA cultures were cycled 25 times, while those using cDNA from TSA and SFM cultures were cycled 28 times.

Table 2.6: Typical PCR Reactions Performed using cDNA as Template

Reaction component	**Volume**	**Final concentration**
10× Standard *Taq* buffer	2 µL	1×
dNTPs (10 mM each)	0.4 µL	200 µM
Forward primer (10 pmol/µL)	1 µL	0.5 pmol/µL
Reverse primer (10 pmol/µL)	1 µL	0.5 pmol/µL
DMSO (100% v/v)	1 µL	5% v/v
cDNA template	2 µL	2 µL
Taq Polymerase (5U/µL)	0.125 µL	0.03125 U/µL
Water	To 20 µL final volume	

Thermal cycling conditions:

Initial denaturing 95°C for 2 minutes

Followed by 25 to 28 cycles (depending on sample used) of:

Denaturing at 95°C for 10 seconds

Annealing at 60°C for 30 seconds

Extension at 68°C for 15 seconds

2.6 Plant Bioassays

2.6.1 Potato Tuber Slice Bioassay

A potato tuber slice bioassay was performed according to a previously described protocol (Loria et al., 1995) with the following changes. Potatoes were peeled and surface

sterilized using 15% v/v bleach (Chlorox) for 10 minutes, after which they were washed twice with sterile water. The tubers were then aseptically sliced into roughly 1 cm thick pieces. The slices were placed into 9 cm diameter sterile glass Petri dishes containing moistened Whatman filter paper. Sterile 6 mm paper disks (Whatman) were placed on top of each slice, and 10^6 spores of *S. scabiei* in a 25 µL volume were inoculated onto the tuber tissue underneath each disk. In a separate assay, 25 µL of filter-sterilized culture supernatant from 4-day old OBB cultures of *S. scabiei* was added to each disk. The Petri dishes were sealed with Parafilm and were incubated in the dark for 7 days at room temperature, after which the potato slices were photographed. The assays were conducted twice in total with 3 replicates per treatment for each assay.

2.6.2 Radish Seedling Bioassay

A radish seedling bioassay was conducted as follows. Half strength Murashige and Skoog (MS) modified basal medium (Phytotech Labs, USA) was prepared, and 15 mL aliquots were placed into 60 glass test tubes (25 × 150 mm). Then, a 9 cm diameter Whatman filter paper was shaped into a plug and placed into each test tube, after which the test tubes were autoclaved. Radish seeds ('Cherry Belle'; McKenzie Seeds, Canada) were surface sterilized by soaking in 70% v/v ethanol with gentle rocking for 5 minutes and then soaking in a solution of 17% v/v bleach (Chlorox) and 0.1% v/v Tween-20 with gentle rocking for 10 minutes. The seeds were rinsed several times with sterile water to remove any remaining bleach. One seed was placed on top of each filter paper in the test tubes, and the filter paper was pushed down until the bottom of the paper was in contact with the MS medium. The tubes were placed at 4°C for 2 days to stratify the seeds, after which they were incubated at room temperature (21 to 24°C) with gentle shaking under a 16-hour photoperiod for 4 days. Then, each test tube was

inoculated with spores of *S. scabiei* (10^6) by pipetting the spores (suspended in 100 µL of sterile water) into the MS medium. A total of 6 plants were treated with each strain of *S. scabiei,* while control plants were treated with 100 µL of water. The plants were then incubated for an additional 3 to 4 weeks, after which they were photographed and measured. Photos of the radish seedling roots were acquired using a Leica S8APO stereomicroscope (Leica Microsystems, Germany). The assay was conducted 3 times in total.

2.6.3 Leaf Infiltration Bioassay

A leaf infiltration bioassay was performed as described before (Fyans et al., 2016) with the following changes. *Nicotiana benthamiana* plants were grown in pots from seed for approximately 9 weeks at room temperature (21 to 24°C) under a 16-hour photoperiod. The potting soil was supplemented with pellet fertilizer (14-14-14; Plant-Prod Smartcote) as per the manufacturer's instructions. Leaves were infiltrated with either 25 µL of filter-sterilized supernatants from 4-day old OBB cultures of *S. scabiei,* or 10^6 spores of *S. scabiei* in 25 µL of water. To infiltrate, a needle was first used to make a pinprick in the leaf. Then, a needleless syringe filled with the liquid to be infiltrated was placed over the hole, and the liquid was injected while applying counter-pressure to the underside of the leaf. The soaked area on the leaf created by the infiltration process was marked with a soft tip marker. A single leaf was used for infiltration of each sample, and a total of 2 to 3 leaves per plant on 3 separate plants were infiltrated in each assay. The plants were incubated at room temperature under a 16-hour photoperiod for 12 days, after which the leaves were removed and photographed. The assay was conducted twice.

2.7 Assessment of *S. scabiei* Morphological Development

A total of 10^6 spores of each *S. scabiei* strain were cultured in triplicate on PMA, SFM, TSA, OBA, ISP-4 and MMG agar plates for a total of 5 days. The plates were photographed every 24 hours.

2.8 Bioinformatics Approaches

The amino acid sequences of Scabin, SCAB_27781 and SCAB_27791 were obtained from the StrepDB (http://strepdb.streptomyces.org.uk/). Possible nuclear localization signals (NLS) in the Scabin amino acid sequence were predicted using the NLS prediction software programs Nucpred (Brameier et al., 2007), NLStradamus (Nguyen et al., 2009), NLS mapper (http://nls-mapper.iab.keio.ac.jp/cgi-bin/NLS_Mapper_form.cgi) and SeqNLS (Lin et al., 2012). The default settings were used for all the tools.

To predict possible secretion signals on Scabin and SCAB_27781, the program Signal-P 5.0 (Almagro Armenteros et al., 2019) was used. The prediction software was run with the "gram-positive" and "long output" settings selected.

The SCAB_27781 domain prediction analysis was performed using the homology prediction software programs Pfam (http://pfam.xfam.org/search/sequence), HHpred,(https://toolkit.tuebingen.mpg.de/tools/hhpred) FUGUE (Shi et al., 2001), Phyre^2 (Kelley et al., 2016) and the National Center for Biotechnology Information (NCBI) Basic Local Alignment Search Tool for proteins (BLASTP) (http://blast.ncbi.nlm.nih.gov/Blast.cgi). All programs were run with the default settings.

2.8.1 BLAST Identification of Homologous Proteins

Homologous proteins were identified using NCBI BLASTP (http://blast.ncbi.nlm.nih.gov/Blast.cgi) with the amino acid sequence of Scabin, SCAB_27781

and SCAB_27791 as the query. The arrangements of the homologous genes within their respective genomes were determined by manual inspection of the annotated genome files. The *rpoB* gene nucleotide sequence for each *Streptomyces* species identified as possessing a homologue to either Scabin or SCAB_27781 was obtained from the NCBI database.

2.8.2 Sequence Alignment and Phylogenetic Tree Building

A phylogenetic tree was constructed using the *rpoB* gene sequences from the different *Streptomyces* species. The sequences were first aligned using Biolign version 4.0.6.2 (https://www.softpedia.com/get/Science-CAD/BioLign.shtml) and then the alignment was imported into the Molecular Evolutionary Genetics Analysis (MEGA7) program. A maximum likelihood tree was generated using the general time reversal (GTR) model with gamma distribution and invariant sites (G+I), and bootstrap analyses were conducted with 1,000 repetitions.

2.9 Analysis of Thaxtomin A Production

S. scabiei strains were cultured in 5 mL of OBB in 6 separate wells of sterile 6-well tissue culture plates. Mycelial cells were harvested from 2 mL of each culture after 4 or 7 days of incubation, and the material was dried and weighed. Supernatants (1 mL) from 4- or 7-day old cultures and were extracted twice using 0.5 mL of ethyl acetate, after which the extracts were combined and dried overnight at room temperature. The residual material was redissolved in 100 µL of HPLC-grade 100% methanol, and the resulting extracts were filtered using a 0.22 µm PTFE syringe filter. HPLC was conducted on an Agilent 1260 Infinity Quaternary LC system with a Poroshell 120 EC-C18 column (4.6 × 50 mm, 2.7 µm particle size; Agilent Technologies Inc.) as previously described (Fyans et al., 2016). Samples were eluted at a rate of

1 mL/min using a 30% acetonitrile and 70% water isocratic mobile phase. The samples were monitored at a wavelength of 380 nm, and the data were collected using the ChemStation software version B.04.03 (Agilent Technologies Canada Inc.). A standard curve was prepared using pure thaxtomin A standards (Millipore Sigma Canada) and was used to calculate the concentration of thaxtomin A in each sample. The thaxtomin A production levels were normalized using the dry cell weights (DCWs) and were reported as ng thaxtomin A/mg DCW.

2.10 Statistics

Statistical analysis was conducted using Minitab 19.2020.1 (Minitab LLC, USA). A one-way ANOVA was performed with a Tukey test for both the radish seedling bioassay and the thaxtomin analysis. For the radish assay, the combined root and shoot length of 14 radish seedlings per treatment (see Section 2.6.2) were used in the ANOVA, while three samples per strain (see Section 2.8) were used in the ANOVA for the thaxtomin production levels. A box plot of the distribution and mean for each strain or treatment was generated in Minitab.

CHAPTER 3: RESULTS

3.1 Homologues of Scabin, SCAB_27781 and SCAB_27791 are Found in Both Pathogenic and Non-Pathogenic *Streptomyces* Species

The *scabin* gene in *S. scabiei* 87-22 is located immediately downstream from *SCAB_27781*, which was previously suggested to encode a putative toxin B subunit (Lyons et al., 2016). The genes are separated by only 136 bp and are oriented in the same direction, suggesting that they may form an operon (Figure 3.1). A putative regulatory gene (*SCAB_27791*) is situated upstream of *SCAB_27781* and is oriented in the same direction, and the intergenic region is again quite short (103 bp) (Figure 3.1), thereby making it a candidate for inclusion in the putative operon.

Figure 3.1: Diagram showing the arrangement of *scabin*, the putative toxin B domain (*27781*) and the putative regulator (*27791*) genes on the *S. scabiei* chromosome. The direction of the arrows indicates the direction of transcription. Diagram not to scale.

The hypothesis was that if these genes are functionally linked, then their arrangement would be conserved in other organisms where the genes are found. To investigate this further, the amino acid sequences of Scabin, SCAB_27781 and SCAB_27791 were used to search the NCBI BLASTP non-redundant protein sequence database. First, proteins exhibiting ≥80% coverage and ≥ 65% amino acid sequence identity with Scabin were chosen for further bioinformatics analysis. Homologues of SCAB_27781 and SCAB_27791 were searched using the same strategy, but the search radius was mainly limited to the genomes of *Streptomyces*

species that were identified as having a *scabin* homologue, with some exceptions. The genome sequence files were manually inspected for the presence of a YVTN domain or beta-propeller-containing protein gene (*SCAB_27781* homologue) and putative regulatory or ATP-binding protein gene (*SCAB_27791* homologue) close to a QVE containing hypothetical protein gene (*scabin* homologue). The position of the *scabin*-like genes in relation to the other nearby genes of interest was then mapped onto a *rpoB* phylogenetic tree to generate a composite figure (Figure 3.2).

This analysis revealed that only some *Streptomyces* species that harbour a *scabin* homologue harbour a homologue for *SCAB_27781*. Homologues of *SCAB_27791* are highly conserved and are almost always found encoded near the *scabin* and/or *SCAB_27781* homologue genes (Figure 3.2). In some species, there is an additional gene present that is predicted to encode a polysaccharide deacetylase family protein. When considering the arrangement of these genes, the phylogenetic tree can be roughly divided by eye into at least three different clades (Figure 3.2): Clade A primarily consists of organisms that contain homologues of the *scabin*, *SCAB_27781* and *SCAB_27791* genes with the same arrangement as in *S. scabiei*; Clade B is predominantly made up of species that harbour the *scabin* and *SCAB_27791* gene homologues but no *SCAB_27781* homologue anywhere in the genome; and Clade C mainly consists of organisms harbouring homologues of all three genes along with the predicted polysaccharide deacetylase family protein-coding gene at the same locus. Importantly, this tree demonstrates that if there are homologues of both *scabin* and *SCAB_27781* found somewhere in the genome of a species, then they are always encoded directly next to one another in the same orientation. Interestingly, no plant pathogenic species were found to be part of Clade B, in which a *scabin* homologue was

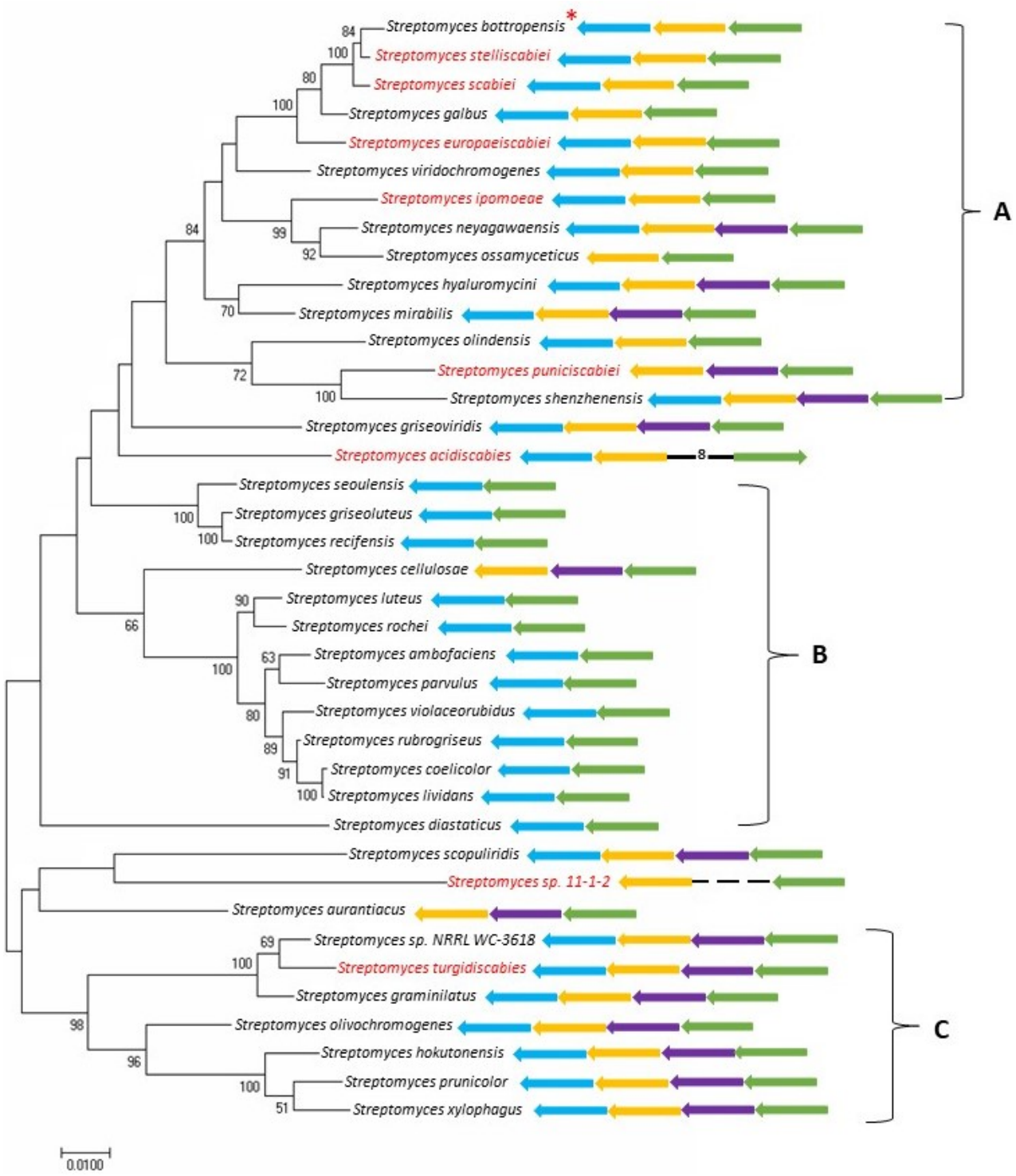
Streptomyces bottropensis *
Streptomyces stelliscabiei
Streptomyces scabiei
Streptomyces galbus
Streptomyces europaeiscabiei
Streptomyces viridochromogenes
Streptomyces ipomoeae
Streptomyces neyagawaensis
Streptomyces ossamyceticus
Streptomyces hyaluromycini
Streptomyces mirabilis
Streptomyces olindensis
Streptomyces puniciscabiei
Streptomyces shenzhenensis
Streptomyces griseoviridis
Streptomyces acidiscabies
Streptomyces seoulensis
Streptomyces griseoluteus
Streptomyces recifensis
Streptomyces cellulosae
Streptomyces luteus
Streptomyces rochei
Streptomyces ambofaciens
Streptomyces parvulus
Streptomyces violaceorubidus
Streptomyces rubrogriseus
Streptomyces coelicolor
Streptomyces lividans
Streptomyces diastaticus
Streptomyces scopuliridis
Streptomyces sp. 11-1-2
Streptomyces aurantiacus
Streptomyces sp. NRRL WC-3618
Streptomyces turgidiscabies
Streptomyces graminilatus
Streptomyces olivochromogenes
Streptomyces hokutonensis
Streptomyces prunicolor
Streptomyces xylophagus
A
B
C
0.0100

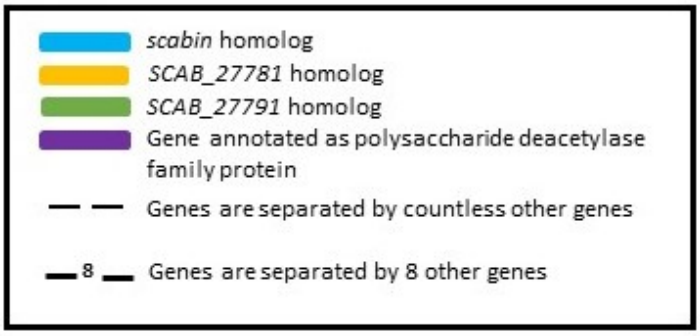

Figure 3.2: Phylogenetic relationships among *Streptomyces* species harbouring homologues of *scabin*, *SCAB_27781* and/or *SCAB_27791*. The tree was constructed using the maximum likelihood method and is based on the *rpoB* nucleotide sequence. Bootstrap values ≥50% are shown at the respective branch points and are based on 1,000 repetitions. The scale bar indicates the number of nucleotide substitutions per site. Plant pathogenic *Streptomyces* species are indicated in red. The red asterisk indicates a species for which both pathogenic and non-pathogenic strains have been described. The block arrows represent the gene homologues identified in each species, with the orientation indicating the direction of transcription. General clades are denoted as A, B and C along the side.

usually present without a corresponding *SCAB_27781* homologue. In all of the pathogenic species analyzed, the *scabin* homologue gene was always found either immediately next to a *SCAB_27781* homologue, or it was missing from the genome altogether, such as in *Streptomyces* sp. 11-1-2 and *S. puniciscabiei* (Figure 3.2).

3.2 Key Substrate Binding Residues Differ Between Scabin Homologues

An alignment of the amino acid sequences of select *scabin* homologues was next conducted in order to look for any differences in the proteins from pathogenic and non-pathogenic species. Interestingly, the Scabin homologues from non-pathogenic species that did not have an associated SCAB_27781 homologue (Figure 3.2) showed changes in amino acid residues known to play a role in the binding of Scabin to double-stranded DNA (Figure 3.3) (Vatta et al., 2021) Such differences had been previously noted in a comparison of Scabin with the *S. coelicolor* ScARP (Yoshida & Tsuge, 2018), but the results shown here indicate that this

trend extends to other Scabin homologues. In contrast, homologues that are encoded next to a SCAB_27781 homologue are highly similar to Scabin in the DNA binding motif, though some differences are present. Notably, the DNA binding motif is absolutely conserved in the Scabin homologues from the scab-causing species *S. europaeiscabiei* and *S. stelliscabiei* (Figure 3.3), suggesting that these homologues bind double-stranded DNA.

Figure 3.3: Amino acid sequence alignment of select *scabin* homologues. Part of the Scabin DNA binding motif that is highly conserved in homologues encoded next to a SCAB_27781 homologue is outlined in red, while the blue box indicates the corresponding sequence in homologues that are not encoded next to a SCAB_27781 homologue in the respective species. Red shaded sequences are from plant pathogenic species, while unshaded sequences are from non-pathogenic species. The asterisks indicate residues important in the binding of DNA by Scabin (top row). The putative NLS sequence is indicated by the black line above the alignment.

3.3 Scabin Contains a Putative Nuclear Localization Signal

Scabin was previously shown to be a secreted protein by Joshi et al. (2010), and analysis of the Scabin amino acid sequence here using Signal-P 5.0 predicted that it is secreted by the general secretion (Sec) system with a 0.7634 likelihood. If Scabin binds DNA as its target

within host cells, then it would first be required to localize to the plant cell nucleus, and this in turn would require the presence of a nuclear localization signal (NLS) within the protein. Analysis of the Scabin amino acid sequence using NLS prediction programs did not identify a putative NLS, but such programs are not designed for predicting NLSs in bacterial proteins. Instead, we turned to a previous study that identified NLS sequences in *Streptomyces* terminal proteins capable of translocation into eukaryotic nuclei (Tsai et al., 2008). The consensus sequence for the *Streptomyces* NLSs reported in this study is K(K/R)x(K/R), and an examination of the Scabin sequence revealed the presence of a perfectly matching sequence (KKTR) within the DNA binding motif (Figure 3.3). The sequence is conserved in most of the *scabin* homologues that are encoded next to *SCAB_27781* homologues but is absent from those proteins that are not associated with a *SCAB_27781* homologue.

3.4 SCAB_27781 has a Predicted Beta-Propeller Domain

To gather information on potential role(s) for SCAB_27781, the amino acid sequence was analysed using Signal-P 0.5, BlastP, Pfam, HHpred, FUGUE and Phyre[2] to identify possible domains. Signal-P 5.0 predicted a Sec-dependant lipoprotein secretion signal with a 0.8374 likelihood. Pfam predicted no significant matches but gave the insignificant Pfam-A domain matches as: 2 separate lactonase 7-bladed beta-propellers (e-values 0.12 and 0.0049 respectively), PQQ-like domain (e-value 78) and NHL repeat (e-value 680). A BlastP search identified homologous proteins annotated as YncE family protein, YVTN-family beta propeller protein, PQQ-dependent catabolism-associated beta-propeller protein, and SMP-30/gluconolactonase/LRE family protein. HHpred predicted a transmembrane domain and gave 250 sequence homology hits, among which the beta subunit of coatomer (e-value 1.5e-28) is of interest. The proteins YncE (e-value 3.3e-23), surface antigen Lp49, (e-value 2e-23), and

Hypothetical bacterial 6-phosphogluconolactonase (e-value 6e-24), are among the HHpred hits, which corroborates some of the predictions made by Pfam and BlastP. FUGUE predicted homology to YbhE from *E. coli*, virginiamycin B lyase and archeal surface layer protein, all with a 99% confidence cut off. Lastly, Phyre[2] predicted homologous regions to 120 proteins, including nitrous oxide reductases and nitrate reductases, all with a confidence of 99.8 or higher.

The interpro entry for lactonase 7-bladed beta propeller contains: YbhE-type bacterial 6-phosphogluconolactonases, which hydrolyse 6-phosphogluconolactone to 6-phosphogluconate in the pentose phosphate pathway, two fungal muconate lactonizing enzymes that reversibly convert cis,cis-muconates to muconolactones in the microbial beta-ketoadipate pathway, and the surface antigen from the human pathogen *Leptospira interrogans* Lp49. These proteins all have a 7-bladed-beta propeller as part of their structure, despite their diverse functions. The entry lists PQQ-dependent catabolism-associated beta-propeller proteins as a related subfamily. Members of this subfamily are described as having a variable number of YVTN-family beta propeller repeats and occur as part of a transport operon associated with the PQQ-dependant breakdown of alcohols.

YncE is a Sec-dependant periplasmic protein from *E coli*. It contains a YVTN-type 7-bladed beta-propeller and has been shown to participate in iron metabolism and has the ability to bind DNA (Baba-Dikwa et al., 2008; Kagawa et al., 2011). However, the exact purpose of YncE in the cell is still largely unknown. According to interpro, NHL repeats have been found to create 6- bladed beta-propeller folds, some of which are found in serine/threonine protein kinases from various pathogenic bacteria, including PknD from *Mycobacterium tuberculosis*. SMP-30/gluconolactonase/LRE family proteins are part of a family of 6 or 7-bladed beta-

propellers found in a variety of enzymes. One example of note is the gluconolactonase PpgL from *Pseudomonas aeruginosa,* which is involved in biofilm formation and invasion (Song et al., 2019).

The coatomer (COPI) complex is associated with clathrin-independent intracellular transport (Cosson & Letourneur, 1997). The beta subunit of coatomer contains a beta-propeller made of WD40 repeats (Ma & Goldberg, 2013; Stenbeck et al., 1993). Virginiamycin B lyase contains a 7-bladed beta-propeller and gives resistance to streptogramin B antibiotics by breaking open and linearizing the molecule (Korczynska et al., 2007). Virginiamycin B lyases can be found in many Gram-positive bacteria, including *S. coelicolor* (Korczynska et al., 2007). The archeal surface layer proteins are 7-bladed beta-propeller containing proteins thought to have a role in intercellular interactions (Jing et al., 2002). Lastly, both the predicted nitrous oxide reductase and nitrate reductase have a 7-bladed beta-propeller as part of their structure (Torres et al., 2016).

3.5 *scabin* is Expressed in Plant-Based Media

To investigate the timing and the conditions that enable expression of the *scabin* and *SCAB_27781* genes, wild-type *S. scabiei* was cultured on OBA, SFM and TSA agar plates for 24, 48 and 72 hrs, after which the cells were harvested and the total RNA was extracted. The RNA sample from the 48 hr SFM culture was found to be degraded, and thus only the 24 and 72 hr samples for this medium were used for further analysis. Semi-quantitative RT-PCR analysis was performed using the RNA samples and PCR primers that anneal within the *scabin* and *SCAB_27781* genes. As a positive control, the expression of the housekeeping gene *gyrA* was assessed in each sample. Figure 3.4 shows that *scabin* and *SCAB_27781* were expressed at the same time points on the plant-based media OBA and SFM, with the greatest level of expression

occurring on OBA. In contrast, neither gene was expressed on the rich medium TSA at any of the time points examined.

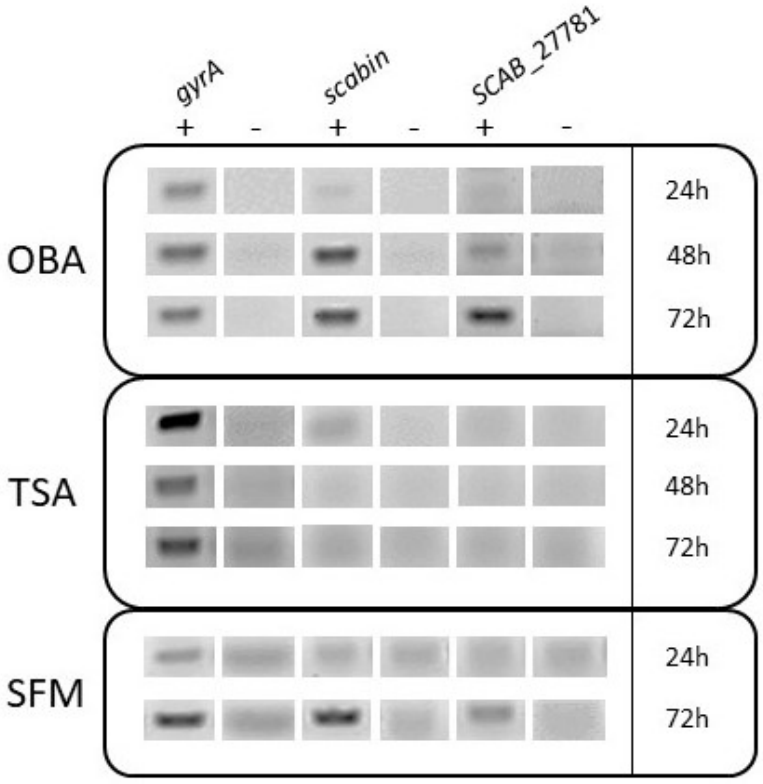

Figure 3.4: Gene expression analysis of *scabin* and *SCAB_27781*. *S. scabiei* 87-22 was cultured on OBA, TSA and SFM for 24, 48 and 72 hours, after which total RNA was extracted and used for semi-quantitative RT-PCR. '+' indicates the products generated from reverse transcription reactions that contained reverse transcriptase, while '-' indicates the products generated from control reactions that lacked reverse transcriptase. PCRs were performing using 25 cycles for the OBA samples, and 28 cycles for the TSA and SFM samples. The housekeeping gene *gyrA* was used as a positive control.

3.6 The *scabin* and *SCAB_27781* Genes are Co-Expressed as a Single Transcript

As noted in Section 3.1. the *scabin* and *SCAB_27781* genes are only separated by a 136 bp intergenic region and are oriented in the same direction, suggesting that they may be co-transcribed. To test whether this is the case, primers were designed to amplify a 730 bp

fragment spanning the intergenic region (Figure 3.5A), and these were used in RT-PCR reactions with the 72 hr OBA RNA sample. As shown in Figure 3.5B, a band of the expected size could be amplified in the test reaction but not in the control reactions, supporting the notion that the two genes are co-expressed on a single transcript.

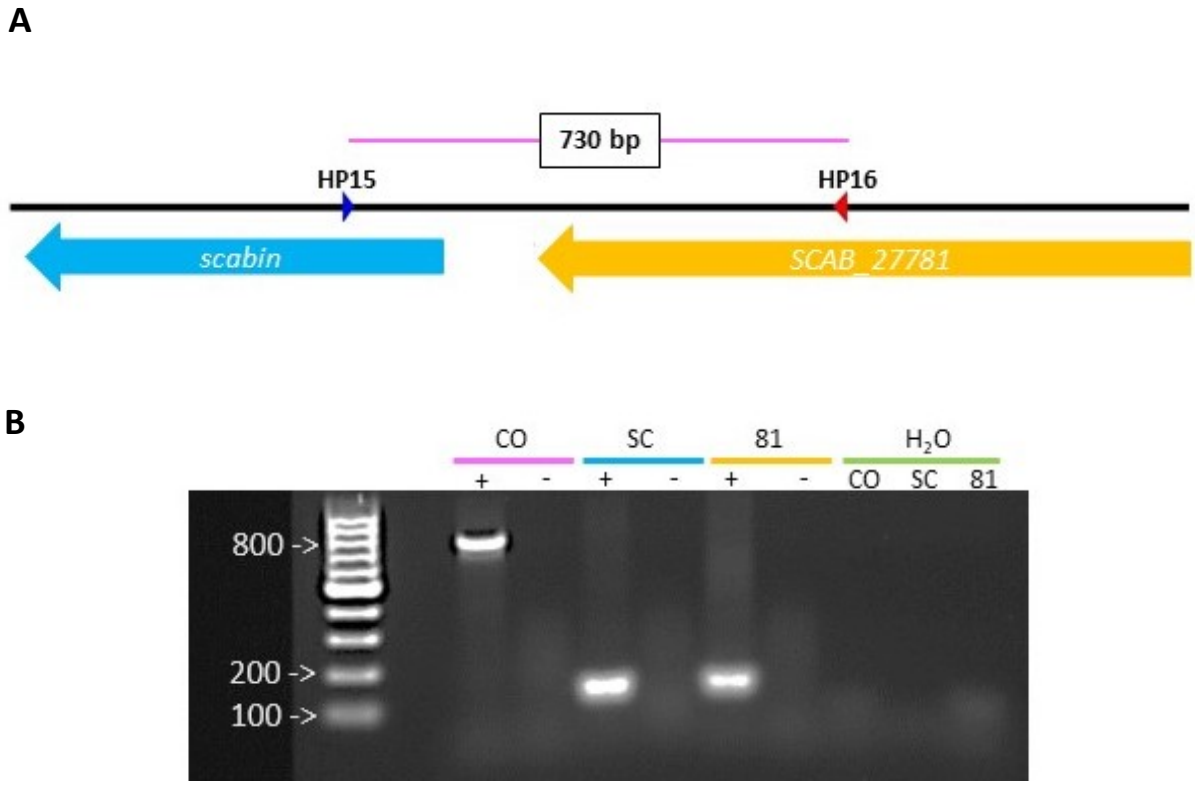

Figure 3.5: **(A)** Primer binding sites for amplification of the intergenic region between *scabin* and *SCAB_27781* (red and blue arrowheads). The expected product size is 730 bp. **(B)** RT-PCR analysis for detecting co-transcription of *scabin* and *SCAB_27781.* Reactions were conducted using the HP15 and HP16 primers shown in **A** (CO), or using primers that amplify the internal regions of the *scabin* (SC) and *SCAB_27781* (81) genes. '+' and '-' are as described in the Figure 3.3 figure legend. Water controls (H_2O) contained water in place of DNA template and were conduced with each primer set.

3.7 Construction of the *scabin* Knockout Strain

To assess the *in vivo* role of Scabin in *S. scabiei,* a *scabin* KO mutant was constructed using the Redirect PCR targeting method (Gust et al., 2003). First, a fragment of *S. scabiei*

genomic DNA containing the *scabin* gene and flanking sequences was PCR amplified using custom designed primers. The resulting 3,200 bp fragment was A-tailed before ligation into the pCR4-TOPO vector following the Invitrogen TOPO TA cloning kit protocol (Figure 3.6). Putative clones were digested with EcoRI as a preliminary screen for the presence of insert (data not shown), and then one clone was sent for sequencing at The Center for Applied Genomics (Toronto, ON) to confirm the identity of the cloned insert and to verify the integrity of the sequence such that no unintended errors were incorporated.

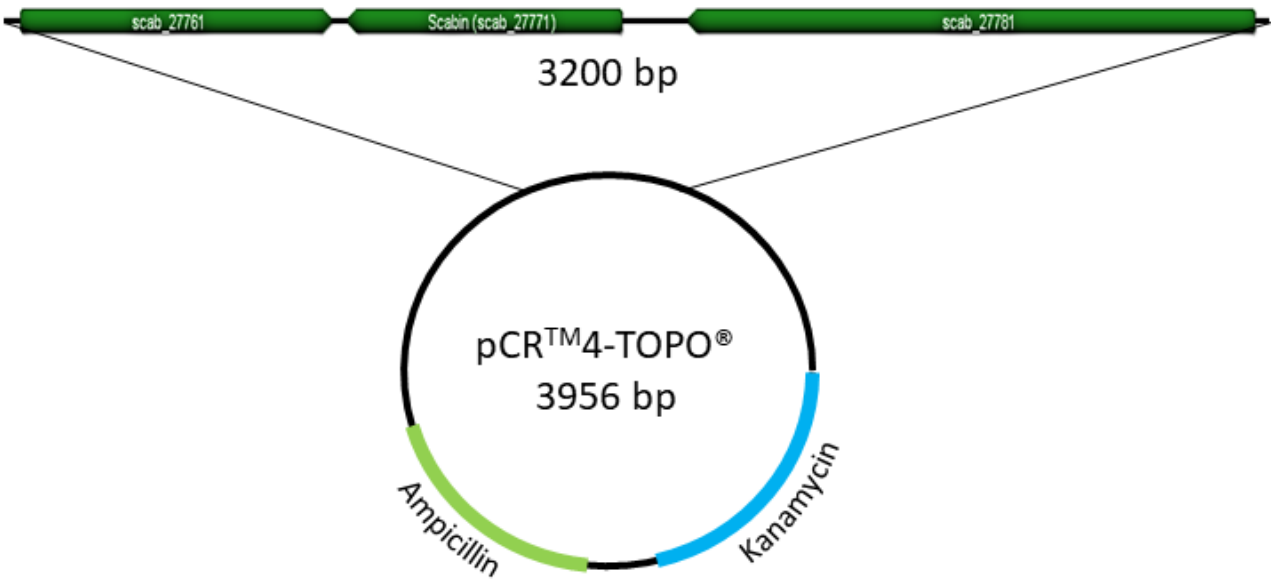

Figure 3.6: Region of interest amplified from *S. scabiei* 87-22 genomic DNA and cloned into the pCR4-TOPO vector. Genes conferring resistance to ampicillin and kanamycin on the vector backbone are shown in green and blue, respectively.

The TOPO plasmid with the correct insert was electroporated into *E. coli* BW25113/ pIJ790 using the protocol in the Redirect manual (Gust et al 2003). This was followed by introduction of a PCR-amplified [ApraR+*oriT*] cassette, which was used to replace the *scabin* gene on the TOPO plasmid via recombination mediated by the Lambda Red proteins. The resulting TOPO plasmid containing the introduced [ApraR+*oriT*] cassette was given the name pDBHP3 (Table 2.1). pDBHP3 was then transformed into *E. coli* ET12456/ pUZ8002 in preparation for conjugation into *S. scabiei*. *Streptomyces* colonies that arose after the conjugation were screened for resistance to apramycin and sensitivity to kanamycin in order to identify strains in which the wild-type *scabin* gene had been replaced by the [ApraR+*oriT*] cassette on the chromosome. Screening was conducted by selective culturing, and successful deletion of the *scabin* gene in three separate mutant isolates (6-3, 11-1, 16-1) was confirmed via PCR (Figure 3.7).

A

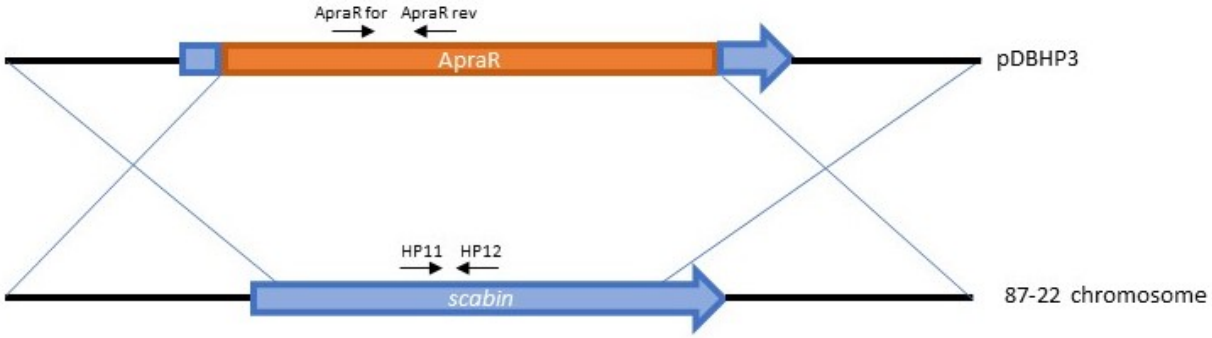

B

	Expected Band Size	
Primer Pair	WT	*scabin* KO
HP11 / HP12	106	0
ApraR for / ApraR rev	0	230

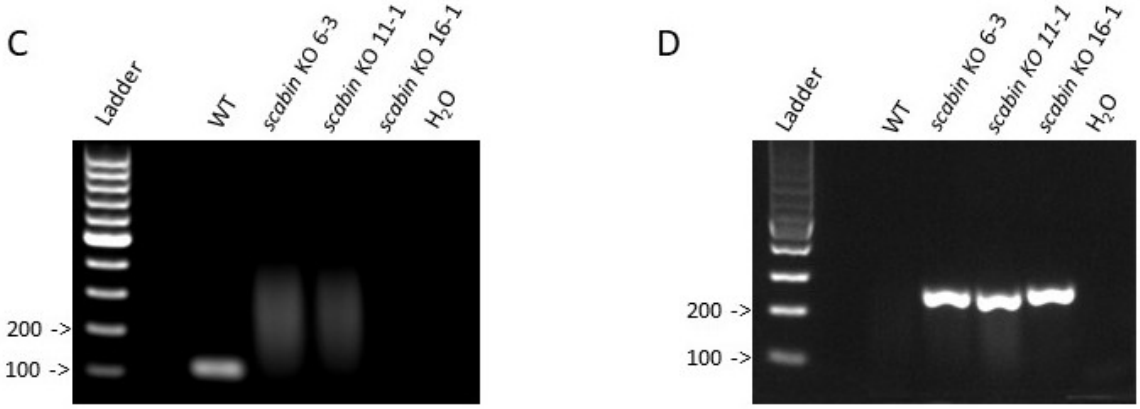

Figure 3.7: **(A)** Diagram showing the recombination expected between the pDBHP3 plasmid and the wild-type (WT) *S. scabiei* chromosome, leading to replacement of the *scabin* gene with the [ApraR+*oriT*] cassette. The approximate locations of primer binding sites used for mutant verification are shown. Not to scale. **(B)** Expected PCR product sizes produced by the primer pairs HP11/HP12 and ApraR for/ApraR rev using WT and mutant (*scabin* KO) genomic DNA as template. **(C, D)** Agarose gel electrophoresis of PCR products generated using WT and KO genomic DNA as template and using the primer pair HP11/HP12 **(C)** and ApraR for/ApraR rev **(D)**. Control reactions contained water in place of genomic DNA. The GeneRuler™ 100bp ladder was used for band size estimation, and relevant ladder band sizes in bp are indicated.

3.8 Pathogenicity Testing of the *scabin* KO and OE Strains

Spore stocks for the three separate *scabin* KO isolates, WT *S. scabiei*, and the previously constructed *scabin* OE strain and associated vector control (VC) (Table 2.1) were prepared and quantified. The stocks were then used in different plant bioassays as discussed below to determine whether Scabin functions as a virulence factor for *S. scabiei.*

3.8.1 Potato Tuber Slice Bioassay

This assay was conducted in order to determine if deletion or overexpression of *scabin* affects the ability of *S. scabiei* to cause damage to excised potato tuber tissue. In addition to inoculating tuber slices with equal numbers of spores of each strain, filter-sterilized OBB culture supernatants were tested in the assay since Scabin was previously reported to be secreted into this medium (Joshi et al., 2010). As shown in Figure 3.8, neither the *scabin* KO strains nor the OE strain caused pitting or necrosis of the tuber tissue that differed from the WT strain. Furthermore, none of the tested culture supernatants caused any obvious damage to the tuber tissue, including supernatant from WT cultures.

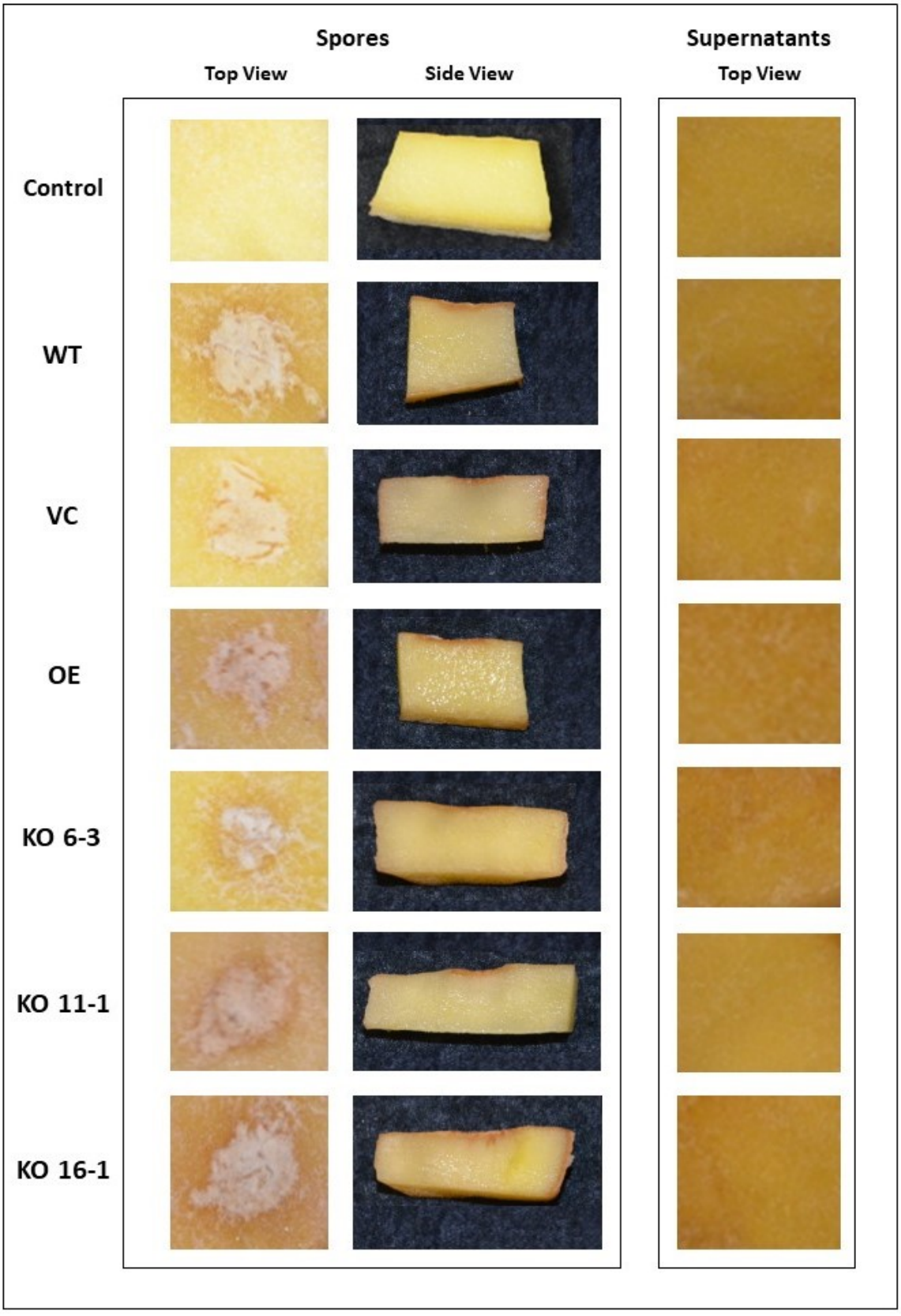
Spores
Supernatants
Top View
Side View
Top View
Control
WT
VC
OE
KO 6-3
KO 11-1
KO 16-1

Figure 3.8: Potato tuber slice bioassay for assessing the pathogenicity of *S. scabiei.* Triplicate tuber slices were inoculated with equal numbers of spores of the different *S. scabiei* strains as well as with filter-sterilized OBB culture supernatants for each strain. Control slices were treated with sterile water for the spore assay, or sterile, uninoculated OBB for the supernatant assay. The slices were incubated in the dark at room temperature for 7 days before being photographed. The assay was conducted two times in total, and representative top and side view photos are shown.

3.8.2 *Nicotiana benthamiana* Leaf Infiltration Bioassay

Although *S. scabiei* is not a foliar pathogen, it was hypothesized that a leaf infiltration bioassay using *N. benthamiana* might reveal phytotoxic effects resulting from the presence of the Scabin mART. An equal number of spores of one *scabin* KO strain (6-3), WT *S. scabiei*, the *scabin* OE strain, the VC strain and a water control were therefore infiltrated through the underside of *N. benthamiana* leaves using a 1 mL syringe. Additionally, as Scabin is known to be secreted, the assay was conducted using cell-free culture supernatants from 4-day OBB cultures of each strain. After 11 days of incubation, the leaves were harvested and photographed to look for differences in discoloration/browning of the infiltration zone (Figure 3.9). Of the 14 leaves infiltrated with the 4-day old culture supernatants, five showed strong chlorosis within the infiltration zones, three displayed mild chlorosis, and six showed no chlorosis within the zones. Of the leaves showing chlorosis, there was no discernible difference between the levels of damage generated by the WT *S. scabiei* supernatants versus supernatants from the *scabin* KO strain. Likewise, the chlorosis generated by the VC and *scabin* OE strains was comparable. No reaction was produced by infiltration of the spores of any of the strains into the leaves (Figure 3.9).

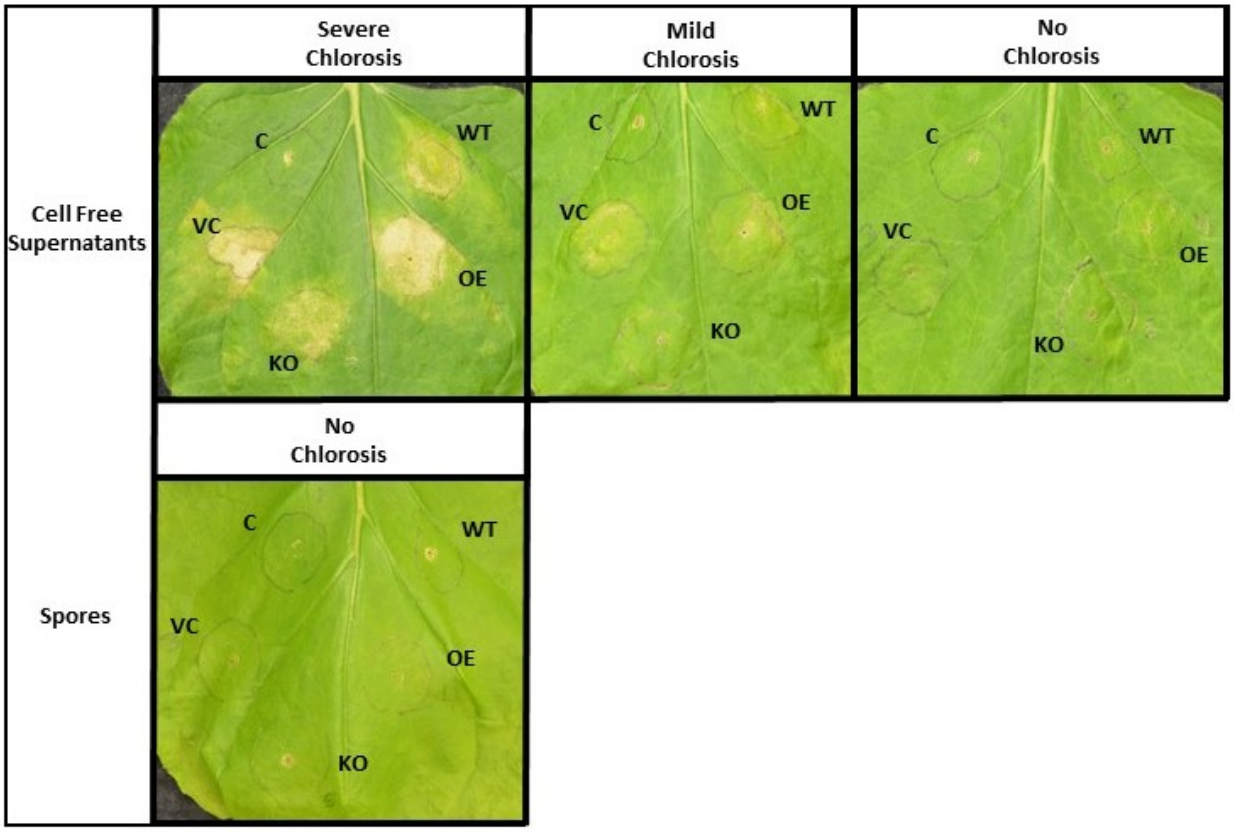

Figure 3.9: Leaf infiltration bioassay. Leaves of *Nicotiana benthaminana* plants were infiltrated with either filter-sterilized culture supernatants or spores of the wild type (WT) strain, *scabin* overexpression strain (OE), *scabin* deletion strain (KO) or the vector control (VC) strain. The control (C) for the culture supernatants was sterile OBB, while that for the spore infiltration was sterile water. As shown in the figure, the infiltration produced a range of reactions from severe chlorosis to no chlorosis. The assay was conducted three times in total, and representative photos are shown.

3.8.3 Radish Seedling Bioassay

Seedlings exposed to *S. scabiei* undergo root and shoot length reduction, radial swelling, and tissue chlorosis and necrosis (Loria et al., 1997). Therefore, to examine the effects of overexpressing or deleting the *scabin* gene, a radish seedling bioassay was conducted as previously described (Joshi et al., 2007). Figure 3.10A shows the necrosis of emerging lateral

roots and the swelling and necrosis of root tips resulting from *S. scabiei* infection, and the observed damage was consistent among all of the plants treated with the different *S. scabiei* strains. The plant roots and shoots were stunted and often necrotic, while the leaves ranged from yellowed with chlorosis to completely brown and falling off. The degree of seedling stunting was similar for all of the different *S. scabiei* treatments (Figure 3.10C).

A

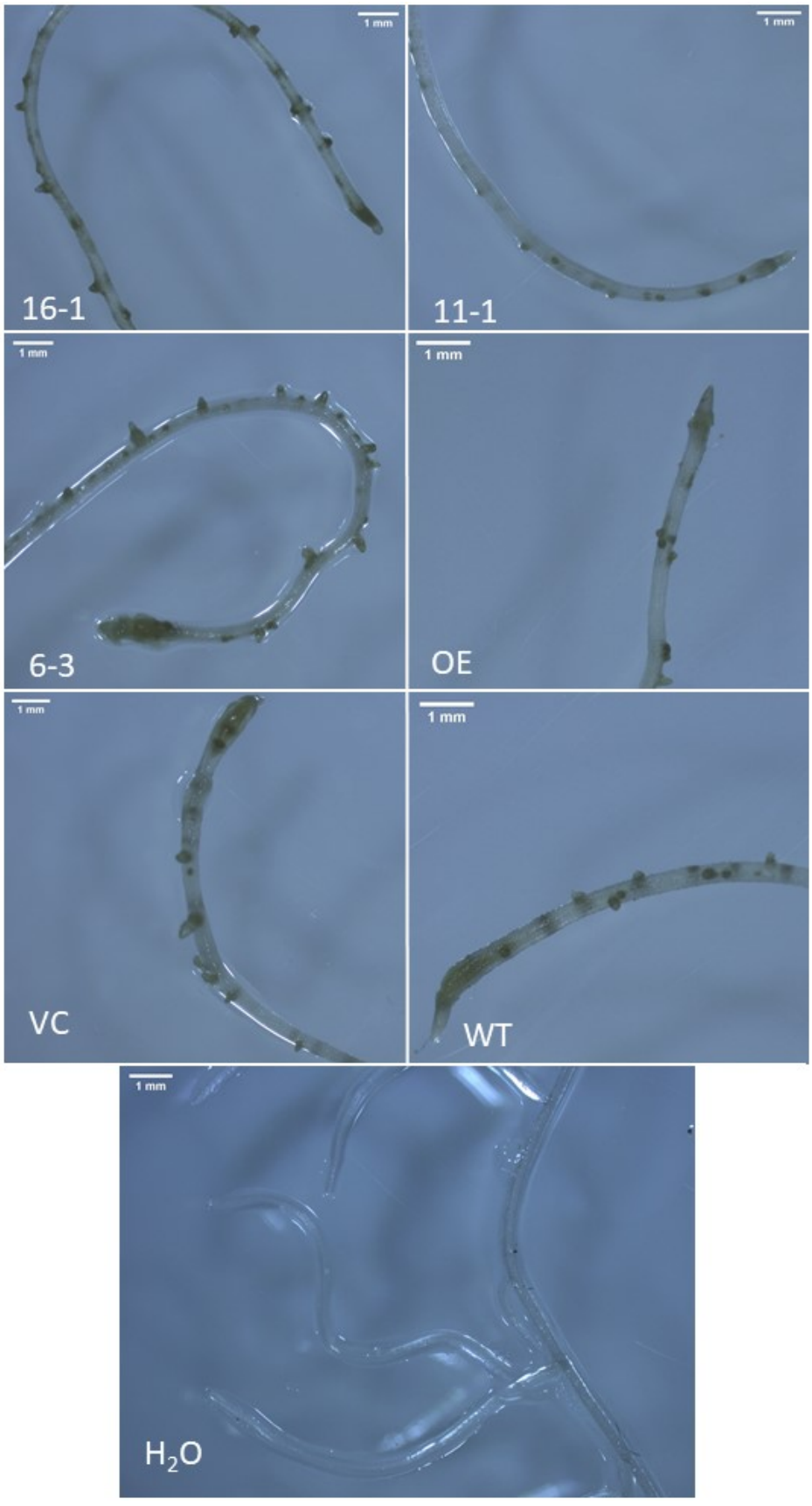

B

H_2O WT OE VC 6-3 11-1 16-1

C

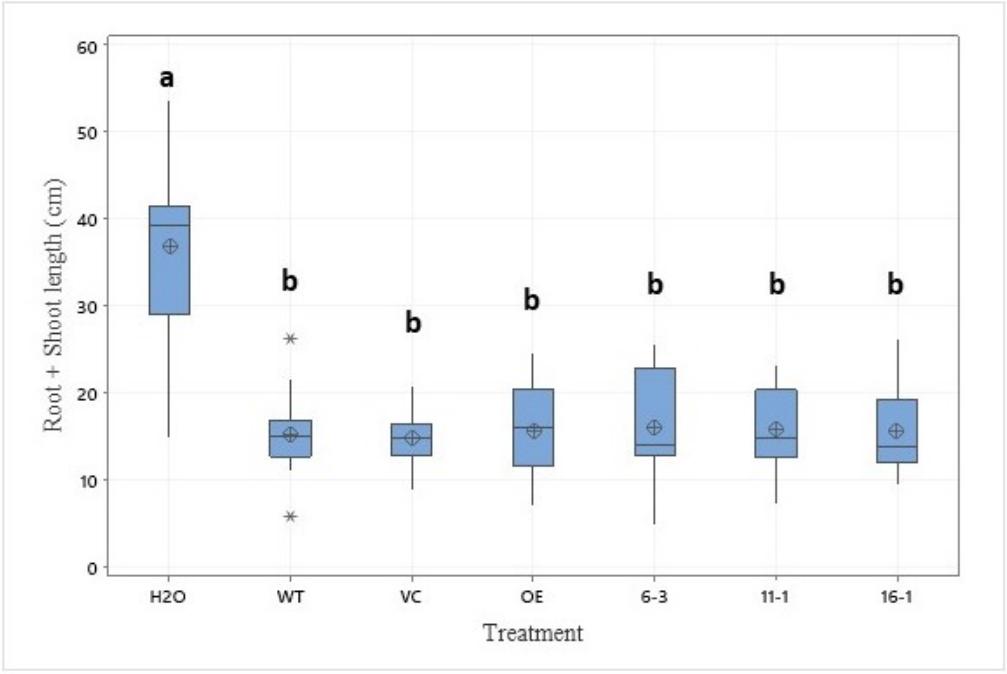

Figure 3.10: **(A)** Damage to radish seedling roots caused by *S. scabiei* wild type (WT), the *scabin* overexpression strain (OE), the three *scabin* KO strains (6-3, 11-1, 16-1) and the vector control strain (VC). Control plants were treated with water (H_2O). The white scale bars in the corner of each photo are equal to 1 mm **(B)** Representative radish seedlings inoculated with water or with the different *S. scabiei* strains listed above. The white scale bars are equal to 1 cm. **(C)** Quantification of radish seedling root and shoot stunting following inoculation with water or with the different *S. scabiei* strains listed above. Groups with the same letters were determined not to be significantly different ($P > 0.05$). Boxes are the interquartile range with the median represented as a horizontal line. Cross-hair symbols represent the mean. Asterisks are outliers in the data, and vertical lines extending from the boxes are the minimum and maximum values in the data set.

3.9 Scabin Does Not Influence Thaxtomin A Production

Thaxtomin A is the main pathogenicity factor that contributed to CS development by *S. scabiei,* and thus I wanted to determine whether overexpressing or deleting the *scabin* gene affects the levels of thaxtomin A produced by this organism. To achieve this, the different *S. scabiei* strains were cultured in OBB for 4 or 7 days, after which the culture supernatants were extracted with organic solvent, and the extracts were analyzed for thaxtomin A using HPLC. As shown in Figure 3.11, both the 4-day and 7-day analysis showed no difference in the level of thaxtomin A produced by the WT and KO strains (Figure 3.11). The level of thaxtomin A generated by the *scabin* OE strain was greater than that of the WT after 7 days incubation; however, it was not significantly different from the amount generated by the VC strain.

A

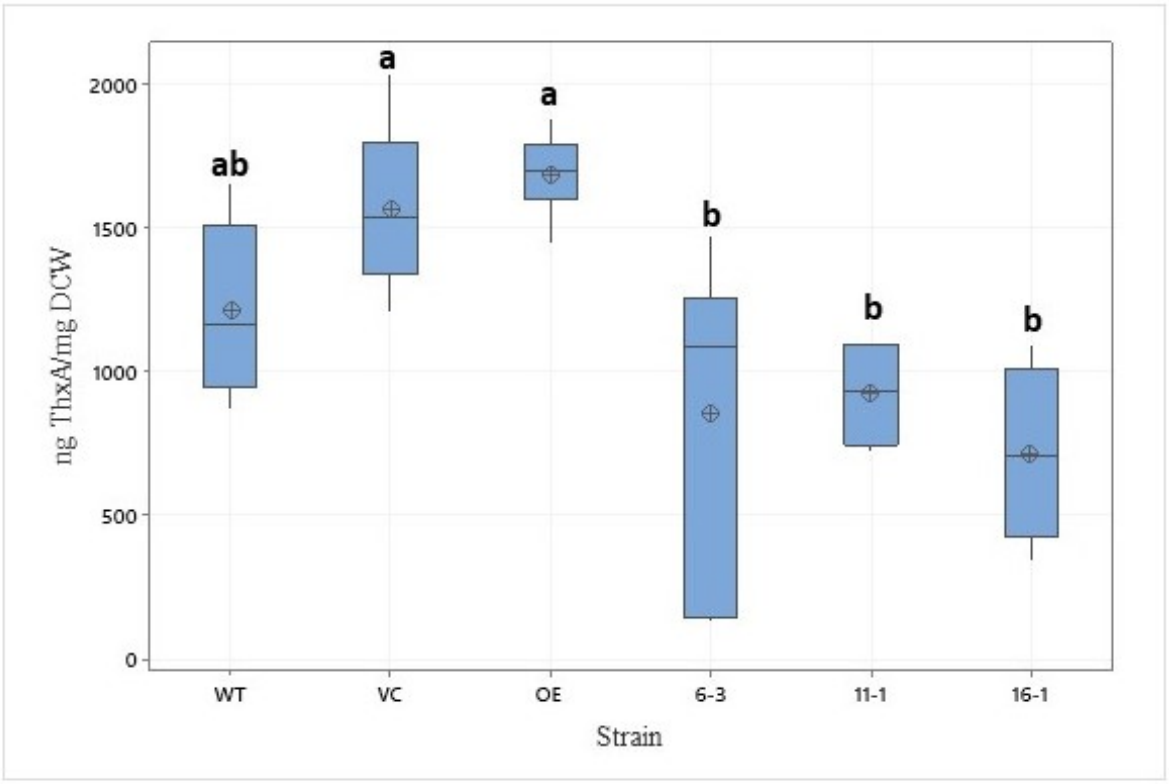
ng ThxA/mg DCW
2000
1500
1000
500
0
a
a
ab
b
b
b
WT
VC
OE
6-3
11-1
16-1
Strain

B

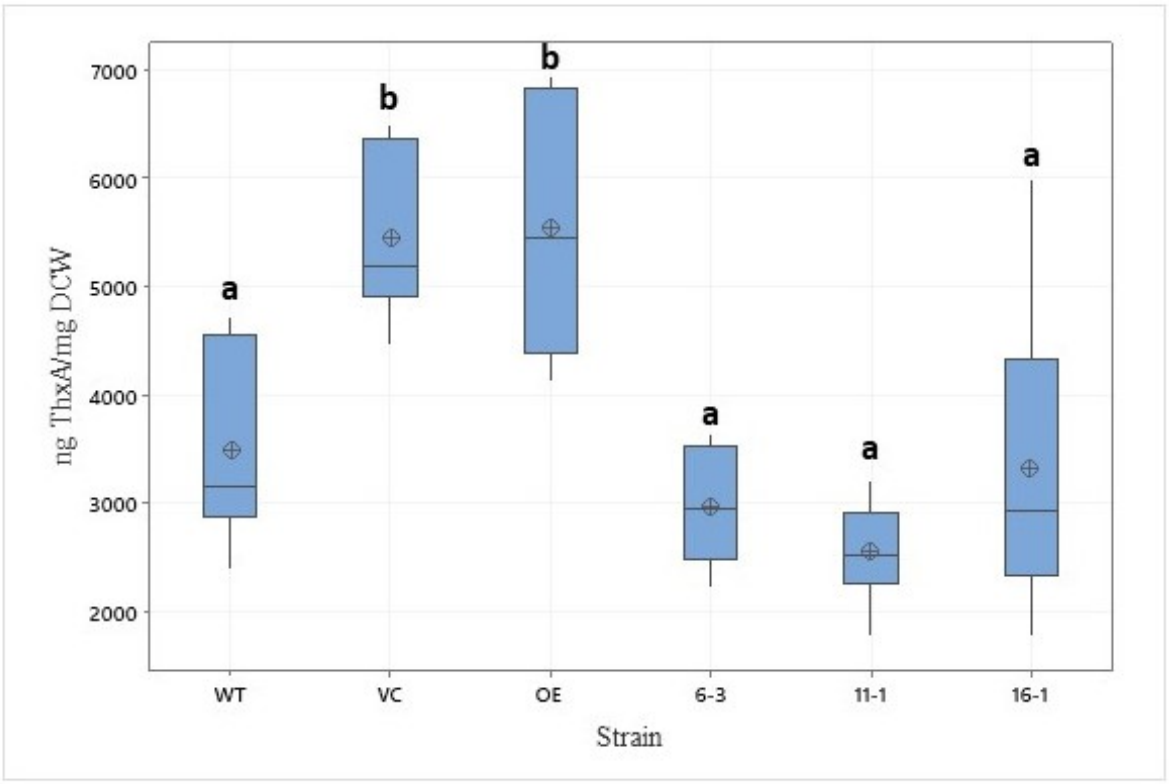
ng ThxA/mg DCW
7000
6000
5000
4000
3000
2000
b
b
a
a
a
a
WT
VC
OE
6-3
11-1
16-1
Strain

Figure 3.11: Thaxtomin A production levels in wild type *S. scabiei* (WT), the vector control strain (VC), the *scabin* overexpression strain (OE) and the three *scabin* KO strains (6-3, 11-1, 16-1). Production was assessed in OBB cultures following incubation for 4 (A) or 7 (B) days. Features of the graph are as described in the Figure 3.10 figure legend. Groups with the same letter were determined not to be significantly different ($P > 0.05$).

3.10 The Morphology of the *scabin* KO and OE Strains is Affected on Certain Culture Media

Szirák et al. (2012) showed that deletion of the gene encoding the Scabin homologue in *S. coelicolor* (ScARP) resulted in morphological changes when the organism was cultured on different media. To further investigate whether Scabin influences the morphological development of *S. scabiei,* the different *S. scabiei* strains (WT, *scabin* OE, VC, *scabin* KO) were cultured on multiple types of media, including OBA, TSA, SFM ISP-4, PMA, and MMG. Within the first 4 days of incubation, the OE strain was delayed in aerial hyphae formation (indicated by the fuzzy appearance of the plate culture) compared to the other strains when cultured on SFM and ISP-4, while the KO strains all produced aerial hyphae more quickly than the other strains on ISP-4 (Figure 3.12). After 4 days of incubation, no obvious differences were observed for any of the strains on all of the media tested (data not shown).

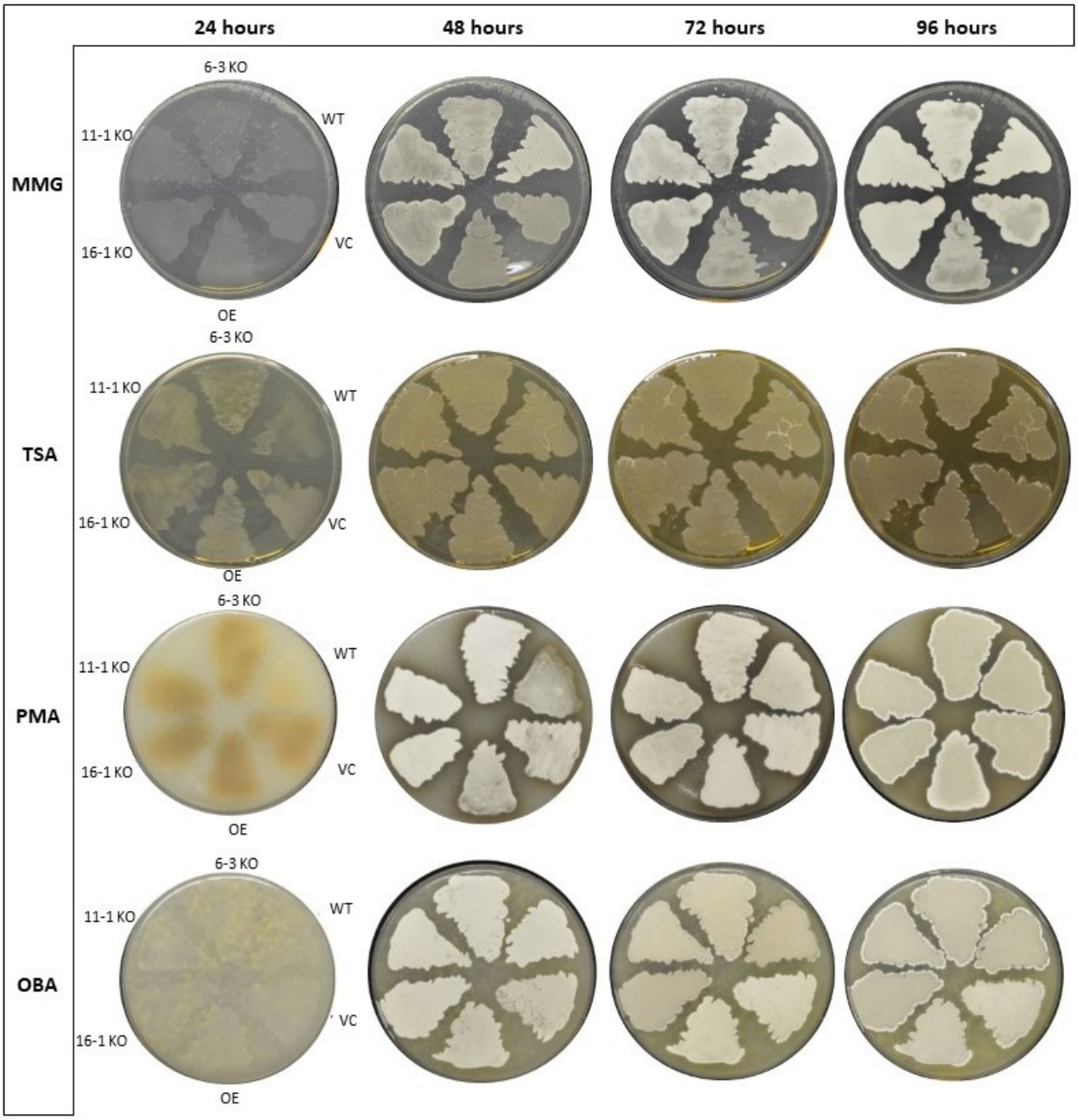
24 hours
48 hours
72 hours
96 hours
MMG
TSA
PMA
OBA
6-3 KO
11-1 KO
16-1 KO
WT
VC
OE

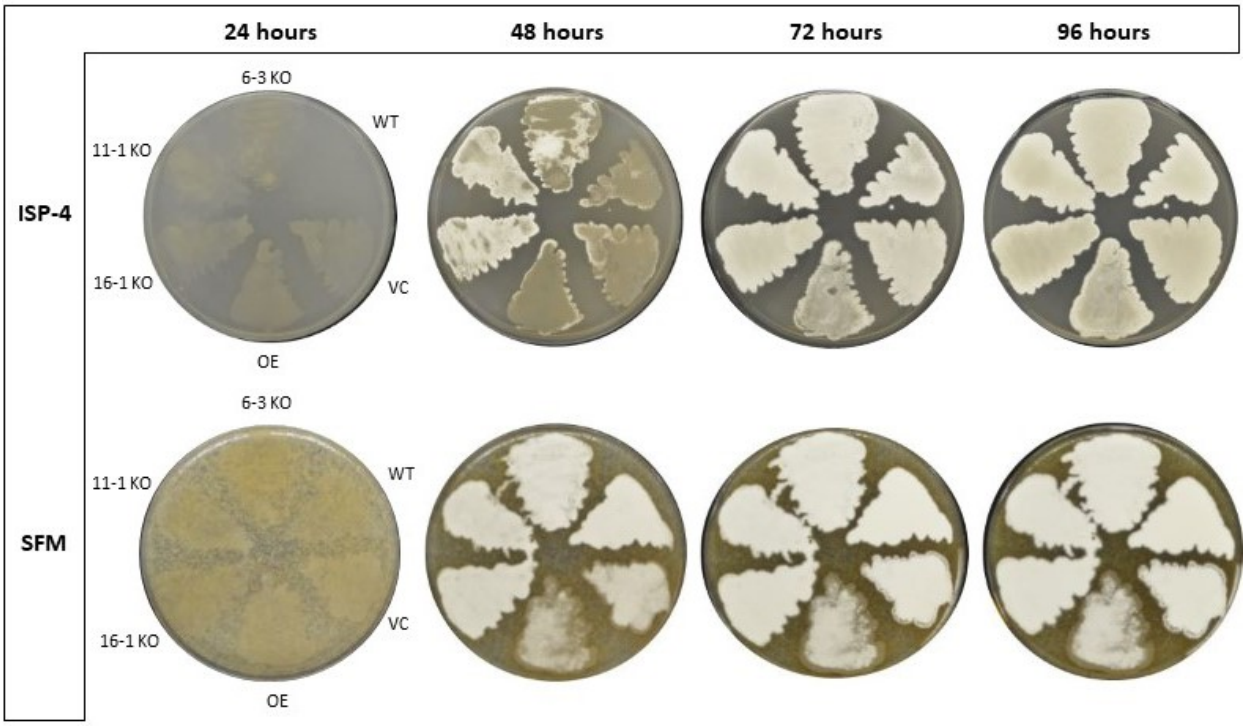

Figure 3.12: Morphological development of the *S. scabiei* strains cultured on different agar media. Photographs of the plates were taken every 24 hours for 4 days. The analysis was performed in triplicate, and representative plates for each culture medium are shown.

CHAPTER 4: DISCUSSION

mART toxins serve as virulence factors for many pathogenic bacteria, including plant pathogens. Therefore, when the Scabin mART was identified in the genome of the plant pathogen *S. scabiei*, it was suspected of being a virulence factor. The targets of mARTs are usually proteins; however, Scabin has the rare ability to target and attach an ADP-ribose moiety to guanosine residues in DNA, RNA, and mononucleotides. This activity is not currently found in any other pathogenesis-associated mARTs, and so if Scabin does play a role in the virulence of *S. scabiei*, it would represent the first of its kind.

4.1 A Bioinformatic Look at Scabin and SCAB_27781

4.1.1 Predicted Functions of Scabin and SCAB_27781

Homology searches revealed that Scabin homologues can be found in other pathogenic *Streptomyces* as well as some non-pathogenic species. Even though Scabin is present in non-pathogenic species, it may still contribute to the virulence of *S. scabiei* and may simply have an alternate function in the non-pathogenic species. This is because the presence of virulence genes in non-pathogenic species has been observed before. For example, concanamycins were first discovered in the culture broth of the non-pathogenic species *Streptomyces disastrochromogenes* (Kinashi et al., 1984). At the time, it was found that concanamycins exhibit anti-cancer, antiviral and antifungal activities, and production of these molecules by *S. disastrochromogenes* was being studied in the context of antibiotic research (Haydock et al., 2005; Kinashi et al., 1984). However, when concanamycin A and B were found to be produced by *S. scabiei*, it was determined that these molecules additionally display potent phytotoxic activity (Natsume et al., 2005; Natsume et al., 1996), and subsequently it has been shown that

concanamycin may play a role in the type of scab lesion that develops from *S. scabiei* infection (Natsume et al., 2017). Likewise, the plant hormone IAA is produced by both pathogenic and plant growth-promoting *Streptomyces* (Bignell et al., 2010). Auxin is a negative regulator of plant immunity, and thus production of the auxin-class molecule IAA by bacteria is thought to play a role in suppressing the plant immune system and allowing the bacteria to inhabit and proliferate within the plant, for better or for worse (Ma & Ma, 2016). Finally, the genes that produce the cononafacoyl phytotoxins can be found in a wide variety of both pathogenic and non-pathogenic bacterial species (Bignell et al., 2018). CFA-Ile was shown to contribute to the pathogenicity of *S. scabiei* by facilitating disease development on seedling roots and inducing tissue hypertrophy on potato tubers (Bignell et al., 2018). Other coronafacoyl phytotoxins play similar roles in the virulence of different pathogens, but it is unclear what function they serve in non-pathogenic bacteria (Bignell et al., 2018).

Homology searches for the putative toxin B domain, SCAB_27781, in other *Streptomyces* showed that many, but not all species harbour a homologue of this protein in addition to a Scabin homologue (Figure 3.2). Importantly, the genes encoding the Scabin and SCAB_27781 homologues were always found immediately next to one another on the chromosome, and they were always oriented in the same direction (Figure 3.2). This suggests that the genes are possibly expressed as an operon and are functionally linked. It is noteworthy that almost all of the plant pathogenic species harbour genes encoding both a Scabin and SCAB_27781 homologue, while most non-pathogenic species either contain both genes or only a gene encoding a Scabin homologue. This is interesting as it points to the possibility of the Scabin homologues having different *in vivo* functions depending on the host species.

Analysis of the Scabin amino acid sequence using SignalP-5.0 indicated that the protein is likely Sec-secreted in *S. scabiei*. Sec-targeted proteins are secreted unfolded and can either remain embedded in the Gram-positive cell wall, or eventually diffuse passively through the peptidoglycan layer to be released extracellularly (Green & Mecsas, 2016). Unlike most Gram-negative pathogenicity effectors, which utilise dedicated secretion systems to be deposited inside host cells, Gram-positive effectors are often secreted by a general secretion system like Sec (Green & Mecsas, 2016). Gram-positive effectors can then catalyze their own translocation across the eukaryotic cell membrane, as is the case with AB toxins (Green & Mecsas, 2016). SCAB_27781 was predicted to be a Sec secreted protein; however, the specific secretion signal is projected to target SCAB_27781 for insertion into the bacterial peptidoglycan as a lipoprotein. If SCAB_27781 is indeed deposited in the bacterial cell wall, then it is unclear how this would fit with its putative role as the toxin B domain for Scabin. It is plausible that Scabin has no need for a B-domain, and that SCAB_27781 plays some other role related to Scabin. The C3 group of mARTs are single domain toxins that lack a B subunit, and it is currently unproven exactly how C3 toxins enter the host cell. However, it was suggested that the toxins may be secreted while the bacterium is growing intracellularly within the host, thereby eliminating the need for the membrane-crossing B domain (Molinari et al., 2006; Vogelsgesang et al., 2007). *S. scabiei* was shown to grow both intercellularly and intracellularly in radish seedling roots (Loria et al., 2008). Therefore, it is possible that Scabin can be secreted directly into the cytosol of plant cells.

Domain analysis of SCAB_27781 showed that it shares structural homology with many beta-propeller containing proteins. Beta-propellers, especially 7-bladed beta-propellers, which make up the majority of the predictions, are structurally conserved but are functionally highly

diverse (Chen et al., 2011). As a result, predicting a cellular function based on the presence of a beta-propeller is notoriously difficult. Beta-propellers can be found in a broad range of proteins such as ligand binding proteins, hydrolases, oxidoreductases, signaling proteins, and structural proteins, just to name a few (Chen et al., 2011; Pons et al., 2012). The predictions for SCAB_27781 fall randomly within these categories, making the prediction of a specific function for SCAB_27781 at this time tenuous at best.

There are some examples of mART toxins that have a beta-propeller as part of their proposed B-domain, such as Chelt from *Vibrio Cholerae* and the Tc toxin family produced by many human and insect pathogens (Fieldhouse et al., 2010; Meusch et al., 2014). Chelt is made up of two domains encoded as a single polypeptide, the toxin domain (Ia/Ib) and the putative translocation domain II (Fieldhouse et al., 2010). Domain II is a predicted beta-propeller with 15% amino acid identity to a 7-bladed beta-propeller lectin from the fungus *Psathyrella velutina*, as well as 11% amino acid identity to human integrin αVb3 (Fieldhouse et al., 2010). The mechanism of entry has not been characterized for Chelt, but it is thought that the beta-propeller domain may function in binding to the host cell surface in a similar manner as the ricin B domain from the ricin AB toxin (Fieldhouse et al., 2010). In the ricin entry mechanism, the B domain binds to cell surface glycolipids and glycoproteins, and this triggers endocytosis of the toxin (Lord et al., 2003). Since SCAB_27781 possesses a beta-propeller, it is possible that it functions in lectin-like cell surface binding as well, but no specific lectin-like beta propeller was among the predictions obtained.

The Tc toxin family contains ARTs with a well characterized entry mechanism involving a large 3 subunit (TcA, TcB and TcC) pore forming complex (Meusch et al., 2014). The TcB subunit includes a 6-bladed beta-propeller that acts as a gate at the end of the beta-

sheet cocoon formed by TcB and TcC (Meusch et al., 2014). The ADP-ribosyltransferase domain, which is cleaved from the C terminal end of TcC, passes through this cocoon unfolded, and interacts with the beta-propeller (Gatsogiannis et al., 2018). This interaction triggers a conformational change in the beta-propeller, opening the pore for passage of the ART into the TcA translocation channel subunit and eventual entry into the host cell. The opening in the beta propeller is the narrowest in the entire complex at 11–15 Å in diameter, but the ART was shown to be able to pass through in its unfolded state (Gatsogiannis et al., 2018). It seems unlikely that the SCAB_27781 protein acts as a pore for Scabin to pass through like the beta-propeller of Tc toxin. This is because in addition to the beta-propeller, the Tc toxin complex has several domains and structures that are required for successful translocation of the ART and which are not found in SCAB_27781 or Scabin.

4.1.2 A Short Sequence in the DNA Binding Region May Control Substrate Preference and Nuclear Localization

An amino acid sequence alignment of Scabin homologues showed differences in some key substrate binding residues. The homologues were roughly split into two groups: those that had the Scabin-like sequence beginning with KK, and those with the ScARP-like sequence beginning with RQ. In Scabin, the three lysines and arginine in the KKTRTEK sequence are part of the DNA-interacting residues that allow Scabin to bind to dsDNA (Vatta et al., 2021). In ScARP, these residues are changed to RQTKTEI, which was previously suggested to have a diminishing effect on the affinity of ScARP for dsDNA (Yoshida & Tsuge, 2018). Instead, ScARP prefers guanosine-containing mononucleotides for a substrate (Yoshida & Tsuge, 2018). Changes to these residues in other homologues likely alter their substrate preferences as well.

Having different affinities for DNA and mononucleotides could be further evidence for a divergence of *in vivo* function among the Scabin homologues.

If Scabin does play a role in the pathogenesis of *S. scabiei* by ADP-ribosylating potato DNA, then it would first need to enter the nucleus of the plant cell. Proteins are targeted to the nucleus by the presence of a nuclear localization signal (NLS). In addition to the DNA binding role of the KKTRTEK, there is evidence that it may function as a nuclear localization signal. A functional nuclear localization consensus sequence K(K/R)X(K/R) was found in plasmid-capping terminal proteins of *Streptomyces* species (Tsai et al., 2008). This sequence KRPRP was shown to be required for localization of the terminal protein to the nucleus of Hela cells (Tsai et al., 2008). The variable residue (X) in the consensus sequence can be proline (P), valine (V), alanine (A), lysine (K) or arginine (R), but not asparagine (N) (Chelsky et al., 1989). In addition, bulky residues such as phenylalanine (F), tryptophan (W) and tyrosine (Y) are not typically placed between K and R residues (Lacasse & Lefebvre, 1995). The acidic residues aspartate (D) and glutamate (E) are not usually found between the K and R; however, these amino acids do appear frequently in the flanking regions along with proline or glycine (G) (Lacasse & Lefebvre, 1995). In Scabin, the X position is occupied by a threonine (T), and while this is not one of the preferred amino acids, it is not on the list of unlikely candidates. Furthermore P, D and E can all be found in the region flanking the possible NLS in Scabin. Moreover, NLSs are often found as part of a DNA binding domain (Lacasse & Lefebvre, 1995), and so the overlap of the possible NLS in *S. scabiei* with residues known to contribute to DNA binding adds validity to this prediction. The substitution of the first KK for RQ in ScARP destroys the NLS consensus sequence. Therefore, if Scabin is able to be targeted to the nucleus

and ScARP is not, then this would be additional evidence that they play different roles in their respective streptomycete.

4.2 The Expression of *scabin* and *SCAB_27781* Suggests a Role in Virulence

Virulence factors are usually not expressed until the pathogen is in the presence of the host. The *scabin* and *SCAB_27781* genes are both clearly expressed on OBA and SFM, which contain the plant-based ingredients oat bran and soy flour, respectively, and they were not expressed on the general bacterial culturing medium TSA. This pattern is similar to that of known virulence genes in *S. scabiei,* including the genes responsible for thaxtomin A and CFA-Ile production (Fyans et al., 2015; Loria et al., 1995). Therefore, the expression pattern of *scabin* and *SCAB_27781* is consistent with their potential role as virulence factors in *S. scabiei*.

Bacteria tend to form groups of functionally-related genes that are expressed all at once in an operon. Genes are predicted to be organized in an operon based on intergenic distance, conserved gene clusters, experimental evidence, functional relation, and sequence elements (Brouwer et al., 2008). The *scabin* and *SCAB_27781* genes are predicted to form an operon based on the first three methods of prediction. The intergenic region between the two genes is relatively short (~ 100 bp), and as noted earlier, the organization of the genes is conserved in many different *Streptomyces* genomes. Using RT-PCR analysis of the intergenic region between the *scabin* and *SCAB_27781* genes, it was demonstrated that the genes are co-transcribed as a single transcript (Figure 3.5), which is strong experimental evidence for these genes forming an operon. Whether the *SCAB_27791* putative regulatory gene, which is separated from *SCAB_27781* by only ~100 bp (Figure 3.1), is part of this operon in *S. scabiei* remains to be determined. However, the conservation of this gene in the immediate proximity to the *scabin*

and *SCAB_27781* genes in other streptomycetes (Figure 3.2) suggests that it may be part of the operon, and/or it is involved in the regulation of *scabin* and *SCAB_27781* gene expression.

4.3 The *scabin* Knockout Mutant Shows Differences in Morphology but not Virulence

At the beginning of the study, it was hypothesized that if Scabin functions as a virulence factor for *S. scabiei,* then deletion of the gene should negatively impact the virulence phenotype of the strain, while overexpression of the gene would be expected to enhance the strain virulence. Thus, a *scabin* KO strain was constructed in this study and was tested in three different plant bioassays alongside *S. scabiei* wild type and a previously constructed strain that overexpresses the *scabin* gene. Overall, it was found that neither the mutant nor the overexpression strain was obviously affected in virulence compared to *S. scabies* 87-22. This however, does not eliminate the possibility that Scabin is a virulence factor, but instead suggests that its mode of action may be more subtle. Similar to Scabin, a gene deletion mutant of the putative virulence factor TomA was indistinguishable from the wild-type strain in a potato tuber tissue bioassay as well as in tomato and radish seedling bioassays (Seipke & Loria, 2008). The assays used in the TomA study and in the study here are designed to characterize phytotoxic effects such as necrosis, swelling, pitting, stunting, etc. However, TomA homologues in other phytopathogenic bacteria play a role in the suppression of host immune responses, and it was suggested that this may be the case for the TomA in *S. scabiei* (Seipke & Loria, 2008). If true, this role would not be obvious in the assays performed. Likewise, Scabin was originally assumed to be cytotoxic based on the history of mART toxins causing the death of the host cells through disruption of key functions (Holbourn et al., 2006). However, mARTs such as HopU1, AvrRPM1 and HopF2 from other plant pathogens are all modulators of plant immunity and do not cause the outright death of cells (Nicaise et al., 2013; Redditt et al., 2019; Wang et al.,

2010). Therefore, it is plausible that Scabin may play a role in immune suppression through direct interaction with immunity-related plant genes or mRNA, and this activity was not captured by the assays used.

Deletion or overexpression of the *scabin* gene had some effect on the morphology of *S. scabiei* on certain culture media (Figure 3.10). On SFM, the OE strain was delayed in sporulation compared to the wild type, whereas the deletion mutant was not affected. This latter result resembles that shown by Szirák and colleagues in their study, in which a ScARP null mutant was phenotypically the same as the wild type on SFM agar (Szirák et al., 2012). However, on MMG and R5 medium, the ScARP null mutant was deficient or delayed in sporulation (Szirák et al., 2012), whereas the *scabin* deletion mutant behaved the same as wild-type *S. scabiei* on MMG and on OBA, PMA, and TSA. Furthermore, the *scabin* deletion mutant underwent morphological differentiation more quickly than the wild-type strain on ISP-4. Production of the secondary metabolite actinorhodin was affected in the ScARP null mutant sometimes increasing and sometimes reducing depending on the media the mutant was grown on (Szirák et al., 2012), whereas thaxtomin A production levels were not significantly impacted in either the *scabin* KO or OE strains (Figure 3.11). Overall, the *scabin* KO and ScARP null mutant appear to have different morphological and physiological phenotypes, which again may point to differences in function between the two mARTs.

4.4 Closing Statements and Future Directions

This study has provided new insights into the potential function of Scabin and the associated SCAB_27781 protein in *S. scabiei*. Many questions remain, however, and can be the focus of future studies. For example, it was demonstrated that the *SCAB_27781* gene is co-

transcribed with the *scabin* gene, which strongly suggests that the two genes are functionally related in some way. However, it is unknown if the two proteins interact with each other to form an AB holotoxin, or if the beta-propeller predicted in SCAB_27781 is capable of any type of receptor or substrate binding in general. This could be assessed through techniques such as tandem affinity purification or co-immunoprecipitation. Furthermore, a gene deletion mutant of *SCAB_27781* as well as a *scabin*/*SCAB_27781* double mutant should be constructed to see if these genetic manipulations have an impact on the virulence and/or morphology of *S. scabiei* as compared to the *scabin* KO constructed in this study.

The possible NLS consensus sequence found in Scabin should be assessed to confirm its ability to target Scabin to the plant cell nucleus. To do so, the suspected NLS sequence or the entire protein could be attached to a green fluorescent protein (GFP) gene on a plasmid, and the subcellular location visualized using fluorescence microscopy as described by Tsai and colleagues (Tsai et al., 2008). The *S. coelicolor* ScARP could be included in the experiment since it is hypothesized that this protein cannot translocate into the nucleus. Modified GFP plasmids specific for use in plant systems could be employed to investigate the subcellular localization of Scabin and ScARP in *Arabidopsis* roots and leaves or in an onion epidermal cell assay (Chiu et al., 1996). Alternatively, a GFP subcellular localization assay could be conducted using a simpler eukaryote such as yeast as a proof of concept (Niedenthal et al., 1996). If it can be shown that Scabin does localize to a eukaryotic nucleus, the next step would be to mutagenize the putative NLS identified in this study to identify the residues required for translocation.

Scabin could feasibly play a role in virulence through modulation of the host immune system. In order to assess this possibility, the expression of immunity-related genes upon

infection with wild-type *S. scabiei* and the *scabin* KO strain should be determined. Furthermore, the level of pathogen-triggered immune responses such as callose deposition and reactive oxygen species accumulation should be assessed. In order to assess differences in colonisation and proliferation ability, the general level of bacterial growth both intercellularly and intracellularly should be examined. This could be achieved using confocal or transmission electron microscopy following infection of radish roots with *scabin* KO, OE and WT strains. Finally, Scabin was shown to have higher activity towards potato DNA as compared to bacterial DNA (Lyons et al., 2016), but it is currently unclear whether or not it can target DNA from other plant species. Therefore, an investigation into whether this activity extends towards the DNA of other known *S. scabiei* plant hosts such as radish would be interesting.

Understanding the mechanisms of plant pathogenicity is important when designing strategies for the prevention or management of plant diseases. Characterizing the virulence factors of *S. scabiei* is especially useful, since no completely reliable strategy for the prevention of CS disease currently exists. In addition to the possible benefits to agriculture and plant disease management, studies on the *in vivo* role of Scabin will contribute to the general understanding of ADP-ribosyltransferase toxins. DNA-targeting mARTs are exceedingly rare, and thus the knowledge of how they might function in an organism is of great interest. Hopefully, the work presented in this thesis leads to a deeper understanding of Scabin in the future.

Works Cited

Agriculture and Agri-Food Canada. (2020). *Potato market information review, 2019-2020*. Retrieved from *http://www.agr.gc.ca/eng/industry-markets-and-trade/market-information-by-sector/horticulture/horticulture-sector-reports/potato-market-information-review-2015-2016/?id=1500402297688*

Almagro Armenteros, J. J., Tsirigos, K. D., Sønderby, C. K., Petersen, T. N., Winther, O., Brunak, S., von Heijne, G., Nielsen, H. (2019). SignalP 5.0 improves signal peptide predictions using deep neural networks. *Nature Biotechnology*, *37*(4), 420–423. *https://doi.org/10.1038/s41587-019-0036-z*

Aung, K., Kim, P., Li, Z., Joe, A., Kvitko, B., Alfano, J. R., & He, S. Y. (2020). Pathogenic bacteria target plant plasmodesmata to colonize and invade surrounding tissues. *The Plant Cell*, *32*(3), 595–611. *https://doi.org/10.1105/tpc.19.00707*

Baba-Dikwa, A., Thompson, D., Spencer, N. J., Andrews, S. C., & Watson, K. A. (2008). Overproduction, purification and preliminary X-ray diffraction analysis of YncE, an iron-regulated Sec-dependent periplasmic protein from *Escherichia coli*. *Acta Crystallographica Section F: Structural Biology and Crystallization Communications*, *64*(10), 966–969. *https://doi.org/10.1107/S1744309108029515*

Babcock, J., Eckwall, E., & Janet, L. (1993). Production and regulation of potato-scab-inducing phytotoxins by Streptomyces scabies. *Journal of General Microbiology*, *139*(7), 1579–1586. *https://doi.org/10.1099/00221287-139-7-1579*

Barnett, S. J., Ballard, R. A., & Franco, C. M. M. (2019). Field assessment of microbial inoculants to control *Rhizoctonia* root rot on wheat. *Biological Control*, *132*(October

2018), 152–160. *https://doi.org/10.1016/j.biocontrol.2019.02.019*

Bérdy, J. (1974). Recent developments of antibiotic research and classification of antibiotics according to chemical Structure. *Advances in Applied Microbiology*, *18*(C), 309–406. *https://doi.org/10.1016/S0065-2164(08)70573-2*

Bignell, D.R.D., Cheng, Z., & Bown, L. (2018). The coronafacoyl phytotoxins: structure, biosynthesis, regulation and biological activities. *Antonie van Leeuwenhoek*, *111*(5), 649–666. *https://doi.org/10.1007/s10482-017-1009-1*

Bignell, D.R.D., Fyans, J. K., & Cheng, Z. (2014). Phytotoxins produced by plant pathogenic *Streptomyces* species. *Journal of Applied Microbiology*, *116*(2), 223–235. *https://doi.org/10.1111/jam.12369*

Bignell, Dawn R. D., Huguet-Tapia, J. C., Joshi, M. V., Pettis, G. S., & Loria, R. (2010). What does it take to be a plant pathogen: genomic insights from *Streptomyces* species. *Antonie van Leeuwenhoek*, *98*(2), 179–194. *https://doi.org/10.1007/s10482-010-9429-1*

Bouarab, K., Melton, R., Peart, J., Baulcombe, D., & Osbourn, A. (2002). A saponin-detoxifying enzyme mediates suppression of plant defences. *Nature*, *418*(6900), 889–892. *https://doi.org/10.1038/nature00950*

Brameier, M., Krings, A., & MacCallum, R. M. (2007). NucPred - Predicting nuclear localization of proteins. *Bioinformatics*, *23*(9), 1159–1160. *https://doi.org/10.1093/bioinformatics/btm066*

Braun, S., Gevens, A., Charkowski, A., Allen, C., & Jansky, S. (2017). potato common scab: a review of the causal pathogens, management practices, varietal resistance screening

methods, and host resistance. *American Journal of Potato Research*, *94*(4), 283–296. *https://doi.org/10.1007/s12230-017-9575-3*

Brouwer, R. W. W., Kuipers, O. P., & Van Hijum, S. A. F. T. (2008). The relative value of operon predictions. *Briefings in Bioinformatics*, *9*(5), 367–375. *https://doi.org/10.1093/bib/bbn019*

Bulgarelli, D., Garrido-Oter, R., Münch, P. C., Weiman, A., Dröge, J., Pan, Y., McHardy, A. C., Schulze-Lefert, P. (2015). Structure and function of the bacterial root microbiota in wild and domesticated barley. *Cell Host and Microbe*, *17*(3), 392–403. *https://doi.org/10.1016/j.chom.2015.01.011*

Bulgarelli, D., Rott, M., Schlaeppi, K., Ver Loren van Themaat, E., Ahmadinejad, N., Assenza, F., Rauf, P., Huettel, B., Reinhardt, R.., Schmelzer, E., Peplies, J., Gloeckner, F. O., Amann, R., Eickhorst, T., Schulze-Lefert, P. (2012). Revealing structure and assembly cues for *Arabidopsis* root-inhabiting bacterial microbiota. *Nature*, *488*(7409), 91–95. *https://doi.org/10.1038/nature11336*

Carpusca, I., Jank, T., & Aktories, K. (2006). *Bacillus sphaericus* mosquitocidal toxin (MTX) and pierisin: The enigmatic offspring from the family of ADP-ribosyltransferases. *Molecular Microbiology*, *62*(3), 621–630. *https://doi.org/10.1111/j.1365-2958.2006.05401.x*

Chater, K. F. (2006). *Streptomyces* inside-out: a new perspective on the bacteria that provide us with antibiotics. *Philosophical Transactions of the Royal Society B: Biological Sciences*, *361*(1469), 761–768. *https://doi.org/10.1098/rstb.2005.1758*

Chater, K. F. (2016). Recent advances in understanding *Streptomyces*. *F1000Research*, *5*(F1000

Faculty Rev), 2795. *https://doi.org/10.12688/f1000research.9534.1*

Chater, K. F., Biró, S., Lee, K. J., Palmer, T., & Schrempf, H. (2010). The complex extracellular biology of *Streptomyces*: REVIEW ARTICLE. *FEMS Microbiology Reviews*, 34(2), 171–198. *https://doi.org/10.1111/j.1574-6976.2009.00206.x*

Chater, K. F., & Chandra, G. (2006). The evolution of development in *Streptomyces* analysed by genome comparisons. *FEMS Microbiology Reviews*, *30*(5), 651–672. *https://doi.org/10.1111/j.1574-6976.2006.00033.x*

Chelsky, D., Ralph, R., & Jonak, G. (1989). Sequence requirements for synthetic peptide-mediated translocation to the nucleus. *Molecular and Cellular Biology*, *9*(6), 2487–2492. *https://doi.org/10.1128/mcb.9.6.2487*

Chen, C. K. M., Chan, N. L., & Wang, A. H. J. (2011). The many blades of the β-propeller proteins: Conserved but versatile. *Trends in Biochemical Sciences*, *36*(10), 553–561. *https://doi.org/10.1016/j.tibs.2011.07.004*

Cheng, Z., Bown, L., Piercey, B., & Bignell, D. R. D. (2019). Positive and negative regulation of the virulence-associated coronafacoyl phytotoxin in the potato common scab pathogen *Streptomyces scabies*. *Molecular Plant-Microbe Interactions*, *32*(10), 1348-1359. *https://doi.org/10.1094/MPMI-03-19-0070-R*

Chiu, W., Niwa, Y., Zeng, W., Hirano, T., Kobayashi, H., & Sheen, J. (1996). Engineered GFP as a vital reporter in plants. *Current Biology*, *6*(3), 325–330. *https://doi.org/10.1016/S0960-9822(02)00483-9*

Chung, E. H., Da Cunha, L., Wu, A. J., Gao, Z., Cherkis, K., Afzal, A. J., Mackey, D., Dangl, J.

L. (2011). Specific threonine phosphorylation of a host target by two unrelated type III effectors activates a host innate immune receptor in plants. *Cell Host and Microbe*, *9*(2), 125–136. *https://doi.org/10.1016/j.chom.2011.01.009*

Clarke, C. R., Kramer, C. G., Kotha, R. R., Wanner, L. A., Luthria, D. L., & Kramer, M. (2019). Cultivar resistance to common scab disease of potato is dependent on the pathogen species. *Phytopathology*, *109*(9), 1544–1554. *https://doi.org/10.1094/PHYTO-09-18-0368-R*

Collier, R., & Else, M. A. (2014). UK fruit and vegetable production - impacts of climate change and opportunities for adaptation. In *Climate change impact and adaptation in agricultural systems* (pp. 88–109). *https://doi.org/10.1079/9781780642895.0088*

Conn, V. M., Walker, A. R., & Franco, C. M. M. (2008). Endophytic actinobacteria induce defense pathways in *Arabidopsis thaliana*. *Molecular Plant-Microbe Interactions®*, *21*(2), 208–218. *https://doi.org/10.1094/MPMI-21-2-0208*

Cosson, P., & Letourneur, F. (1997). Coatomer (COPI)-coated vesicles: Role in intracellular transport and protein sorting. *Current Opinion in Cell Biology*, *9*(4), 484–487. *https://doi.org/10.1016/S0955-0674(97)80023-3*

Currie, C. R., Scott, J. A., Summerbell, R. C., & Malloch, D. (1999). Fungus-growing ants use antibiotic-producing bacteria to control garden parasites. *Nature*, *398*(April), 701–704. *https://doi.org/10.1038/19519*

Davies, J. (2006). Where have all the antibiotics gone? *Canadian Journal of Infectious Diseases and Medical Microbiology*, *17*(5), 287–290. *https://doi.org/10.1155/2006/707296*

Day, B., Dahlbeck, D., Huang, J., Chisholm, S. T., Li, D., & Staskawicz, B. J. (2005).

Molecular basis for the RIN4 negative regulation of RPS2 disease resistance. *Plant Cell*, *17*(4), 1292–1305. *https://doi.org/10.1105/tpc.104.030163*

Dees, M. W., & Wanner, L. A. (2012). In search of better management of potato common scab. *Potato Research*, *55*(3–4), 249–268. *https://doi.org/10.1007/s11540-012-9206-9*

Duval, I., Brochu, V., Simard, M., Beaulieu, C., & Beaudoin, N. (2005). Thaxtomin A induces programmed cell death in *Arabidopsis thaliana* suspension-cultured cells. *Planta*, *222*(5), 820–831. *https://doi.org/10.1007/s00425-005-0016-z*

Edwards, J., Johnson, C., Santos-Medellín, C., Lurie, E., Podishetty, N. K., Bhatnagar, S., Eisen, J. A., Sundaresan, V. (2015). Structure, variation, and assembly of the root-associated microbiomes of rice. *Proceedings of the National Academy of Sciences of the United States of America*, *112*(8), E911–E920. *https://doi.org/10.1073/pnas.1414592112*

Embley, T. M. (1994). The molecular phylogeny and systematics of the actinomycetes. *Annual Review of Microbiology*, *48*(1), 257–289. *https://doi.org/10.1146/annurev.micro.48.1.257*

Errakhi, R., Dauphin, A., Meimoun, P., Lehner, A., Reboutier, D., Vatsa, P., Briand, J., Madiona, K., Rona, J. P., Barakate, M., Wendehenne, D., Beaulieu, C., Bouteau, F. (2008). An early Ca2+ influx is a prerequisite to thaxtomin A-induced cell death in *Arabidopsis thaliana* cells. *Journal of Experimental Botany*, *59*(15), 4259–4270. *https://doi.org/10.1093/jxb/ern267*

Fellermann, M., Huchler, C., Fechter, L., Kolb, T., Wondany, F., Mayer, D., Michaelis, J., Stenger, S., Mellert, K., Möller, P., Barth, T. F. E., Fischer, S., Barth, H. (2020). Clostridial C3 toxins enter and intoxicate human dendritic cells. *Toxins*, *12*(9) 563. *https://doi.org/10.3390/toxins12090563*

Feng, B., Liu, C., Shan, L., & He, P. (2016). Protein ADP-ribosylation takes control in plant–bacterium interactions. *PLoS Pathogens*, 12(12) e1005941. *https://doi.org/10.1371/journal.ppat.1005941*

Fieldhouse, R. J., Turgeon, Z., White, D., & Merrill, A. R. (2010). Cholera- and anthrax-like toxins are among several new ADP-Ribosyltransferases. *PLoS Computational Biology*, *6*(12) e1001029. *https://doi.org/10.1371/journal.pcbi.1001029*

Freeman, V. J. (1951). Studies on the virulence of bacteriophage-infected strains of *Corynebacterium diphtheriae*. *Journal of Bacteriology*, *61*(6), 675–688. *https://doi.org/10.1128/jb.61.6.675-688.1951*

Fu, Z. Q., Guo, M., Jeong, B. R., Tian, F., Elthon, T. E., Cerny, R. L., Staiger, D., Alfano, J. R. (2007). A type III effector ADP-ribosylates RNA-binding proteins and quells plant immunity. *Nature*, *447*(7142), 284–288. *https://doi.org/10.1038/nature05737*

Fyans, J. K., Altowairish, M. S., Li, Y., & Bignell, D. R. D. (2015). Characterization of the coronatine-like phytotoxins produced by the common scab pathogen *Streptomyces scabies*. *Molecular Plant-Microbe Interactions*, *28*(4), 443–454. *https://doi.org/10.1094/MPMI-09-14-0255-R*

Fyans, J. K., Bown, L., & Bignell, D. R. D. (2016). Isolation and characterization of plant-pathogenic *Streptomyces* species associated with common scab-infected potato tubers in newfoundland. *Phytopathology*, *106*(2), 123–131. *https://doi.org/10.1094/PHYTO-05-15-0125-R*

Gatsogiannis, C., Merino, F., Roderer, D., Balchin, D., Schubert, E., Kuhlee, A., Hayer-Hartl, M., Raunser, S. (2018). Tc toxin activation requires unfolding and refolding of a β-

propeller. *Nature*, *563*(7730), 209–233. *https://doi.org/10.1038/s41586-018-0556-6*

Goudjal, Y., Toumatia, O., Sabaou, N., Barakate, M., Mathieu, F., & Zitouni, A. (2013). Endophytic actinomycetes from spontaneous plants of Algerian Sahara: Indole-3-acetic acid production and tomato plants growth promoting activity. *World Journal of Microbiology and Biotechnology*, *29*(10), 1821–1829. https://doi.org/10.1007/s11274-013-1344-y

Government of Canada C. F. I. A. (2015). PI-009: seed potato tuber inspection. Retrieved from Government of Canada website: *https://inspection.canada.ca/plant-varieties/potatoes/guidance-documents/pi-009/eng/1383933490053/1383934020925?chap=0.*

Government of Canada C. F. I. A. (2021) Canadian grade conpendium: volume 2 fresh fruit or vegetables. Retrieved from Government of Canada website: *https://inspection.canada.ca/about-cfia/acts-and-regulations/list-of-acts-and-regulations/documents-incorporated-by-reference/canadian-grade-compendium-volume-2/eng/1519996239002/1519996303947?chap=3#s31c3*

Goyer, C., & Beaulieu, C. (1997). Host range of *Streptomycete* strains causing common scab. *Plant Disease*, *81*(8), 901–904. *https://doi.org/10.1094/PDIS.1997.81.8.901*

Grant, M., Brown, I., Adams, S., Knight, M., Ainslie, A., & Mansfield, J. (2000). The RPM1 plant disease resistance gene facilitates a rapid and sustained increase in cytosolic calcium that is necessary for the oxidative burst and hypersensitive cell death. *The Plant Journal*, *23*(4), 441–450. *https://doi.org/10.1046/j.1365-313x.2000.00804.x*

Green, E. R., & Mecsas, J. (2016). Bacterial secretion systems: An overview. *Virulence*

Mechanisms of Bacterial Pathogens, *4*(1), 213–239. *https://doi.org/10.1128/9781555819286.ch8*

Gust, B., O'Rourke, S., Bird, N., Kieser, T., & Chater, K. (2003). Recombineering in *Streptomyces coelicolor*. *FEMS Online Protocols*, 1–22. Retrieved from *http://recombineering.ncifcrf.gov/*

Han, L., Dutilleul, P., Prasher, S. O., Beaulieu, C., & Smith, D. L. (2008). Assessment of common scab-inducing pathogen effects on potato underground organs via computed tomography scanning. *Phytopathology*, *98*(10), 1118–1125. *https://doi.org/10.1094/PHYTO-98-10-1118*

Haydock, S. F., Appleyard, A. N., Mironenko, T., Lester, J., Scott, N., & Leadlay, P. F. (2005). Organization of the biosynthetic gene cluster for the macrolide concanamycin A in *Streptomyces neyagawaensis* ATCC 27449. *Microbiology*, *151*(10), 3161–3169. *https://doi.org/10.1099/mic.0.28194-0*

Healy, F. G., Wach, M., Krasnoff, S. B., Gibson, D. M., & Loria, R. (2000). The txtAB genes of the plant pathogen *Streptomyces acidiscabies* encode a peptide synthetase required for phytotoxin thaxtomin A production and pathogenicity. *Molecular Microbiology*, *38*(4), 794–804. *https://doi.org/10.1046/j.1365-2958.2000.02170.x*

Hill, J., & Lazarovits, G. (2005). A mail survey of growers to estimate potato common scab prevalence and economic loss in Canada. *Canadian Journal of Plant Pathology*, *27*(1), 46–52. *https://doi.org/10.1080/07060660509507192*

Hiltunen, L. H., Weckman, A., Ylhäinen, A., Rita, H., Richter, E., & Valkonen, J. P. T. (2005). Responses of potato cultivars to the common scab pathogens, *Streptomyces scabies* and *S.*

turgidiscabies. *Annals of Applied Biology*, *146*(3), 395–403. *https://doi.org/10.1111/j.1744-7348.2005.040083.x*

Holbourn, K. P., Shone, C. C., & Acharya, K. R. (2006). A family of killer toxins: Exploring the mechanism of ADP-ribosylating toxins. *FEBS Journal*, *273*(20), 4579–4593. *https://doi.org/10.1111/j.1742-4658.2006.05442.x*

Holmes, R. K. (2000). Biology and molecular epidemiology of diphtheria toxin and the tox gene. *The Journal of Infectious Diseases*, *181*(s1), S156–S167. *https://doi.org/10.1086/315554*

Hou, S., Mu, R., Ma, G., Xu, X., Zhang, C., Yang, Y., & Wu, D. (2011). *Pseudomonas syringae* pv. *phaseolicola* effector HopF1 inhibits pathogen-associated molecular pattern-triggered immunity in a RIN4-independent manner in common bean (*Phaseolus vulgaris*). *FEMS Microbiology Letters*, *323*(1), 35–43. *https://doi.org/10.1111/j.1574-6968.2011.02356.x*

Hsu, S.-Y. (2010). *IAA Production by Streptomyces scabies and its role in plant-microbe interaction* (Cornell University). Retrieved from *https://hdl.handle.net/1813/17227*

Hwang, M. S. H., Morgan, R. L., Sarkar, S. F., Wang, P. W., & Guttman, D. S. (2005). Phylogenetic characterization of virulence and resistance phenotypes of *Pseudomonas syringae*. *Applied and Environmental Microbiology*, *71*(9), 5182–5191. *https://doi.org/10.1128/AEM.71.9.5182-5191.2005*

Inoue, H., Nojima, H., & Okayama, H. (1990). High efficiency transformation of *Escherichia coli* with plasmids. *Gene*, *96*(1), 23–28. *https://doi.org/10.1016/0378-1119(90)90336-P*

Jankevicius, G., Ariza, A., Ahel, M., & Ahel, I. (2016). The toxin-antitoxin system dartg

catalyzes reversible adp-ribosylation of DNA. *Molecular Cell*, *64*(6), 1109–1116. *https://doi.org/10.1016/j.molcel.2016.11.014*

Jeong, B. R., Lin, Y., Joe, A., Guo, M., Korneli, C., Yang, H., Wang, P., Yu, M., Cerny, R. L., Staiger, D., Alfano, J. R., Xu, Y. (2011). Structure function analysis of an ADP-ribosyltransferase type III effector and its RNA-binding target in plant immunity. *Journal of Biological Chemistry*, *286*(50), 43272–43281. *https://doi.org/10.1074/jbc.M111.290122*

Jing, H., Takagi, J., Liu, J., & Springer, T. A. (2002). Archaeal surface layer proteins contain β propeller, PKD, and β helix domains and are related to metazoan cell surface proteins. *Structure*, *10*(10), 1453–1464. *https://doi.org/10.1016/S0969-2126(02)00840-7*

Johnson, E. G., Joshi, M. V., Gibson, D. M., & Loria, R. (2007). Cello-oligosaccharides released from host plants induce pathogenicity in scab-causing *Streptomyces* species. *Physiological and Molecular Plant Pathology*, *71*(1–3), 18–25. *https://doi.org/10.1016/j.pmpp.2007.09.003*

Jørgensen, R., Purdy, A. E., Fieldhouse, R. J., Kimber, M. S., Bartlett, D. H., & Merrill, A. R. (2008). Cholix toxin, a novel ADP-ribosylating factor from *Vibrio cholerae*. *Journal of Biological Chemistry*, *283*(16), 10671–10678. *https://doi.org/10.1074/jbc.M710008200*

Joshi, M., Rong, X., Moll, S., Kers, J., Franco, C., & Loria, R. (2007). *Streptomyces turgidiscabies* secretes a novel virulence protein, Nec1, which facilitates infection. *Molecular Plant-Microbe Interactions*, *20*(6), 599–608. *https://doi.org/10.1094/MPMI-20-6-0599*

Joshi, M. V., & Loria, R. (2007). *Streptomyces turgidiscabies* possesses a functional cytokinin biosynthetic pathway and produces leafy galls. *Molecular Plant-Microbe Interactions*,

20(7), 751–758. *https://doi.org/10.1094/MPMI-20-7-0751*

Joshi, M. V., Mann, S. G., Antelmann, H., Widdick, D. A., Fyans, J. K., Chandra, G., Hutchings, M. I., Toth, I., Hecker, M., Loria, R., Palmer, T. (2010). The twin arginine protein transport pathway exports multiple virulence proteins in the plant pathogen *Streptomyces scabies*. *Molecular Microbiology*, *77*(1), 252–271. *https://doi.org/10.1111/j.1365-2958.2010.07206.x*

Kagawa, W., Sagawa, T., Niki, H., & Kurumizaka, H. (2011). Structural basis for the DNA-binding activity of the bacterial B-propeller protein YncE. *Acta Crystallographica Section D: Biological Crystallography*, *67*(12), 1045–1053. *https://doi.org/10.1107/S0907444911045033*

Kaltenpoth, M., Göttler, W., Herzner, G., & Strohm, E. (2005). Symbiotic bacteria protect wasp larvae from fungal infestation. *Current Biology*, *15*(5), 475–479. *https://doi.org/10.1016/j.cub.2004.12.084*

Kaup, O., Gräfen, I., Zellermann, E. M., Eichenlaub, R., & Gartemann, K. H. (2005). Identification of a tomatinase in the tomato-pathogenic actinomycete *Clavibacter michiganensis subsp. michiganensis* NCPPB382. *Molecular Plant-Microbe Interactions*, *18*(10), 1090–1098. *https://doi.org/10.1094/MPMI-18-1090*

Kelley, L. A., Mezulis, S., Yates, C. M., Wass, M. N., & Sternberg, M. J. (2016). The Phyre2 web portal for protein modeling, prediction and analysis. *Nature Protocols*, *10*(6), 845–858. *https://doi.org/10.1038/nprot.2015-053*

Kers, J. A., Wach, M. J., Cameron, K. D., Gibson, D. M., Loria, R., Morello, J. E., Joshi, M. V., Bukhalid, R. A. (2005). A large, mobile pathogenicity island confers plant pathogenicity

on *Streptomyces* species. *Molecular Microbiology*, *55*(4), 1025–1033. *https://doi.org/10.1111/j.1365-2958.2004.04461.x*

Kieser, T., Hopwood, D. A., Bibb, M., Chater, K., & Buttner, M. (2000). *Practical Streptomyces Genetics*. Norwich: John Innes Foundation.

Kim, H. S., Desveaux, D., Singer, A. U., Patel, P., Sondek, J., & Dangl, J. L. (2005). The Pseudomonas syringae effector AvrRpt2 cleaves its C-terminally acylated target, RIN4, from *Arabidopsis* membranes to block RPM1 activation. *Proceedings of the National Academy of Sciences of the United States of America*, *102*(18), 6496–6501. *https://doi.org/10.1073/pnas.0500792102*

Kim, J. N., Kim, Y., Jeong, Y., Roe, J. H., Kim, B. G., & Cho, B. K. (2015). Comparative genomics reveals the core and accessory genomes of *streptomyces* species. *Journal of Microbiology and Biotechnology*, *25*(10), 1599–1605. *https://doi.org/10.4014/jmb.1504.04008*

Kinashi, H., Someno, K., & Sakaguchi, K. (1984). Isolation and characterization of concanamycins A, B and C. *The Journal of Antibiotics*, *37*(11), 1333–1343. *https://doi.org/10.7164/antibiotics.37.1333*

King, R. R., & Calhoun, L. A. (2009). The thaxtomin phytotoxins: Sources, synthesis, biosynthesis, biotransformation and biological activity. *Phytochemistry*, *70*(7), 833–841. *https://doi.org/10.1016/j.phytochem.2009.04.013*

King, R. R., Lawrence, C. H., & Clark, M. C. (1991). Correlation of phytotoxin production with pathogenicity of *Streptomyces scabies* isolates from scab infected potato tubers. *American Potato Journal*, *68*(10), 675–680. *https://doi.org/10.1007/BF02853743*

Korczynska, M., Mukhtar, T. A., Wright, G. D., & Berghuis, A. M. (2007). Structural basis for streptogramin B resistance in *Staphylococcus aureus* by virginiamycin B lyase. *Proceedings of the National Academy of Sciences of the United States of America*, *104*(25), 10388–10393. *https://doi.org/10.1073/pnas.0701809104*

Kurth, F., Mailänder, S., Bönn, M., Feldhahn, L., Herrmann, S., Große, I., Buscot, F., Schrey, S. D., Tarkka, M. T. (2014). *Streptomyces*-induced resistance against oak powdery mildew involves host plant responses in defense, photosynthesis, and secondary metabolism pathways. *Molecular Plant-Microbe Interactions*, *27*(9), 891–900. *https://doi.org/10.1094/MPMI-10-13-0296-R*

Lacasse, E. C., & Lefebvre, Y. A. (1995). Nuclear localization signals overlap DNA- or RNA-binding domains in nucleic acid-binding proteins. *Nucleic Acids Research*, *23*(10), 1647–1656. *https://doi.org/10.1093/nar/23.10.1647*

Lee, J. Y., Wang, X., Cui, W., Sager, R., Modla, S., Czymmek, K., Zybaliov, B., van Wijk, K., Zhang, C., Lu, H., Lakshmanana, V. (2011). A plasmodesmata-localized protein mediates crosstalk between cell-to-cell communication and innate immunity in *Arabidopsis*. *Plant Cell*, *23*(9), 3353–3373. *https://doi.org/10.1105/tpc.111.087742*

Legault, G. S., Lerat, S., Nicolas, P., & Beaulieu, C. (2011). Tryptophan regulates thaxtomin A and indole-3-acetic acid production in *Streptomyces scabiei* and modifies its interactions with radish seedlings. *Phytopathology*, *101*(9), 1045–1051. *https://doi.org/10.1094/PHYTO-03-11-0064*

Li, Liu, J., Díaz-Cruz, G., Cheng, Z., & Bignell, D. R. D. (2019). Virulence mechanisms of plant-pathogenic *Streptomyces* species: An updated review. *Microbiology (United*

Kingdom), *165*(10), 1025–1040. *https://doi.org/10.1099/mic.0.000818*

Li, X., Lei, X., Zhang, C., Jiang, Z., Shi, Y., Wang, S., Wang, L., Hong, B. (2016). Complete genome sequence of *Streptomyces globisporus* C-1027, the producer of an enediyne antibiotic lidamycin. *Journal of Biotechnology*, *222*, 9–10. *https://doi.org/10.1016/j.jbiotec.2016.02.004*

Lin, J. R., Mondal, A. M., Liu, R., & Hu, J. (2012). Minimalist ensemble algorithms for genome-wide protein localization prediction. *BMC Bioinformatics*, *13*(1), 157. *https://doi.org/10.1186/1471-2105-13-157*

Locht, C., Coutte, L., & Mielcarek, N. (2011). The ins and outs of pertussis toxin. *FEBS Journal*, *278*(23), 4668–4682. *https://doi.org/10.1111/j.1742-4658.2011.08237.x*

Lord, M. J., Jolliffe, N. A., Marsden, C. J., Pateman, C. S. C., Smith, D. C., Spooner, R. A., Watson, P. D., Roberts, L. M. (2003). Ricin: Mechanisms of cytotoxicity. *Toxicological Reviews*, *22*(1), 53–64. *https://doi.org/10.2165/00139709-200322010-00006*

Lorenzi, J.-N., Lespinet, O., Leblond, P., & Thibessard, A. (2021). Subtelomeres are fast-evolving regions of the *Streptomyces* linear chromosome. 7(6) *Microbial Genomics*. *https://doi.org/10.1099/mgen.0.000525*

Loria, R., Bukhalid, R. A., Creath, R. A., Leiner, R. H., Olivier, M., & Steffens, J. C. (1995). Differential production of thaxtomins by pathogenic *Streptomyces* species in vitro. *Phytopathology*, *85*(5), 537–541. *https://doi.org/10.1094/Phyto-85-537*

Loria, Rosemary, Bignell, D. R. D., Moll, S., Huguet-Tapia, J. C., Joshi, M. V., Johnson, E. G., Seipke, R. F., Gibson, D. M. (2008). Thaxtomin biosynthesis: the path to plant

pathogenicity in the genus *Streptomyces*. *Antonie van Leeuwenhoek*, *94*(1), 3–10. *https://doi.org/10.1007/s10482-008-9240-4*

Loria, Rosemary, Bukhalid, R. A., Fry, B. A., & King, R. R. (1997). Plant pathogenicity in the genus *Streptomyces*. *Plant Disease*, *81*(8), 836–846. *https://doi.org/10.1094/PDIS.1997.81.8.836*

Loria, Rosemary, Kers, J., & Joshi, M. (2006). Evolution of Plant Pathogenicity in *Streptomyces* . *Annual Review of Phytopathology*, *44*(1), 469–487. *https://doi.org/10.1146/annurev.phyto.44.032905.091147*

Lyons, B., Ravulapalli, R., Lanoue, J., Lugo, M. R., Dutta, D., Carlin, S., & Merrill, A. R. (2016). Scabin, a Novel DNA-acting ADP-ribosyltransferase from *Streptomyces scabies*. *Journal of Biological Chemistry*, *291*(21), 11198–11215. *https://doi.org/10.1074/jbc.M115.707653*

Ma, K.-W., & Ma, W. (2016). Phytohormone pathways as targets of pathogens to facilitate infection. *Plant Molecular Biology*, *91*(6), 713–725. *https://doi.org/10.1007/s11103-016-0452-0*

Ma, W., & Goldberg, J. (2013). Rules for the recognition of dilysine retrieval motifs by coatomer. *EMBO Journal*, *32*(7), 926–937. *https://doi.org/10.1038/emboj.2013.41*

MacNeil, D. J., Gewain, K. M., Ruby, C. L., Dezeny, G., Gibbons, P. H., & MacNeil, T. (1992). Analysis of *Streptomyces avermitilis* genes required for avermectin biosynthesis utilizing a novel integration vector. *Gene*, *111*(1), 61–68. *https://doi.org/10.1016/0378-1119(92)90603-M*

Martin-Hernandez, A. M., Dufresne, M., Hugouvieux, V., Melton, R., & Osbourn, A. (2000). Effects of targeted replacement of the tomatinase gene on the interaction of *Septoria lycopersici* with tomato plants. *Molecular Plant-Microbe Interactions*, *13*(12), 1301–1311. *https://doi.org/10.1094/MPMI.2000.13.12.1301*

Meusch, D., Gatsogiannis, C., Efremov, R. G., Lang, A. E., Hofnagel, O., Vetter, I. R., Aktories, K., Raunser, S. (2014). Mechanism of Tc toxin action revealed in molecular detail. *Nature*, *508*(1), 61–65. *https://doi.org/10.1038/nature13015*

Molinari, G., Rohde, M., Wilde, C., Just, I., Aktories, K., & Chhatwal, G. S. (2006). Localization of the C3-like ADP-ribosyltransferase from *Staphylococcus aureus* during bacterial invasion of mammalian cells. *Infection and Immunity*, *74*(6), 3673–3677. *https://doi.org/10.1128/IAI.02013-05*

Nakano, T., Matsushima-Hibiya, Y., Yamamoto, M., Takahashi-Nakaguchi, A., Fukuda, H., Ono, M., Takamura-Enya, T., Kinashi, H., Totsuka, Y. (2013). ADP-ribosylation of guanosine by SCO5461 protein secreted from *Streptomyces coelicolor*. *Toxicon*, *63*(1), 55–63. *https://doi.org/10.1016/j.toxicon.2012.11.019*

Nakano, T., Takahashi-Nakaguchi, A., Yamamoto, M., & Watanabe, M. (2014). Pierisins and CARP-1: ADP-Ribosylation of DNA by ARTCs in Butterflies and Shellfish. In *Current Topics in Microbiology and Immunology: Endogenous ADP-Ribosylation* (2015 editi, pp. 127–149). *https://doi.org/10.1007/82_2014_416*

Natsume, M., Komiya, M., Koyanagi, F., Tashiro, N., Kawaide, H., & Abe, H. (2005). Phytotoxin produced by *Streptomyces spp.* causing potato russet scab in Japan. *Journal of General Plant Pathology*, *71*(5), 364–369. *https://doi.org/10.1007/s10327-005-0211-6*

Natsume, M., Ryu, R., & Abe, H. (1996). Production of Phytotoxins, Concanamycins A and B by *Streptomyces spp*. Causing Potato Scab. *Japanese Journal of Phytopathology*, *62*(4), 411–413. *https://doi.org/10.3186/jjphytopath.62.411*

Natsume, M., Tashiro, N., Doi, A., Nishi, Y., & Kawaide, H. (2017). Effects of concanamycins produced by *Streptomyces scabies* on lesion type of common scab of potato. *Journal of General Plant Pathology*, *83*(2), 78–82. *https://doi.org/10.1007/s10327-017-0696-9*

Nguyen Ba, A. N., Pogoutse, A., Provart, N., & Moses, A. M. (2009). NLStradamus: A simple Hidden Markov Model for nuclear localization signal prediction. *BMC Bioinformatics*, *10*, 1–11. *https://doi.org/10.1186/1471-2105-10-202*

Nicaise, V., Joe, A., Jeong, B., Korneli, C., Boutrot, F., Westedt, I., Staiger, D., Alfano, J. R., Zipfel, C. (2013). Pseudomonas HopU1 modulates plant immune receptor levels by blocking the interaction of their mRNAs with GRP7. *The EMBO Journal*, *32*(5), 701–712. *https://doi.org/10.1038/emboj.2013.15*

Niedenthal, R. K., Riles, L., Johnston, M., & Hegemann, J. H. (1996). *Yeast Functional Analysis Reports Green Fluorescent Protein as a Marker for Gene Expression and Subcellular Localization in Budding Yeast*. *12*, 773–786. *https://doi.org/10.1002/(SICI)1097-0061(19960630)12:8<773::AID-YEA972>3.0.CO;2-L*

Oda, T., Hirabayashi, H., Shikauchi, G., Takamura, R., Hiraga, K., Minami, H., Hashimoto, H., Yamamoto, M., Wakabayash, K., Shimizu, T., Sato, M. (2017). Structural basis of autoinhibition and activation of the DNA-targeting ADP-ribosyltransferase pierisin-1. *Journal of Biological Chemistry*, *292*(37), 15445–15455. *https://doi.org/10.1074/jbc.M117.776641*

Palazzo, L., Mikoč, A., & Ahel, I. (2017). ADP-ribosylation: new facets of an ancient modification. *The FEBS Journal*, *284*(18), 2932–2946. *https://doi.org/10.1111/febs.14078*

Pareja-Jaime, Y., Roncero, M. I. G., & Ruiz-Roldán, M. C. (2008). Tomatinase from *Fusarium oxysporum* f. sp. *lycopersici* is required for full virulence on tomato plants. *Molecular Plant-Microbe Interactions*, *21*(6), 728–736. *https://doi.org/10.1094/MPMI-21-6-0728*

Perry, H. C. (2019). *In Vivo Characterization of Scabin, a Novel mART Toxin Family Member from the Common Scab Pathogen Streptomyces scabies*. Memorial University of Newfoundland.

Pons, T., Gómez, R., Chinea, G., & Valencia, A. (2012). Beta-propellers: Associated Functions and their Role in Human Diseases. *Current Medicinal Chemistry*, *10*(6), 505–524. *https://doi.org/10.2174/0929867033368204*

Redditt, T. J., Chung, E. H., Karimi, H. Z., Rodibaugh, N., Zhang, Y., Trinidad, J. C., Kim, J. H., Zhou, Q., Shen, M., Dangl, J. L., Mackey, D., Innes, R. W. (2019). AvrRpm1 functions as an ADP-ribosyl transferase to modify NOI domain-containing proteins, including *Arabidopsis* and soybean RPM1-interacting protein4. *The Plant Cell*, *31*(11), 2664–2681. *https://doi.org/10.1105/tpc.19.00020R2*

Redenbach, M., Scheel, J., & Schmidt, U. (2000). Chromosome topology and genome size of selected actinomycetes species. *Antonie van Leeuwenhoek, International Journal of General and Molecular Microbiology*, *78*(3–4), 227–235. *https://doi.org/10.1023/A:1010289326752*

Riedlinger, J., Schrey, S. D., Tarkka, M. T., Hampp, R., Kapur, M., & Fiedler, H. P. (2006). Auxofuran, a novel metabolite that stimulates the growth of fly agaric, is produced by the

mycorrhiza helper bacterium *Streptomyces* strain AcH 505. *Applied and Environmental Microbiology*, *72*(5), 3550–3557. *https://doi.org/10.1128/AEM.72.5.3550-3557.2006*

Rungin, S., Indananda, C., Suttiviriya, P., Kruasuwan, W., Jaemsaeng, R., & Thamchaipenet, A. (2012). Plant growth enhancing effects by a siderophore-producing endophytic streptomycete isolated from a Thai jasmine rice plant (*Oryza sativa* L. cv. KDML105). *Antonie van Leeuwenhoek, International Journal of General and Molecular Microbiology*, *102*(3), 463–472. *https://doi.org/10.1007/s10482-012-9778-z*

Sabaratnam, S., & Traquair, J. A. (2002). Formulation of a *Streptomyces* biocontrol agent for the suppression of Rhizoctonia damping-off in tomato transplants. *Biological Control*, *23*(3), 245–253. *https://doi.org/10.1006/bcon.2001.1014*

Sadeghi, A., Karimi, E., Dahaji, P. A., Javid, M. G., Dalvand, Y., & Askari, H. (2012). Plant growth promoting activity of an auxin and siderophore producing isolate of *Streptomyces* under saline soil conditions. *World Journal of Microbiology and Biotechnology*, *28*(4), 1503–1509. *https://doi.org/10.1007/s11274-011-0952-7*

Sambrook, J., & Russell, D. (2001). *Molecular Cloning: A Laboratory Manual* (Third). New York: Cold Spring Harbor Laboratory Press.

Sánchez, J., & Holmgren, J. (2008). Cholera toxin structure, gene regulation and pathophysiological and immunological aspects. *Cellular and Molecular Life Sciences*, *65*(9), 1347–1360. *https://doi.org/10.1007/s00018-008-7496-5*

Schmitt, M. P., & Holmes, R. K. (1991). Iron-dependent regulation of diphtheria toxin and siderophore expression by the cloned *Corynebacterium diphtheriae* repressor gene dtxR in *C. diphtheriae* C7 strains. *Infection and Immunity*, *59*(6), 1899–1904.

https://doi.org/10.1128/iai.59.6.1899-1904.1991

Scholte, K., & Labruyere, R. E. (1985). Netted scab: a new name for an old disease in Europe. *Potato Research*, *28*(4), 443–448. *https://doi.org/10.1007/BF02357520*

Seipke, R. F., Kaltenpoth, M., & Hutchings, M. I. (2012). *Streptomyces* as symbionts: an emerging and widespread theme? *FEMS Microbiology Reviews*, *36*(4), 862–876. *https://doi.org/10.1111/j.1574-6976.2011.00313.x*

Seipke, R. F., & Loria, R. (2008). *Streptomyces scabies* 87-22 possesses a functional tomatinase. *Journal of Bacteriology*, *190*(23), 7684–7692. *https://doi.org/10.1128/JB.01010-08*

Shi, J., Blundell, T. L., & Mizuguchi, K. (2001). FUGUE: Sequence-structure homology recognition using environment-specific substitution tables and structure-dependent gap penalties. *Journal of Molecular Biology*, *310*(1), 243–257. *https://doi.org/10.1006/jmbi.2001.4762*

Simon, N. C., Aktories, K., & Barbieri, J. T. (2014). Novel bacterial ADP-ribosylating toxins: structure and function. *Nature Reviews Microbiology*, *12*(9), 599–611. *https://doi.org/10.1038/nrmicro3310*

Singer, A. U., Desveaux, D., Betts, L., Chang, J. H., Nimchuk, Z., Grant, S. R., Dangl, J. L., Sondek, J. (2004). Crystal structures of the type III effector protein AvrPphF and its chaperone reveal residues required for plant pathogenesis. *Structure*, *12*(9), 1669–1681. *https://doi.org/10.1016/j.str.2004.06.023*

Skaar, E. P. (2010). The battle for iron between bacterial pathogens and their vertebrate hosts.

PLoS Pathogens, *6*(8), e1000949. *https://doi.org/10.1371/journal.ppat.1000949*

Song, Y.-J., Wang, K.-L., Shen, Y.-L., Gao, J., Li, T., Zhu, Y.-B., Li, C.-C., He, L.-H., Zhou, Q.-X., Zhao, N.-L., Zhao, C., Yang, J., Huang, Q., Mu, X.-Y., Dou, D.-F., Liu, C., He, J.-H., Sun, B., Bao, R. (2019). Structural and functional insights into PpgL, a metal-independent β-propeller gluconolactonase that contributes to *Pseudomonas aeruginosa* virulence. *Infection and Immunity*, *87*(4), 1–13. *https://doi.org/10.1128/IAI.00847-18*

Stead, D., & Wale, S. (2004). *Non-water control measures for potato common scab*. Retrieved from *https://ahdb.org.uk/review-of-research-on-non-water-based-approaches-to-control-of-potato-common-scab*

Stenbeck, G., Harter, C., Brecht, A., Herrmann, D., Lottspeich, F., Orci, L., & Wieland, F. T. (1993). β'-COP, a novel subunit of coatomer. *EMBO Journal*, *12*(7), 2841–2845. *https://doi.org/10.1002/j.1460-2075.1993.tb05945.x*

Stiles, B. G., Wigelsworth, D. J., Popoff, M. R., & Barth, H. (2011). Clostridial Binary Toxins: Iota and C2 Family Portraits. *Frontiers in Cellular and Infection Microbiology*, *1*(December), 1–14. *https://doi.org/10.3389/fcimb.2011.00011*

Sun, Q. Y., Ding, L. W., He, L. L., Sun, Y. Bin, Shao, J. L., Luo, M., & Xu, Z. F. (2009). Culture of *Escherichia coli* in SOC medium improves the cloning efficiency of toxic protein genes. *Analytical Biochemistry*, *394*(1), 144–146. *https://doi.org/10.1016/j.ab.2009.07.023*

Szirák, K., Keserű, J., Biró, S., Schmelczer, I., Barabás, G., & Penyige, A. (2012). Disruption of SCO5461 gene coding for a mono-ADP-ribosyltransferase enzyme produces a conditional pleiotropic phenotype affecting morphological differentiation and antibiotic production in

Streptomyces coelicolor. *Journal of Microbiology*, *50*(3), 409–418. *https://doi.org/10.1007/s12275-012-1440-y*

Taechowisan, T., Peberdy, J. F., & Lumyong, S. (2003). Isolation of endophytic actinomycetes from selected plants and their antifungal activity. *World Journal of Microbiology and Biotechnology*, *19*(4), 381–385. *https://doi.org/10.1023/A:1023901107182*

Torres, M. J., Simon, J., Rowley, G., Bedmar, E. J., Richardson, D. J., Gates, A. J., & Delgado, M. J. (2016). Nitrous oxide metabolism in nitrate-reducing bacteria: physiology and regulatory mechanisms. In *Advances in Microbial Physiology* (1st ed., Vol. 68). *https://doi.org/10.1016/bs.ampbs.2016.02.007*

Tsai, H. H., Huang, C. H., Lin, A. M., & Chen, C. W. (2008). Terminal proteins of *Streptomyces* chromosome can target DNA into eukaryotic nuclei. *Nucleic Acids Research*, *36*(10), 1–8. *https://doi.org/10.1093/nar/gkm1170*

Vatta, M., Lyons, B., Heney, K. A., Lidster, T., & Merrill, A. R. (2021). Mapping the DNA-binding motif of scabin toxin, a guanine modifying enzyme from *Streptomyces scabies*. *Toxins*, *13*(1), 55. *https://doi.org/10.3390/toxins13010055*

Viaene, T., Langendries, S., Beirinckx, S., Maes, M., & Goormachtig, S. (2016). *Streptomyces* as a plant's best friend? *FEMS Microbiology Ecology*, *92*(8), 1–10. *https://doi.org/10.1093/femsec/fiw119*

Vogelsgesang, M., Pautsch, A., & Aktories, K. (2007). C3 exoenzymes, novel insights into structure and action of Rho-ADP-ribosylating toxins. *Naunyn-Schmiedeberg's Archives of Pharmacology*, *374*(5–6), 347–360. *https://doi.org/10.1007/s00210-006-0113-y*

Wang, Y., Li, J., Hou, S., Wang, X., Li, Y., Ren, D., Chen, S., Tang, X., Zhou, J.-M. (2010). A *Pseudomonas syringae* ADP-ribosyltransferase inhibits *Arabidopsis* mitogen-activated protein kinase kinases. *Plant Cell*, *22*(6), 2033–2044. *https://doi.org/10.1105/tpc.110.075697*

Wanner, L. A., & Kirk, W. W. (2015). *Streptomyces* – from basic microbiology to role as a plant pathogen. *American Journal of Potato Research*, *92*(2), 236–242. *https://doi.org/10.1007/s12230-015-9449-5*

Ward, A. C., & Allenby, N. E. (2018). Genome mining for the search and discovery of bioactive compounds: The *Streptomyces* paradigm. *FEMS Microbiology Letters*, *365*(24), 1–20. *https://doi.org/10.1093/femsle/fny240*

Waterer, D. (2002). Impact of high soil pH on potato yields and grade losses to common scab. *Canadian Journal of Plant Science*, *82*(3), 583–586. *https://doi.org/10.4141/P01-046*

Watve, M. G., Tickoo, R., Jog, M. M., & Bhole, B. D. (2001). How many antibiotics are produced by the genus *Streptomyces*? *Archives of Microbiology*, *176*(5), 386–390. *https://doi.org/10.1007/s002030100345*

Wilton, M., Subramaniam, R., Elmore, J., Felsensteiner, C., Coaker, G., & Desveaux, D. (2010). The type III effector HopF2 Pto targets *Arabidopsis* RIN4 protein to promote *Pseudomonas syringae* virulence. *Proceedings of the National Academy of Sciences*, *107*(5), 2349–2354. *https://doi.org/10.1073/pnas.0904739107*

Yim, G., Huimi Wang, H., & Davies, J. (2007). Antibiotics as signalling molecules. *Philosophical Transactions of the Royal Society B: Biological Sciences*, *362*(1483), 1195–1200. *https://doi.org/10.1098/rstb.2007.2044*

Yoshida, T., & Tsuge, H. (2018). Substrate N 2 atom recognition mechanism in pierisin family DNA-targeting, guanine-specific ADP-ribosyltransferase ScARP. *Journal of Biological Chemistry*, *293*(36), 13768–13774. *https://doi.org/10.1074/jbc.AC118.004412*

Zhang, X., Clark, C. A., & Pettis, G. S. (2003). Interstrain inhibition in the sweet potato pathogen *Streptomyces ipomoeae*: Purification and characterization of a highly specific bacteriocin and cloning of its structural gene. *Applied and Environmental Microbiology*, *69*(4), 2201–2208. *https://doi.org/10.1128/AEM.69.4.2201-2208.2003*

Appendix

The appendix consists of the NCBI accession numbers for the genome file, RpoB protein accession numbers and corresponding *rpoB* nucleotide sequence coordinates for each streptomycete used in the creation of the phylogenetic tree (Figure 3.2).

Table S1: RpoB protein and nucleotide accession numbers for select streptomycetes

***Streptomyces* species**	**Genome accession**	**Genome coordinates**	**Protein accession**
Streptomyces acidiscabies	NZ_LYDS01000365	Complement 5983 -9468	WP_075733393.1
Streptomyces ambofaciens	NZ_CP012382	4731924 - 4735409	WP_053135571.1
Streptomyces aurantiacus	NZ_AOPZ01000478	Complement 29456 – 32941	WP_016645186.1
Streptomyces bottropensis	KB405078	Complement 1121251 – 1124736	EMF54941.1
Streptomyces cellulosae	NZ_JOEV01000018	Complement 189673 - 193158	WP_030671898.1
Streptomyces coelicolor	NZ_CP042324	5078169 - 5081654	WP_011029792.1
Streptomyces diastaticus	BLLN01000002	1472796 - 1476278	GFH70887.1
Streptomyces europaeiscabiei	NZ_PCGU01000049	Complement 13564 - 17049	WP_046706205.1
Streptomyces galbus	NZ_JRHJ01000054	105388 - 108873	WP_033528320.1
Streptomyces graminilatus	NZ_LIQQ01000263	Complement 5099 - 8581	WP_055528983.1
Streptomyces griseoluteus	NZ_BNBQ01000012	Complement 137746 - 141231	WP_135789392.1
Streptomyces griseoviridis	NZ_CP034687	Complement 3665191 - 3668676	WP_127178490.1

Streptomyces hokutonensis	NZ_BARG01000058	Complement 47787 - 51272	WP_026179099.1
Streptomyces hyaluromycini	NZ_BCFL01000016	Complement 1419342 - 1422827	WP_089099473.1
Streptomyces ipomoeae	NZ_SPAY01000131	45821 - 49306	WP_009330720.1
Streptomyces lividans	CP009124	3408840 - 3412325	AIJ13994.1
Streptomyces luteus	KN039947	Complement 2219678 - 2223163	KFG74266.1
Streptomyces mirabilis	NZ_KN050740	Complement 317195 - 320680	WP_037719158.1
Streptomyces neyagawaensis	NZ_LIQW01000434	Complement 5092 - 8577	WP_055540098.1
Streptomyces olindensis	JJOH01000017	217218 - 220703	KDN76514.1
Streptomyces olivochromogenes	NZ_BDQI01000007	Complement 175992 - 179477	WP_067367154.1
Streptomyces ossamyceticus	NZ_RJKY01000001	3699029 - 3702514	WP_055515271.1
Streptomyces parvulus	CP015866	4308991 - 4312476	ANJ08977.1
Streptomyces prunicolor	NZ_BARF01000005	29863 - 33348	WP_026150159.1
Streptomyces puniciscabiei	NZ_VFNX01000001	2379885 - 2383370	WP_055706210.1
Streptomyces recifensis	NZ_MUNH01000012	12196 - 15681	WP_086689997.1
Streptomyces rochei	JAAGMZ010000042	17018 - 20503	NEC70170.1
Streptomyces rubrogriseus	NZ_JAAGMQ010000783	Complement 11740 - 15225	WP_109034201.1
Streptomyces scabies	NC_013929	Complement 4190843 - 4194328	WP_013001438.1

Streptomyces scopuliridis	NZ_AZSP01000234	Complement 73992 - 77474	WP_030351423.1
Streptomyces seoulensis	CP032229	3666146 - 3669631	QBJ91844.1
Streptomyces shenzhenensis	NZ_PENI01000044	Complement 27303 - 30788	WP_121894863.1
Streptomyces sp. *11-1-2*	CP022545	6482813 - 6486295	ASQ96280.1
Streptomyces sp. *NRRL WC-3618*	NZ_LGDW01000463	Complement 5067 - 8549	WP_053745800.1
Streptomyces stelliscabiei	KQ257875	34361 - 37161	KND35109.1
Streptomyces turgidiscabies	AEJB01000664	8218 - 11700	ELP61643.1
Streptomyces violaceorubidus	NZ_JODM01000001	227696 - 231181	WP_030145442.1
Streptomyces viridochromogenes	NZ_LGUQ01000254	Complement 40734 - 44219	WP_048585312.1
Streptomyces xylophagus	NZ_JNWO01000023	140468 - 143953	WP_043682780.1